AD-A075 467 ITT ELECTRO-OPTICAL PRODUCTS DIV ROANOKE VA F/G 20/6
BIDIRECTIONAL COUPLER FOR FULL DUPLEX TRANSMISSION ON A SINGLE --ETC(U)
AUG 79 A R NELSON, G A GASPARIAN, G W BICKEL DAAB07-77-C-1798
UNCLASSIFIED CORADCOM-77-1798-F NL

1 OF 2
AD
A075467

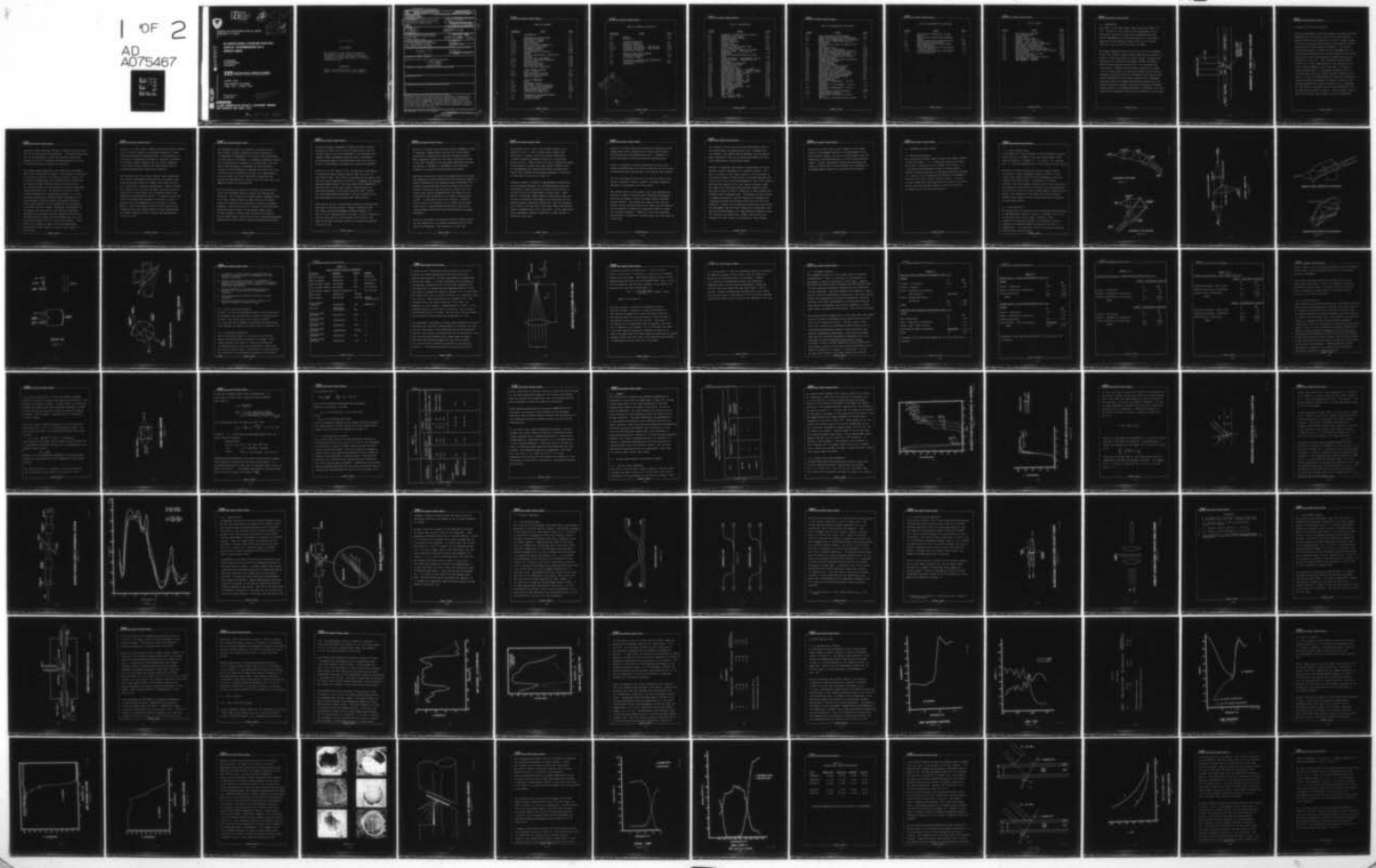

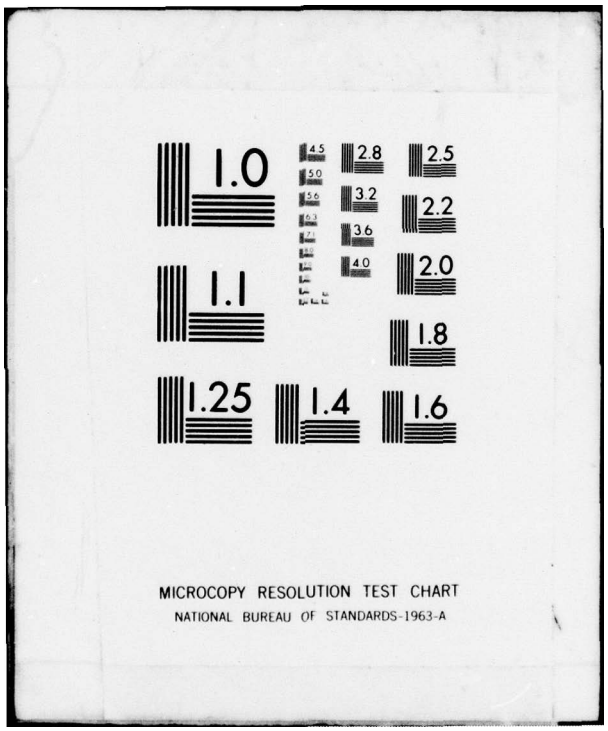
1.0
1.1
1.25
1.4
1.6
1.8
2.0
2.2
2.5
2.8
3.2
3.6
4.0
4.5
5.0
5.6
MICROCOPY RESOLUTION TEST CHART
NATIONAL BUREAU OF STANDARDS-1963-A

LEVEL II

12039073

(12)

RESEARCH AND DEVELOPMENT TECHNICAL REPORT
CORADCOM-77-1798-F

AD A075467

BI-DIRECTIONAL COUPLER FOR FULL DUPLEX TRANSMISSION ON A SINGLE FIBER

A.P.NELSON
G.A.GASPARIAN
G.W.BICKEL

ITT ELECTRO-OPTICAL PRODUCTS DIVISION
7635 Plantation Rd., Roanoke, Va. 24019. Telephone (703) 563-0371

AUGUST 1979

FINAL REPORT FOR PERIOD
1 MAY 1977 - 15 MAY 1979

Prepared for:
CENCOMS

CORADCOM
US ARMY COMMUNICATION RESEARCH & DEVELOPMENT COMMAND
FORT MONMOUTH, NEW JERSEY 07703

N O T I C E S

DISCLAIMERS

The citation of trade names and names of manufacturers in this report is not to be construed as official Government indorsement or approval of commercial products or services referenced herein.

DISPOSITION

Destroy this report when it is no longer needed. Do not return it to the originator.

Unclassified

SECURITY CLASSIFICATION OF THIS PAGE (When Data Entered)

REPORT DOCUMENTATION PAGE

READ INSTRUCTIONS BEFORE COMPLETING FORM

1. REPORT NUMBER: CORADCOM-77-1798-F

2. GOVT ACCESSION NO.

3. RECIPIENT'S CATALOG NUMBER

4. TITLE (and Subtitle): Bi-directional Coupler for Full Duplex Transmission on a Single Fiber.

5. TYPE OF REPORT & PERIOD COVERED: Final Rept. May 1, 1977 - May 15, 1979

6. PERFORMING ORG. REPORT NUMBER: 1 May 77 - 15 May 79

7. AUTHOR(s): A. R. Nelson, G. A. Gasparian, G. W. Bickel

8. CONTRACT OR GRANT NUMBER(s): DAAB07-77-C-1798

9. PERFORMING ORGANIZATION NAME AND ADDRESS: ITT Electro-Optical Products Division, P.O. Box 7065, Roanoke, Virginia 24019

10. PROGRAM ELEMENT, PROJECT, TASK AREA & WORK UNIT NUMBERS: 1L162701AH92MA13 MA

11. CONTROLLING OFFICE NAME AND ADDRESS: U.S. Army Communications R&D Command, ATTN: DRDCO-COM-RM-4, CENCOMS, Fort Monmouth, New Jersey 07703

12. REPORT DATE: AUG 1979

13. NUMBER OF PAGES: 188

14. MONITORING AGENCY NAME & ADDRESS (if different from Controlling Office): 11 Aug 79

15. SECURITY CLASS. (of this report): Unclassified

15a. DECLASSIFICATION/DOWNGRADING SCHEDULE

16. DISTRIBUTION STATEMENT (of this Report)

Approved for public release, distribution unlimited

12 190

17. DISTRIBUTION STATEMENT (of the abstract entered in Block 20, if different from Report)

18. SUPPLEMENTARY NOTES

19. KEY WORDS (Continue on reverse side if necessary and identify by block number)

10 to the -8th power

20. ABSTRACT (Continue on reverse side if necessary and identify by block number)

The primary objective of this contract is the development of a bi-directional coupler for single optical fiber transmission systems and the implementation of two such couplers in a full duplex link with simulated length of up to 8 km, 20 Mb/s data rate, and 10^{-9} BER. The primary approach adapted for this task is the fiber dichroic coupler. Other approaches were also investigated. When used in a duplex optical data link, this three port device constitutes a wavelength selective bi-directional coupler.

DD FORM 1 JAN 73 1473 EDITION OF 1 NOV 65 IS OBSOLETE

Unclassified

SECURITY CLASSIFICATION OF THIS PAGE (When Data Entered)

189750

TABLE OF CONTENTS

TABLE OF CONTENTS (Continued)

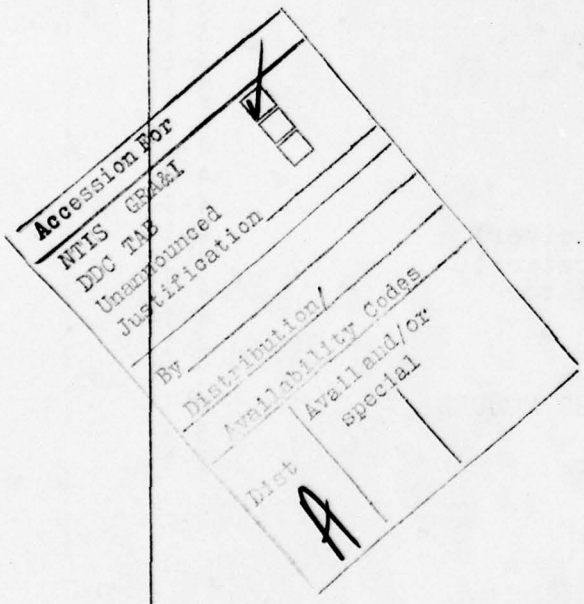

LIST OF ILLUSTRATIONS

LIST OF ILLUSTRATIONS (Continued)

LIST OF ILLUSTRATIONS (Continued)

LIST OF TABLES

1.0 INTRODUCTION

This report is the Final Report under Contract No DAAB07-77-C-1798. The goal of this effort was the development of a bi-directional coupler for single fiber transmission systems and the implementation of two such couplers in a full scale duplex link, with simulated length of up to 8 km, 20 Mb/s (NRZ) data rate, and 10^{-8} bit error rate (BER).

The primary approach adopted for this task was the development of the Fiber Dichroic Coupler shown schematically in Figure 1-1, based on a fiber beam splitter coupler design. Although other techniques were considered as possible methods to achieve bidirectional operation, the ability to use wavelength discrimination to achieve near end optical isolation was deemed to be a critical factor in achieving ultimate system operation. Techniques using two different wavelength sources emerged from initial considerations as primary candidates for development. Techniques which were dropped from further consideration were spatial duplexing or angular distribution duplexing techniques without benefit of wavelength separation. Electronic cross talk cancellation techniques were explicitly excluded by the original

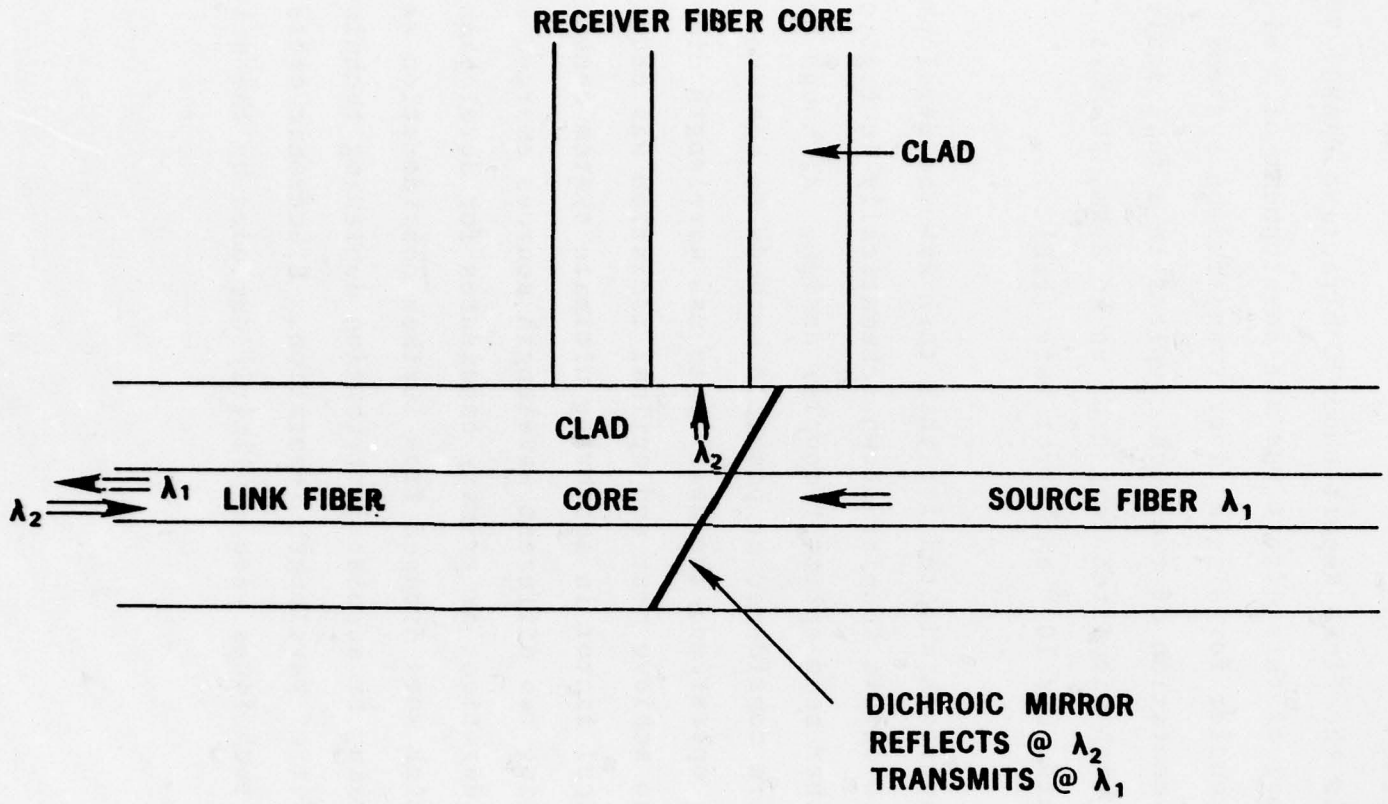

SCHEMATIC OF FIBER DICHROIC COUPLER

FIGURE 1-1

statement of work for the program.

Further consideration of possible methods to achieve wavelength duplexing led to the primary choice of the Fiber Dichroic Coupler because of the potential for low cost, compact rugged construction, potential minimization of environmental effects, and potential for high optical performance. This optical performance potential included not only throughput but also low internally generated cross talk and capability of discriminating against cross talk generated through reflections and backscatter in the link. Other techniques which had many, but not all, of these characteristics were considered as potential backup techniques for this program. For example, coupler designs based on conventional focussing optics to transform small spot size, highly divergent radiation from a fiber to a large, collimated beam and conventional dispersive elements (prisms and gratings) or dichroic reflectors, were considered potentially inferior because of size, ruggedness, and cost factors, although from the outset performance could be expected to be equal or superior. Other couplers, such as the fused biconical taper coupler, were not considered as

potential primary approaches because of higher insertion losses and lack of backscatter discrimination. It should be noted that some of the advantages of using two different source wavelengths can still be obtained with these couplers by the use of passive filtering at sources and detectors.

The primary coupler approach to this effort was the development of the Fiber Dichroic Coupler. This coupler is fabricated by the direct insertion of a dichroic reflector surface into the fiber throughput path and the addition of a third fiber to receive the light reflected from the dichroic mirror. The dichroic surface has the property of selective wavelength transmission/reflection. The dichroics utilized in bidirectional operation are complimentary filters, i.e., short wavelength transmission (long wavelength transmission) and long wavelength reflection (short wavelength reflection). Thus the main emphasis of this program was the development of the Fiber Dichroic Coupler. Additional requirements for the program were the study of other potential duplexing techniques and potential trade-offs against each other and the Fiber Dichroic Coupler and the implementation of a full duplex bidirectional link on a single fiber channel. These efforts are reported in detail in the following report. An overview of these efforts is given in the remainder of this section.

Section 2.0 of this report (Technique and Design Study) consists of (1) a study of methods of wavelength duplexing in fiber optics using standard focussing optics, (2) presentation of the results of experiments designed to determine limitations of the Fiber Dichroic Coupler, and (3) a brief comparison of the Fiber Dichroic Coupler with other methods used in achieving bidirectional single fiber operation.

The focussing optics (or lensed coupler) study investigated the potential performance characteristics of couplers using prism and grating dispersive elements and dichroic mirrors in a conventional collimated configuration. Optical throughput, internal cross talk, and external cross talk rejection capabilities of each coupler were calculated based on the assumption of monochromatic sources. It should be noted that detailed considerations presented in Sections 6.0 and 7.0 indicate that this assumption is not justified in actual devices. One of the primary results of this study was the recognition that all couplers which use lens transformation will suffer diffraction losses varying from approximately 0.3 dB to 0.7 dB.

The experimental effort to determine limitations of the Fiber Dichroic Coupler consisted of three experiments to (1) determine the degradation in dichroic mirror performance at large angles of incidence, (2) determine degradation effects due to using dichroic reflectors in optical beams with relatively high divergence corresponding to fiber numerical aperture, and (3) determine if degradation effects will occur in dichroic mirror operation with spot sizes (approximately 50 μm) of fiber core cross section due to beam walk off. Significant degradation was found in the first two cases, with negative results for beam walk off.

The final portion of Section 2.0 discusses the potential for using three different specific couplers for bidirectional operation. Two of these use focussing optics (standard lenses in one case, graded refractive index lenses in the other) along with dichroic mirror reflection to achieve wavelength duplexing. Both will of course be subject to the diffraction losses discussed in detail in the lensed coupler study. The third coupler covered in this section is the fused biconical taper coupler, which does not use a wavelength duplexing mechanism but can be used to achieve bidirectional operation

through wavelength independent coupling between two fibers. Although this device can be used in bidirectional links operating either at the same wavelength or two different wavelengths, higher throughput losses and lack of wavelength discrimination against link backscatter would limit its usefulness in applications requiring fully optimized components.

Section 3.0 of this report covers the details of the efforts to develop the Fiber Dichroic Coupler (FDC) for use in bidirectional links. This effort was divided into two phases with the first phase consisting of an effort to implement the original proposed coupler design. The first phase effort demonstrated the feasibility of the basic coupler concept through the measured performance of the short-wave pass (SWP) couplers but also demonstrated limitations of the first design by the poor performance of the long-wave pass (LWP) devices.

These results led to a second phase in which two modifications were made to the basic design. Couplers fabricated under this effort achieved throughputs typically between -1.1 and -2.0 dB in transmission and less than -2.7 dB in reflection. Internal backscatter in these couplers was typically less than -40 dB, while external backscatter rejection was between 11 dB and 15 dB.

Section 4.0 discusses the additional optical components needed to implement a demonstration link for full bidirectional operation on a single fiber using the developed couplers. These components include the link fiber, additional filters to take full advantage of the wavelength duplexing technique, and methods to implement an independent dual-wavelength attenuator to determine maximum system link length.

Additional filters were used in the demonstration link since, even though the couplers demonstrated discrimination capability against backscatter at the opposing channel wavelength, the ultimate system performance could be achieved only with additional filtering at the weak receiver channel (1.06 μm). Filters were actually implemented for both channels in anticipation of the availability of stronger long-wavelength sources. In the case of the .85 μm receiver, a dichroic filter proved to be preferred over a "spike" (narrow band) filter since it discriminated as effectively against the long-wavelength source cross talk and had better throughput efficiency.

As part of the effort to determine the most suitable filters for this application, the spectral characteristics of both sources were measured. The potential for cross talk

contributions due to source "out-of-band" emission (e.g., emission in the $\lambda > 0.95$ μm region from a GaAlAs laser operating at a nominal .85 μm) was clearly identified. A similar potential presumably exists for 1.06 μm laser devices as well. These results will have a significant impact on the design of couplers and other optical elements used for implementing full duplex bidirectional operation over single fiber channels by wavelength duplexing, as discussed in some detail in Sections 6.0 and 7.0.

Although a number of methods of implementing an appropriate dual-wavelength attenuator for the demonstration link were investigated, actual fabrication proved to be difficult in at least one case and undesirable in other cases. Consequently a relatively simple method for evaluating cross talk was used to determine link margin in one direction with the opposing channel transmitter turned off. With the attenuator set to achieve the desired bit error rate (BER), the opposing channel transmitter was set to full power: in all cases there was no measurable increase in BER due to either optical or electrical cross talk.

Section 5.0 of this report gives pertinent information on the digital fiber optic transmitter and receiver units used in the bidirectional link demonstration unit. Included is a brief discussion of source and detector characteristics.

Section 6.0 presents a detailed calculation of cross talk effects including source out-of-band radiation and the results of testing the full bidirectional link using the FDC couplers.

The cross talk analysis goes into the spectral detail of the sources, detectors, filters, couplers, and other components important in determining cross talk levels.

The spectral detail of the primary cross talk components are analyzed in order to determine where additional development effort may be needed to achieve ultimate optical isolation between channels. For example the analysis shows that additional source filtering between the sources and the couplers will be required to reduce the significant effect of source "out-of-band" radiation. Finally the cross talk components are spectrally integrated to estimate total cross talk expected in the link.

The remainder of the section discusses measurements made on the bidirectional link demonstration unit, including link loss budgets, link length limiting elements (the low optical power available in the 1.06 μm source) and effects of cross talk (unobservable in the present setup).

Section 7.0 summarizes the results of measurements on lensed dichroic couplers fabricated for a separate program. This data is included in this report because of its pertinence to the overall problem of bidirectional wavelength duplexing and because of its very close correspondence to one of the couplers which was the subject of the lens coupler technique study. The coupler was fabricated using precision aspheric lenses and state-of-the-art dichroic reflectors in near perpendicular incidence with collimated light. Performance of these devices is roughly equivalent to the FDC couplers in throughput and significantly better for internal cross talk and cross talk rejection. Because of the relatively conventional optics used, the development time for these couplers was considerably less than for the FDC couplers, but large quantity production costs may ultimately be significantly higher, and the extra performance not really usable or achievable by other methods.

Section 8.0 of this report gives a summary of the primary results of the program relative to the development of the Fiber Dichroic Coupler, its use in a bidirectional link, and comparison of FDC characteristics to a bulk lensed dichroic coupler. Finally some general conclusions concerning the status of bidirectional link performance and development of wavelength duplex couplers for such links are presented.

2.0 TECHNIQUE AND DESIGN STUDY

2.1 Macroscopic Coupling

The technique and design study portion of this effort consists of three main parts: (1) a theoretical analysis of three bulk coupler techniques: prism, grating, and dichroic: (2) a theoretical and experimental study of various effects related to angular incidence in multilayer dielectric coatings (3) finally, a brief comparison and analysis is included of couplers other than the fiber dichroic coupler. All three of these studies have been reported on in detail in the First, Second, and Third Quarterly Reports, and the results will be summarized in the following sections.

2.1.1 Basic Generic Types

In the analysis of the performance of bulk directional couplers, discussion will be limited to the three basic generic types shown in Figures 2-1 through 2-3: (1) prism, (2) grating, and (3) the bulk implementation of the dichroic mirror coupler.

The first two types, grating and prism, are quite similar in operation, using a dispersive element to effect a relatively small change in beam direction depending on the wavelength of the incident beam. Operating on a different principle, the third coupler (dichroic mirror) uses constructive and destructive interference of reflected or transmitted waves from dielectric layers to cause a large change in beam direction However, the separation of the light into the two beams is generally more complete using the dispersion types as opposed to the dichroic mirror.

2.1.2 Mechanizations

Our analysis will be concerned with two different mechanizations or implementations (shown in Figures 2-4 through 2-6) of each of the three basic coupler types. Obviously, other configurations are also possible, but the analysis must be limited to a reasonable number of models for the sake of manageability. The following criteria were used in selecting these possible mechanizations:

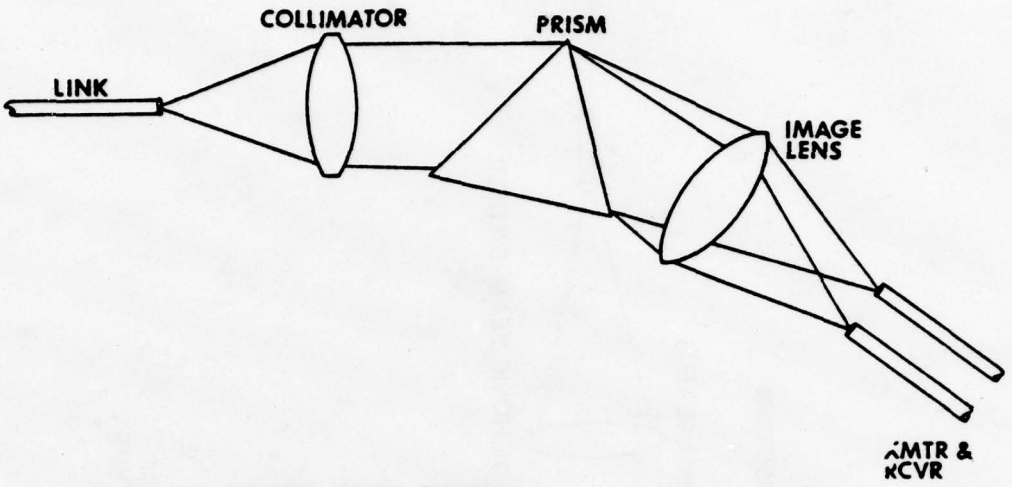

DISPERSION TYPE PRISM

Figure 2-1

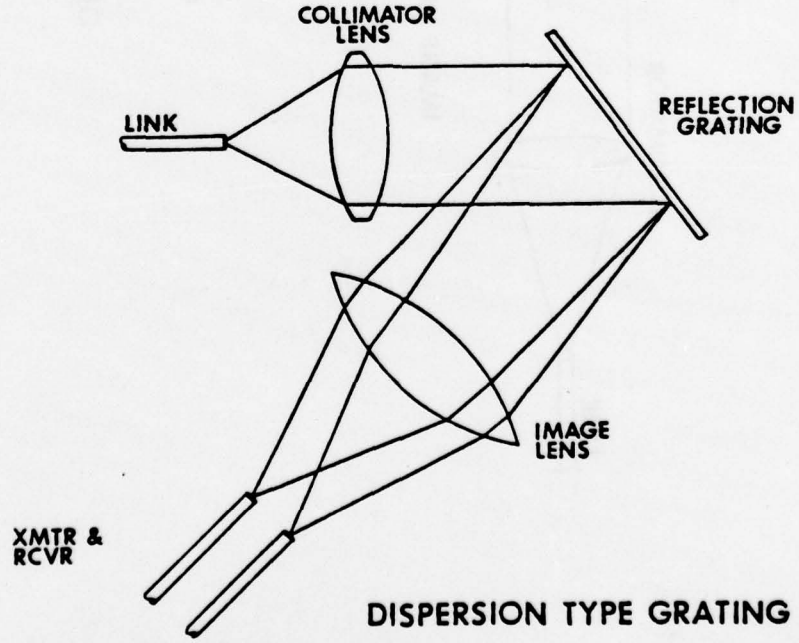

DISPERSION TYPE GRATING

Figure 2-2

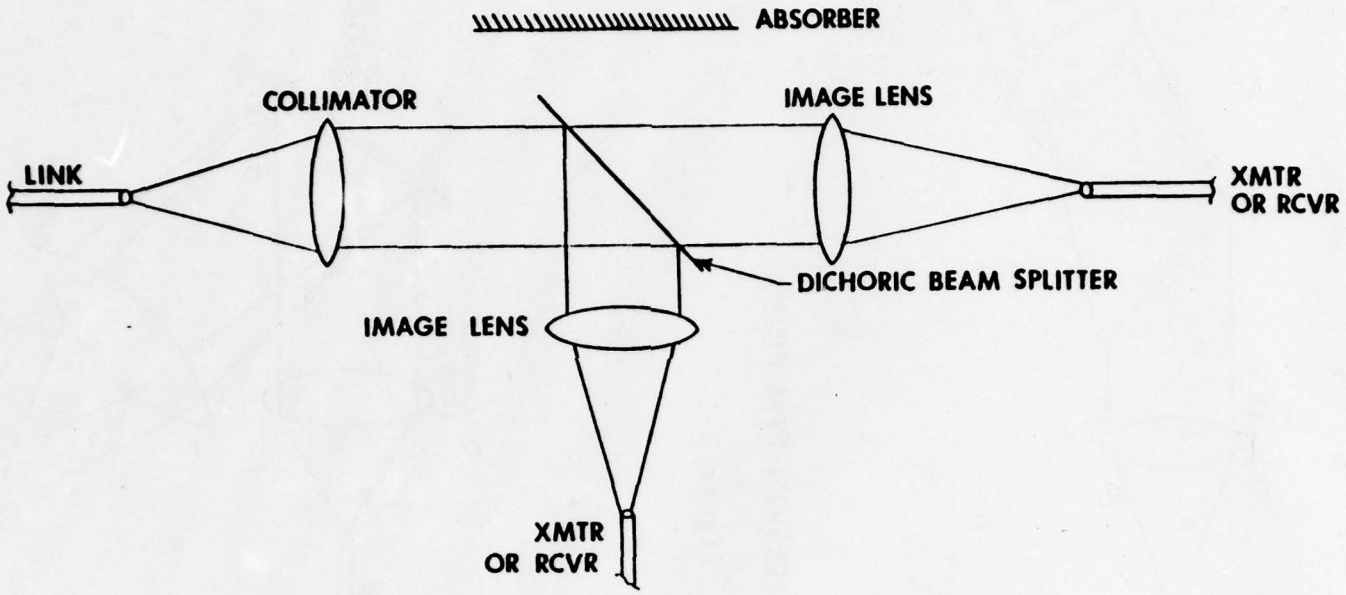

DICHORIC MIRROR TYPE

Figure 2-3

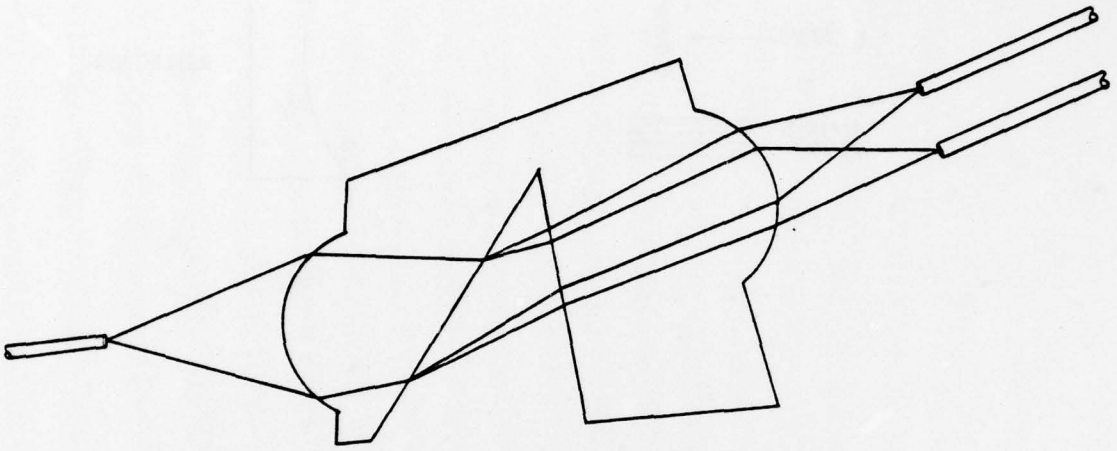

NEGATIVE PRISM - REFRACTIVE COLLIMATION

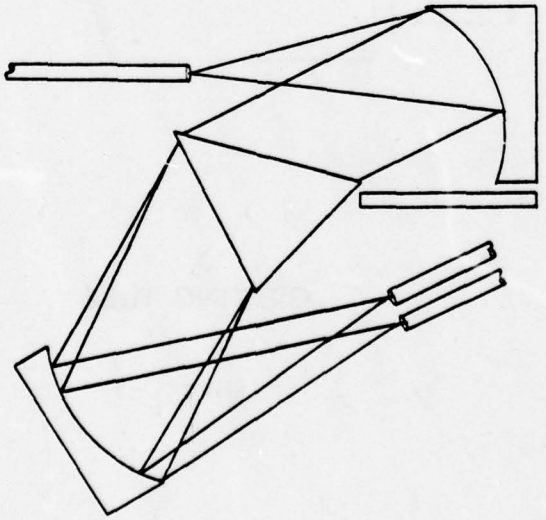

POSITIVE PRISM- REFLECTIVE COLLIMATION

Figure 2-4

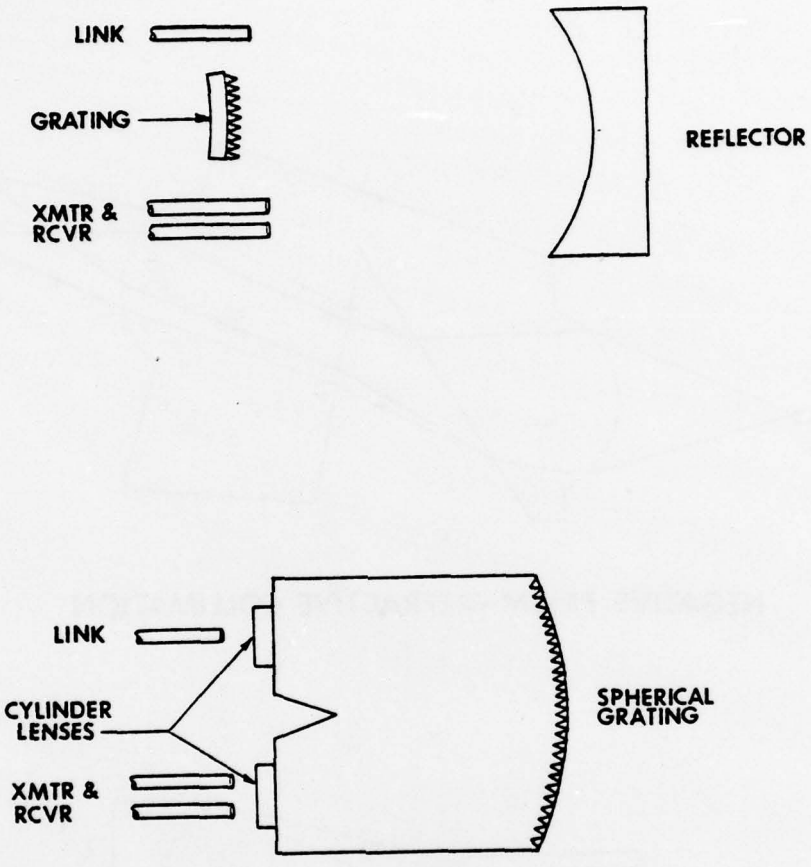

GRATING TUBE

Figure 2-5

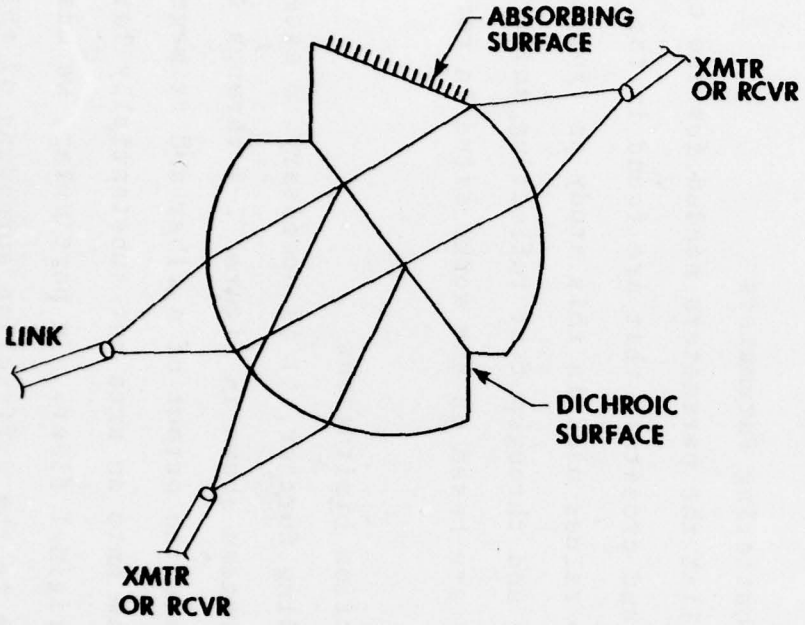

SOLID DICHROIC FILM TYPE

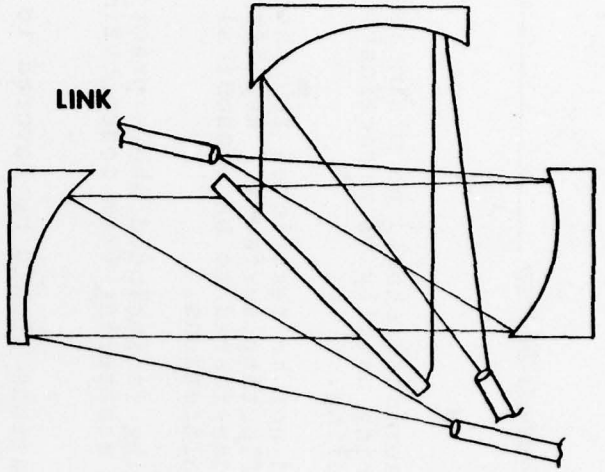

CONVENTIONAL

DICHROIC COUPLER

Figure 2-6

A. The number of surfaces should be minimized because surface scattering usually is predominant over bulk material scattering.

B. Analysis should not be restricted to spherical refracting or reflecting surfaces. Replicated or molded aspherics are considered to be economical in moderately high volume applications.

C. Optical shielding is included where practical to prevent direct scattering from contributing to crosstalk.

D. Solid configurations should be favored to increase ruggedness.

E. Replicated gratings may be plane or spherical but should be limited to reflective types.

2.1.3 Basic Scattering Parameters

In Table 1 we list the parameters needed for the calculations of throughput and crosstalk that are found in the following sections. The values used in this study as typical for scattering and throughput at reflecting and transmitting glass surfaces are based on the works cited in references 4-8.

2.1.4 Diffraction Limitations

Before proceeding further, it is necessary to ascertain whether the systems shown in Figures 2-4 through 2-6 can indeed collimate the output of a fiber and reimage the collimated beam onto an area not substantially larger than that of the original fiber. In particular, we must calculate the losses due to the diffraction spreading of the optical beam.

TABLE 2-1

VALUE OF BASIC OPTICAL PARAMETERS

LOCATION	PROCESS	VALUE	COMMENT
Mirror Surface	Scattering	.1%	Lambertian
Mirror Surface	Throughput	99+%	(ar coating)
Lens Surface (glass)	Scattering	.1%	Lambertian
Lens Surface (glass)	Throughput	99+%	(ar coating)
Lens Surface (glass)	Fresnel Reflection	.2%	(ar coating)
Bulk Glass	Scattering	.02%/mm	
Bulk Plastic	Scattering	.012%/mm	(methyl methacrylate)
Lens Surface (Plastic)	Scattering	.5%	Lambertian
Grating	Scattering (efficiency)	80%	
Dichroic Beam Splitter	Reflection	98+%	λ_1
Dichroic Beam Splitter	Transmission	.2%	λ_1
Dichroic Beam Splitter	Scattering	1-2%	λ_1
Dichroic Beam Splitter	Transmission	85-90%	λ_2
Dichroic Beam Splitter	Reflection	10%	λ_2
Dichroic Beam Splitter	Scattering	1-2%	λ_2

Consider first a diffraction limited system, which can in practice be closely approached at the very short focal lengths characteristic of these instruments by paraboloidal mirrors and lenses. In order to maximize the throughput by intercepting substantially all of the light emanating from the fiber end, we require that the numerical aperture of the lens equal or exceed the numerical aperture (N.A.) of the fiber. For fibers with a N.A. of 0.22 to 0.25 we will stipulate a lens N.A. of 0.25. This translates to an F-number of 2.0. The diameter of the airy disk is then $D_A = 2.44\ \lambda(F\#)$, (independent of focal length.) Substituting $F\# = 2$ and $\lambda = 1.06$ microns we find $D_A = (2.44)(1.06)(2) = 5.17$ microns. This is 10.3% of the core diameter 50 μm of the fiber. From this we can infer that diffraction losses will be about the same order of magnitude, ie., 10%.

Our approximate calculation of these losses proceeds as follows: Consider first the case of decollimation or focusing the light into the fiber after it has passed through the bidirectional coupler. The original collimated beam can be considered to consist of plane waves oriented over a small range of angles. Each plane wave passing through the lens will be focused to a spot and form a diffraction pattern[4] as illustrated in Figure 2-7. The diffraction pattern in the focal plane for

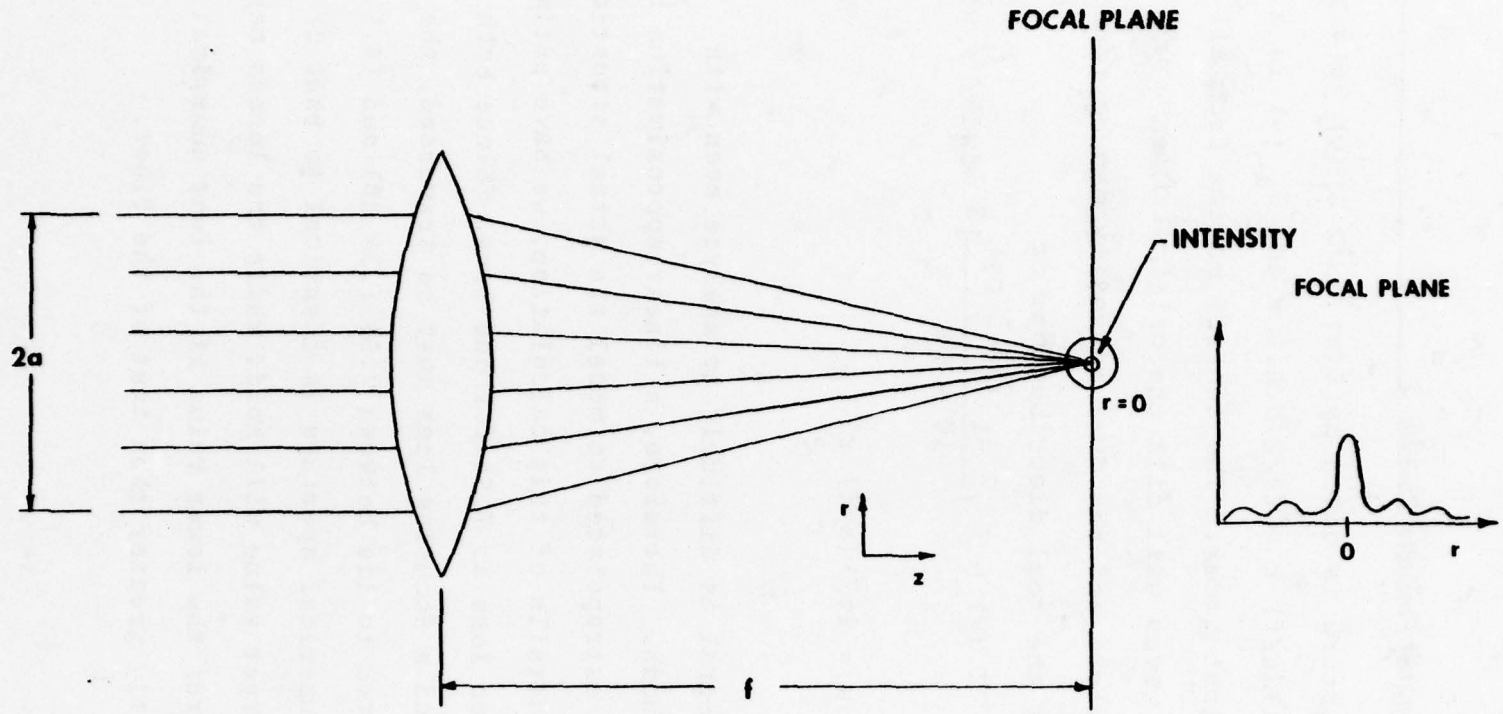

DIFFRACTION PATTERN AFTER LENS

Figure 2-7

a circular aperture is given by $I(v) = [2 J_1 (v) /v]^2 I$ where $v = (2\pi/\lambda)(a/f)\ r = (2\pi/\lambda)(N.A.)\ r$ and $J_1 (v)$ is a Bessel Function of first order. The central maxima from all of the focused plane waves will fill the original fiber core, a circle of 50 μm diameter, and the total intensity can be found by integrating over the toal distribution, or

$$I(V) = \int \left[\frac{2 J_1 (1\vec{v} - \vec{w}1)}{1\vec{v} - \vec{w}\ell}\right]^2 wdwd\theta / \int wdwd\theta$$

where $w = 2\pi/\lambda (a/f)\ r'$

The above integral is difficult to analyze even with numerical methods. Therefore, a linear approximation has been used and extrapolated to model the actual situation. Omitting the details of this calculation, we have estimated the diffraction loss as 7.5% for one lens. Since both a collimating and a focusing lens must be traversed, the total loss is expected to lie between 7.5% (.34 dB) and 14.5% (.68). If the lens numerical aperture is identical to that of the fiber, the larger value will hold; while the losses may be reduced somewhat towards the lower value if the lens numerical aperture is significantly greater than that of the fiber.

It is not possible to raise the throughput simply by increasing the numerical aperture of the lenses, since the fiber core and NA are the limiting factors in the system. However, it is possible to significantly reduce the diffraction spreading losses for the receiver wavelength by making the receiver fiber core larger than the other fibers. This is possible because of PIN and APD detectors have a much larger area than the laser or LED sources or the core size of standard long distance fibers that are used in the remainder of the link.

2.1.5 Throughput Analysis

The throughput analysis for each coupler type is relatively straightforward. There is a potential for differences in performance in the two directions in each coupler. However, the prism and grating types of coupler are sufficiently close to being completely reciprocal devices that the differences will be negligible. The only asymmetry that appears in these devices is due to differences in absortion in the prism materia between the transmitter and receiver wavelengths, typically less than 0.1%, and to differences in grating efficiency between the two wavelengths, which can be reduced to a second order effect by proper choice of blaze. Both will be neglected

The dichroic mirror beamsplitter, on the other hand, has fundamentally different performance in the reflection branch from that in the transmission branch. Further, there is some doubt that optimum long-wavelength-transmittance and short-wavelength-transmittance dichroic filters would have completely complimentary performance. This analysis assumes that they can, and uses performance parameters known to be available in short-wavelength-transmittance filters.

In Tables 2-2 to 2-4, we have summarized the data collected in the previous section for the prism, grating and dichroic mirror devices of Figures 2-4 through 2-6, respectively. As can be seen from the Tables, the larges losses occur with the

TABLE 2-2

Positive Prism, Reflective Collimation (Fig. 2.4)

LOSSES	%	dB
Mirrors - Diffraction	14.5	-.68
Mirrors - Coating	2	-.09
Prism - Absorption & Scattering Bulk Material	Negligible	-
Prism - Surface Reflection & Scattering	2	-.09
TOTAL	18	-.86

Negative Prism, Refractive Collimation (Fig. 2.4)

LOSSES	%	dB
Lens Diffraction	18	-.68
Lens - Reflection & Scattering	2	-.09
Prism - Refl & Scatt @ surf	2	-.09
Bulk Material Refl & Scattering	Negligible	-
TOTAL	18	-.86

Throughput is the same from transmitter to link as from link to receiver.

TABLE 2-3

Grating Type 1 - Normal Configuration (Fig. 2.5)

LOSSES	%	dB
Mirror - Diffraction	14.5	-.68
Mirror - Reflection & Scattering	2	-.09
Grating Efficiency	20	-0.97
TOTAL	33	-1.74

Grating Type 2 - Solid Configuration (Fig. 2.5)

LOSSES	%	dB
Lenses - Diffraction	14.5	-.68
Lenses - Reflection & Scattering	1	-.04
Grating Efficiency	20	-0.97
Bulk Material - Refl & Scattering	Negligible	-
TOTAL	32.2	-1.69

Throughput is the same from transmitter to link as from link to receiver.

TABLE 2-4

Dichroic Filter Type 1 - Reflective Collimation (Fig. 2-6)

LOSSES - REFLECTION DIRECTION	%	dB
Mirrors - Diffraction	14.5	-.68
Mirrors - Absorption & Scattering	2	-.09
Dichroic Transmission & Scattering	1	-0.04
TOTAL	17	-0.81

LOSSES - TRANSMISSION DIRECTION	%	dB
Mirrors - Diffraction	14.5	-.68
Mirrors - Absorption & Scattering	2	-.09
Dichroic Reflection & Scattering	12	-0.56
TOTAL	26.4	-1.33

TABLE 2-4a

Dichroic Filter Type 2 - Solid Block (Fig. 2-6)

	LOSSES - REFLECTION DIRECTION	
	%	dB
Refractive Surface - Refl & Scat	2	-.09
Refractive Surfaces - Diffraction	14.5	-.68
Dichroic Trans & Scattering	1	-0.04
TOTAL	17	-.81

	LOSSES - TRANSMISSION DIRECTION	
	%	dB
Refractive Surfaces - Refl & Scat	2	-.09
Refractive Surfaces - Diffraction	14.5	-.68
Dichroic Refl & Scattering	12	-0.56
TOTAL	26.4	-1.33

grating coupler, due to the grating efficiency, and the dichroic mirror coupler in the transmission mode due to the relatively low mirror throughput.

In an actual link these losses will be taken twice for the grating and prism devices. Due to the asymmetric nature of the dichroic mirror coupler, the total link loss will be the sum of traversing the coupler once in the reflective mode and once in the transmission mode.

2.1.6 Crosstalk Analysis

Since details of the crosstalk analysis for each coupler type have been covered in previous quarterly reports, this report will use one example (the positive prism, reflective collimation type) to indicate the method of crosstalk analysis, and will summarize the results for each coupler type. This analysis will treat the coupler as a separate entity, with backscatter components originating in the link, transmitter or receiver being considered signals. Thus, it will be necessary to consider separately the effects of these backscatter components on system performance. Necessarily some assumptions concerning the size and geometry of the couplers must be made in order to use the known values of material's parameters to estimate the effects of scattering on the crosstalk performance. These assumptions, unless specifically indicated to be otherwise, are at the more pessimistic boundary of reasonable design.

The tunnel diagram Figure 2-8 shows the coupler "unfolded" around the reflective surfaces for clearer visualization of the optical path lengths involved. In other words, the reflecting surfaces are shown as very thin refractive elements, in order to show the optical distances within the system as physical distances. The technique is commonly used in the analysis of prism systems.

The fiber, having a numerical aperture of 0.25, observes a semi-angle of $\theta = \text{SIN}^{-1}$ .25 at the reflective surface. The solid angle subtended by the reflecting surface at the fiber is then:

$$W = 2\pi[1 - \text{COS}(\text{SIN}^{-1} .25)] = .2 \text{ steradians}$$

The fraction of the input light incident on that surface that is scattered and reenters the fiber or is crosscoupled to the adjacent fiber will be:

$$E_s = \frac{W}{2\pi} K_n$$

where K_n is the scattering coefficient of the N_{th} surface, which will range from 10^{-4} to 10^{-3} depending on the surface quality.

The radiation scattered by elements in the collimated beam will be coupled into the receiver fiber only if it lies

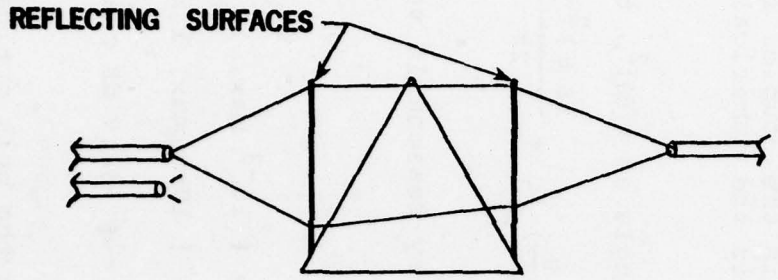

PRISM TUNNEL DIAGRAM

Figure 2-8

within the divergence angle of the collimated beam. To an accuracy of better than 3 percent the beam divergence half angle is:

$$\Delta\theta = \frac{2\,d\,(N.A.)}{D}$$

Where d is the fiber core diameter
D is the coupler lens diameter
N.A. is the numerical aperature (of the lens)

if we approximate the solid angle as $\pi(\Delta\theta)^2$, then

$$E_{s-s} = \left(\frac{W}{2\pi}\right) K_1 + \frac{(\Delta\theta)^2}{2\pi} \left(K_2 + K_3 + K_4\right).$$

Since $W = .2 \gg (\Delta\theta)^2$ for any reasonable values of D, the first term will dominate.

Substituting:

$K_1 = K_2 = K_3 = K_4 = [\ 10^{-3}$ max, 10^{-4} min]

and: D = [10mm max, 1 mm min]

gives: E_{s-s} = [-44.9 dB max, -55.0 dB min]

Calculating the scattering in the bulk optical glass or plastic also requires an estimate of the size of the coupler. If an equilateral prism is used, the altitude must equal D, and its base will be $\sqrt{3}\,D$. The average path length in the prism body will be 1/2 the length of the base or $\frac{\sqrt{3}\,D}{2}$.

The crosstalk will be:

$$E_{S-B} = \frac{(\Delta\theta)^2}{4\pi} \quad \frac{\sqrt{3}\,D}{2} \quad K_B \text{ , where } K_B$$

is the bulk scattering coefficient per millimeter.

Taking D = [10 mm max, 1 mm min]

$$K_B = [2 \times 10^{-4}/\text{mm max},\ 1.3 \times 10^{-4}/\text{mm min}]$$

gives

$$E_{S-B} = [-80.6 \text{ dB max}, -92 \text{ dB min}]$$

which is negligible compared to the surface scattering effects. This same procedure has been carried out for the other mechanizations, and the results are summarized in Table 2-5.

2.1.7 Link Backscatter Isolation

One of the primary reasons for using wavelength duplexing in a bidirectional fiber optic link is to be able to use wavelength discrimination to reduce crosstalk effects arising from backscatter in the fiber itself. Thus the ability of a coupler to provide some of this needed discrimination will be an important element in the evaluation of coupler devices. The isolation provided to the receiver by the coupler from this backscatter will vary with the type of coupler. Inspection of the coupler optical diagrams shows that for the prism and grating types of couplers the link backscatter isolation will be equal to the

TABLE 2-5

SUMMARY OF BULK COUPLER STUDY

DEVICE AND CONFIGURATION	THROUGHPUT (dB)		INTERNAL BACKSCATTER (dB)		EXTERNAL BACKSCATTER REJECTION (dB)
	TRANSMITTER	RECEIVER	MAX	MIN	
PRISM: BOTH	-.86	-.86	-45	-55	SAME AS INTERNAL
GRATING: MIRRORS	-1.70	-1.70	-45	-55	SAME AS INTERNAL
LENSES	-1.70	-1.70	-34	-44	
DICHROIC					
TRANSMITTER REFLECTION BAND	-.81	-1.30	-56 to -80		~ -20
RECEIVER REFLECTION BAND	-1.30	- .81	-56 to -60		~ -10

direct transmitter to receiver isolation, since the major portion of the fiber backscatter radiation will retrace its original path and re-enter the transmitter, only the scattered portion being available to enter the receiver as crosstalk.

Since these mechanizations are optically symmetrical about a mid-plane, the analysis of the fraction of the scattered radiation which actually becomes crosstalk will be identical to the transmitter receiver crosstalk analysis and will not be repeated here.

In the case of the dichroic beamsplitter coupler, a direct leakage term exists, being the fraction of transmitter wavelength reflected from a transmitting dichroic or the fraction transmitted by a reflecting dichroic (i.e., the coefficient T, in the crosstalk analysis). Since this term is at least two order of magnitude larger than any scattering terms for this coupler, the scattering terms may be neglected. This term will vary from 0.1 (= -10dB) to 5×10^{-3} (= -23 dB) depending on the quality of the dichroic and whether the link-to-receiver optical path is reflective or transmissive through the dichroic.

2.1.8 SUMMARY

The value of the throughput and crosstalk parameters investigated in this study are summarized in Table 2-5, and the overall performance of the three approaches to the bulk bidirectional coupler are ranked in Table 2-6. As can be seen from Table 2-5, the three methods give results that are fairly similar for both thoughput losses and internal backscatter rejection. The major differences in performance is in the external backscatter (light reflected from the link fiber) rejection, where the grating and prism have fundamentally different and better performance than the dichroic mirror. If a bulk bidirectional coupler were to be developed, it would seem preferrable, therefore, to follow the prism approach. However, for a fiber integrated device, it is difficult to imagine a reasonable implementation of either the prism or grating coupler, while the dichroic mirror, with its wide directional separation of the two wavelengths, can be used in a fiber format without bulk lenses.

2.2 Incident Angle Effects in Multilayer Coatings

2.2.1 Dichroic Angle Dependence

One concern with the fiber dichroic coupler is that the large incident cone angle involved, $\pm 10^{o}$ in the fiber, will cause a degradation of the performance of the dichroic coating. Since

TABLE 2-6

THEORETICAL STUDY - RESULTS SUMMARY

(RANK OF COUPLER TYPE VS. OPTICAL PARAMETERS)

TYPE	PARAMETER		
	THROUGHPUT	INTERNAL BACKSCATTER	EXTERNAL BACKSCATTER REJECTION
GRATING	3	3	2
PRISM	1	2	1
DICHROIC	2	1	3

the fiber dichroic approach uses intimate contact of the fibers for compactness, simplicity, and reduction of throughput loss, it is not possible to include collimation with this method. Results of a preliminary experiment to determine the angular sensitivity of a standard dichroic coating (OCLI blue dichroic) are shown in Figure 2.9. For this test the light was collimated and the angle of incidence of the light beam to the dichroic surface changed from 30° to 60°, which corresponds to an internal angle of incidence in the glass of 19°to 35°. These angles are not the same as the incident angle for the fiber beamsplitter cut at 45°, which must accomodate an angular range of 35° to 55°, but the effects are similar. From the graph it can be seen that the transition region shifts about .1 μm as the incident angle changes from 30° to 60° or from 19 to 35° internally. In addition, other features of the patterns do not overlap, so that averaging over the angular range should give a smoother curve, without the extremes of height or depth and with a longer, less steep, transition region.

2.2.2 Dichroic Cone Angle Dependence

A second experiment was performed with another similar bulk dichroic (OCLI red dichroic) using several cone angles: N.A. =.25 (±15°), N.A. =.125 (±7.5°), and collimated light. The results for 0° incidence are shown in Figure 2-10. Clearly,

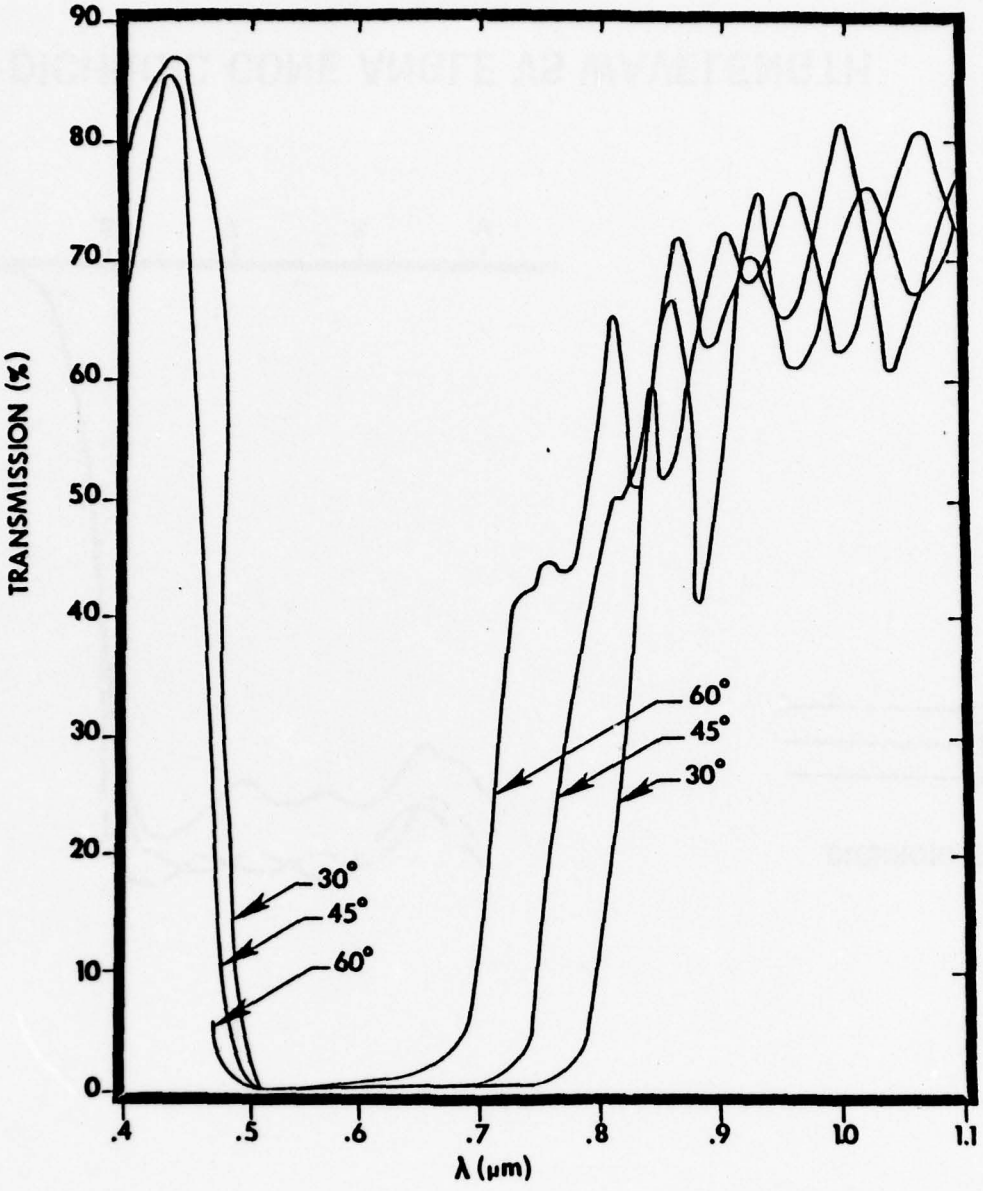

DICHROIC FILTER 30°,45° AND 60° ANGLE OF INCIDENCE

Figure 2-9

302 12073

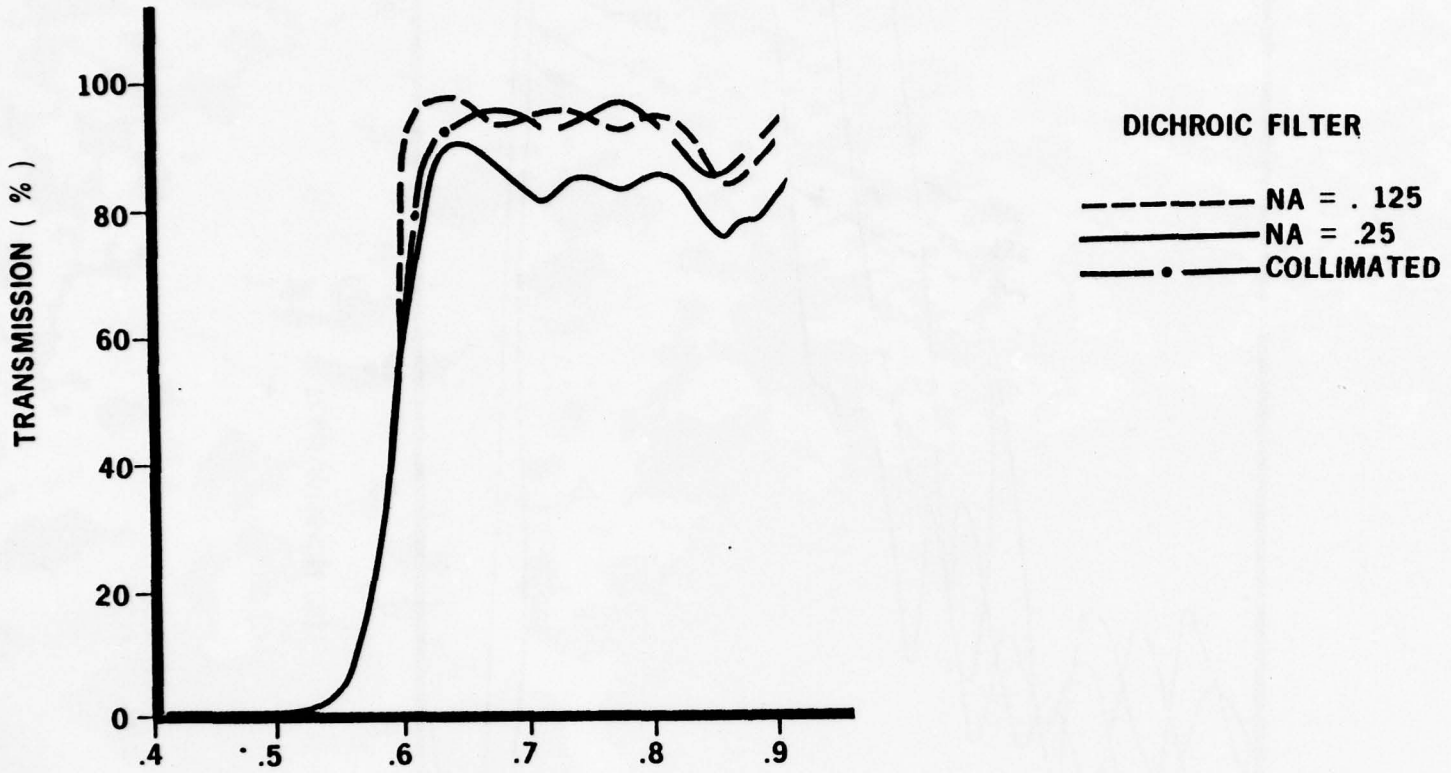

DICHROIC CONE ANGLE VS WAVELENGTH

Figure 2-10

for this case there is very little effect on the performance of the dichroic coating, and thus the extent of the deterioration due to the finite cone angle depends not only on the width of the cone angle, but also on the angle of incidence. This can be partly explained by examining a model using a single layer dielectric film for simplicity. Referring to Figure 2-11, we can write the phase difference ϕ between reflected rays 1 and 2 as:

$$\phi = \frac{2\pi}{\lambda} [2dn_2 \cos \theta_2]$$

where θ_2 is the angle in the dielectric, d is the layer thickness and n_2 the index of refraction. Differentiating, we obtain the dependence of the change in ϕ on a spread in angle θ_2 or

$$\frac{d\phi}{d\theta_2} = \left| \frac{4\pi d}{\lambda} \sin \theta_2 \right|$$

Since sin θ increases with θ, cone angle effects are more important as the angle of incidence increases. For example, at $\theta_1 = 0$, Sin $\theta_2 = 0$ while Sin $\theta_2 \simeq .5$ for $\theta_1 = 45^o$ and $n_2/n_1 = 1.5$.

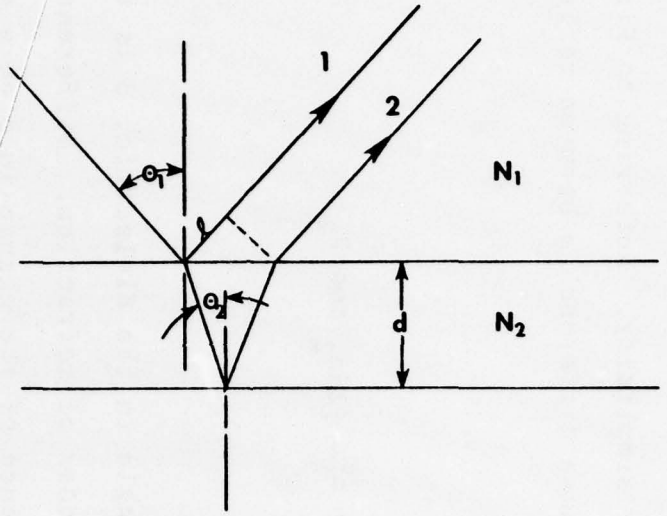

REFRACTION & REFLECTION OF A SINGLE LAYER FILM

Figure 2-11

Another effect that leads to less degradation at 0^{o} incidence is the symmetry of the path length for cone angles centered on 0^{o}. Thus, the transmission at $+10^{o}$ is the same as at -10^{o}, and the effective angular cone is one-half the angular spread for $45^{o} \pm 10^{o}$ incidence.

A third measurement of angle effects was made using a witness, or test, sample of glass from a dichroic coating run made by Corion Instrument Co. in the process of coating our beam-splitters. This dichroic coating is designed for 45^{o} incidence from and into a glass medium, and thus is identical to the siutation in the original fiber dichroic couplers. As shown in Figure 2-12, the experiment requires two 45^{o} glass prisms for the incident and exiting light beams.

The results obtained using the witness sample for three different cone angles (collimated, N.A. = .124, and N.A. = .25) are shown in Figure 2-13. As predicted from the measurements of Figure 2-9, there is a general loss of resolution for the largest N.A. The transition region width increases to 2500Å for N.A.=.25 from 1300Å for collimated light. Also, the maximum transmission has decreased from about 90% to 80%, while the minimum transmission has increased from 15% to 20%. This degradation in performance with cone angle is lessened by decreasing the incident angle to 25^{o} as opposed to 45^{o} in the original fiber dichorics.

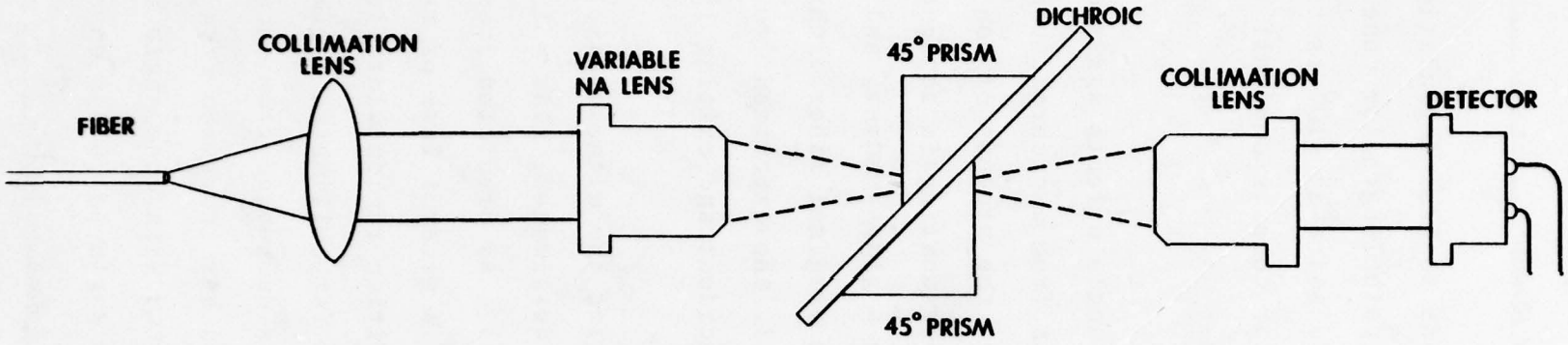

DICHROIC WITNESS SAMPLE EXPERIMENTAL STATION

Figure 2-12

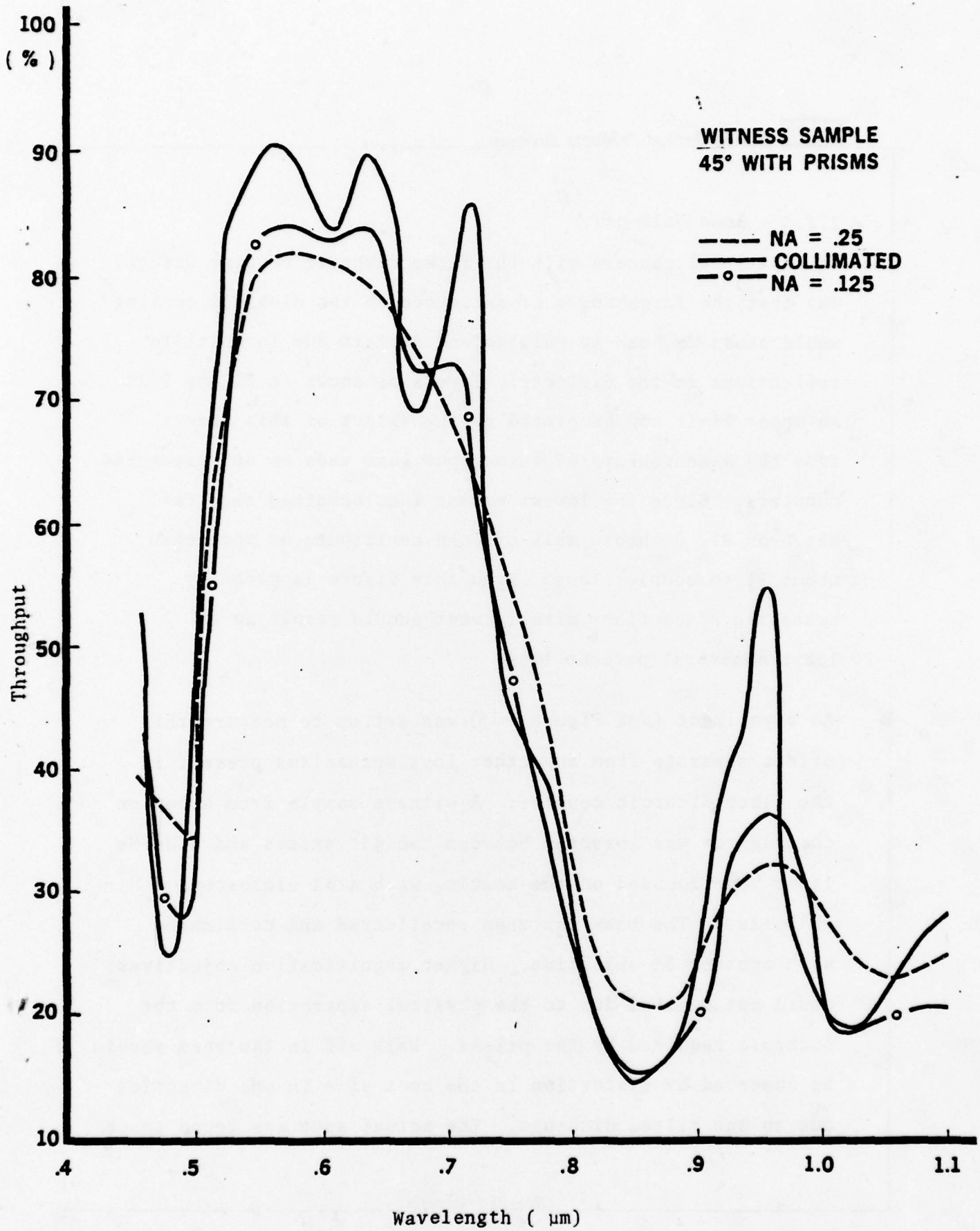

Figure 2-13

302 12034

2.2.3 Beam Walk-off

An additional concern with the fiber dichroic coupler design, was that the large angle of incidence on the dichroic coating would cause the beam to enlarge and distort due to multiple reflections in the dielectric layers as shown in Figure 2-14. An upper limit can be placed on the extent of this effect from the measurements of throughput loss made on our assembled couplers. Since the lowest excess loss obtained thus far has been 9%, dichroic walk-off can contribute no more than about 9% to coupler loss. Even this figure is probably excessive since fiber misalignment should result in at least a several percent loss.

An experiment (see Figure 2-14) was set up to measure this effect separate from any other loss mechanisms present in the fiber dichroic coupler. A witness sample from a Corion coating run was inserted between two 45° prisms and a He-Ne laser beam focused on the coating with a 5X microscope objective. The beam was then recollected and collimated with another 5X objective. Higher magnification objectives could not be used due to the physical separation from the dichroic required by the prisms. Walk off in the beam should be observed by distortion in the spot size in one direction due to the tilted dichroic. The actual spot was found to be

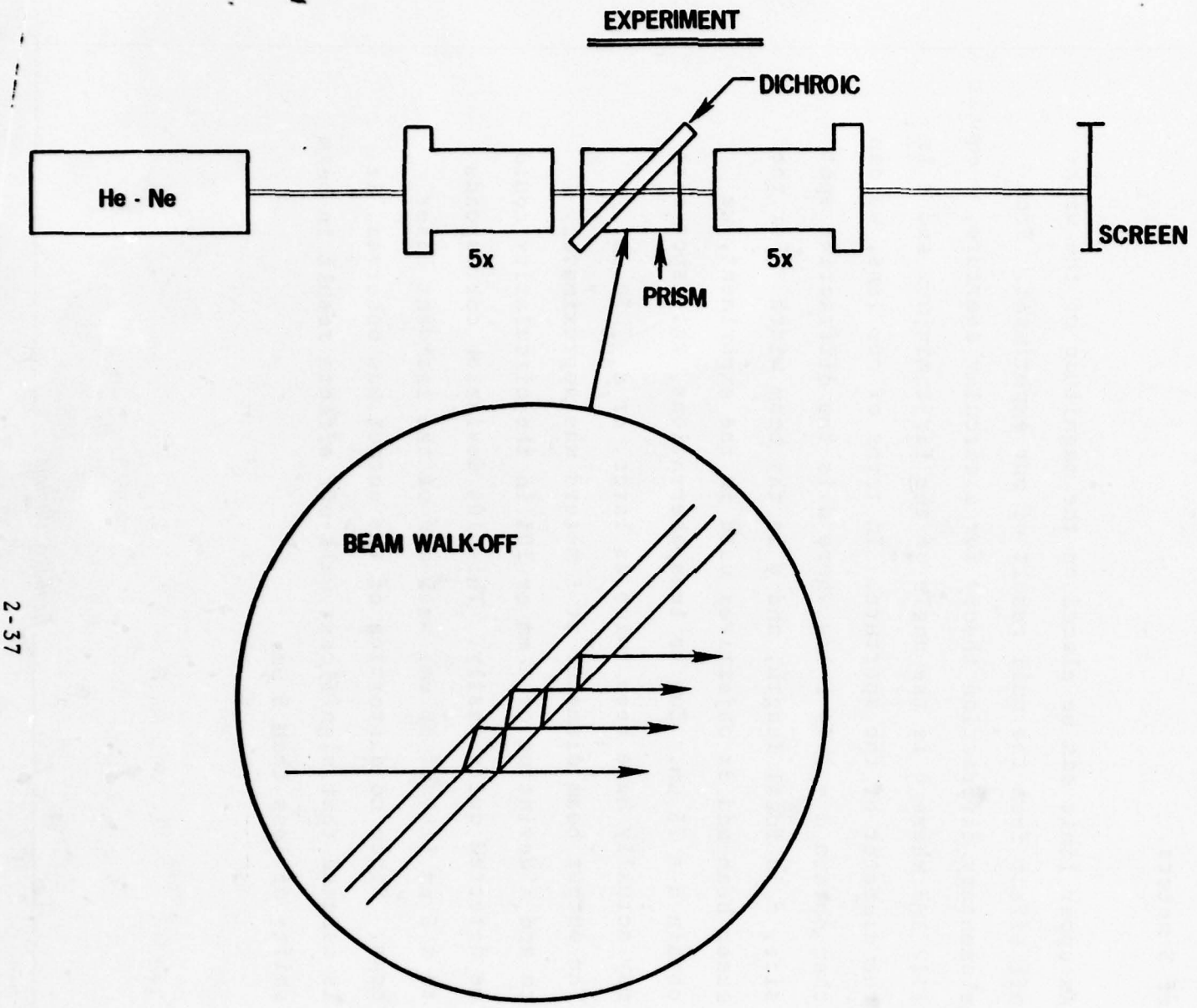

BEAM WALK-OFF EXPERIMENT

Figure 2-14

302 10258

uniformly circular in nature within the limits of our observational abilities and remained so for at least distances of 5 meters.

An upper limit can be placed on the magnitude of the walk-off effect from the null result of our experiment. From elementary diffraction theory for a circular aperture, θ equals $1.22\ \lambda/d$ where θ is the angle of the first minimum and d is the diameter of the aperture. In terms of our lens, we can then obtain $d = 2.44\ f\ \lambda/w$ where d is the diffraction spot size, f is focal length, and w is the beam width. For the laser beam and 5x objectives used in the experiment, we obtain $d = 25\ \mu m$. Due to lens aberrations, this spot size may actually have been twice as large, or $d_{act} \sim 50\ \mu m$. The output beam diameter at 5 meters was approximately 1 cm and a deviation of 1 mm or 10% in the circularity could be detected quite easily. This 10% deviation corresponds to a 5 μm (10% of 50 μm) walk-off of the incident laser beam. Since no distortion of the output was observed, it is assumed that significant walk-off effects result in beam shifts of less than 5 μm.

2.3 Alternate Approaches

2.3.1 The Biconical Taper

The third part of the technique study phase deals with alternate approaches to the fiber dichroic coupler. One possible candidate is the fused biconical taper shown in Figure 2-15. The device is contructed by bringing two fibers into intimate contact, twisting, and exerting tension, while heat is applied to fuse the fibers together. Coupling from one fiber to the other occurs by leakage from a descending taper in the input fiber. Since this coupler does not use wavelength discrimination, a minimum throughput loss of 6 dB is suffered for both couplers in a symmetrical duplex link (Figure 2-16). It is possible for transmission in one direction in an unsymmetrical link (Figure 2-17) to have a loss of less than 6 dB, but then the loss in the reverse direction will be proportionally larger than 6 dB, so that the total loss for both directions will be more than 12 dB. The minimum total loss situation occurs when both devices are symmetrical 3 dB couplers, and in that case the total loss for either direction is 6 dB. However, if the link loss is larger for one wavelength than the other, or if source optical power and detector sensitivity at the two wavelengths are different, then it may be advantageous to use the biconical taper approach in the unsymmetrical mode so as to yield equal bit error rate for both wavelengths.

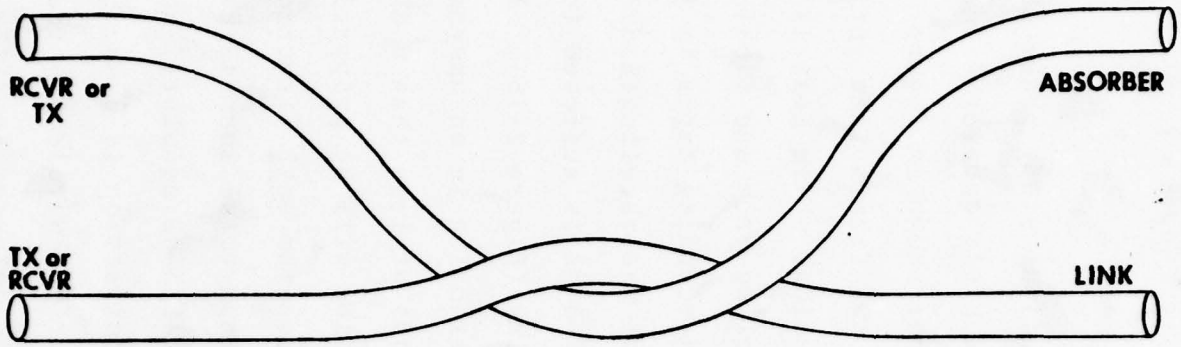

FUSED BICONICAL TAPER

Figure 2-15

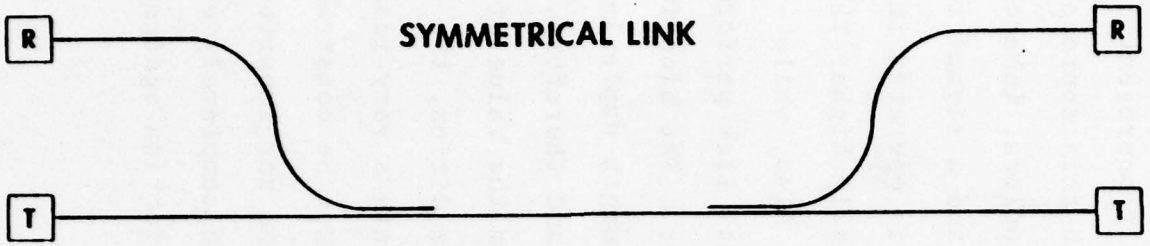

Figure 2-16

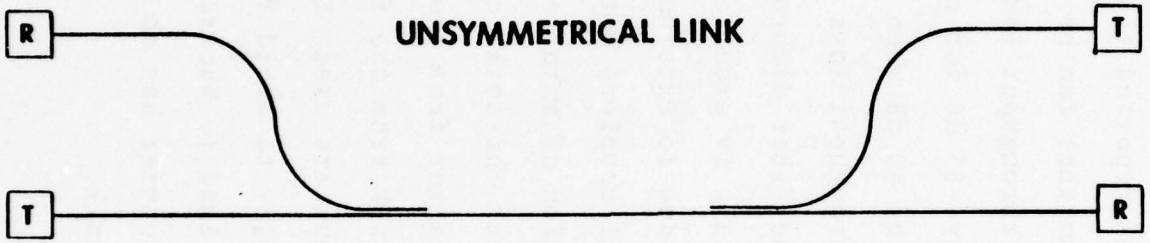

Figure 2-17

Results have been reported in the literature[1] on the construction of the biconical taper and its use in a duplex link. The results reported thus far probably represent close to the maximum that can be achieved with this approach: 7 dB total throughput loss for two couplers, inherent crosstalk down by -55 dB for one coupler, and a signal to crosstalk ratio of 40 dB when the coupler is operated in an actual link. The throughput loss is substantially higher than that predicted for the fiber dichroic coupler. Also, while -55 dB inherent crosstalk is excellent, the actual link performance is much lower due to external backscatter. The biconical taper coupler, and all couplers not using wavelength duplexing, have zero dB rejection of external crosstalk and therefore, it is impossible to lower the total crosstalk from the value of the external backscatter from the fiber. In addition, the -40 dB external crosstalk from the fiber represents a very ideal situation. All couplers used in the link must be constructed extremely carefully to avoid reflections and any imperfections that might lead to backscatter must be completely eliminated since this coupler has no inherent protection against external crosstalk.

[1] B. S. Kawasaki and K. O. Hill, Applied Optics 16, p. 1794 (1977).

2.3.2 Other Alternate Approaches

The drawbacks inherent with all non-wavelength discriminating couplers, such as the biconical taper, lead one to consider alternate approaches that do use wavelength division. One such approach is the dichroic coupler used with a Selfoc^{R} lens, such as shown in Figure 2-18, and reported on in the literature[2]. The losses for this coupler were 1.2 and 1.6 dB for two different wavelengths between .8 and .9 μm. Inherent crosstalk values of -40 to -50 dB were obtained, and there is external crosstalk rejection of at least 10 dB using this coupler. Although this is in effect a bulk coupler, the potential for miniaturization is very good.

There are others possible versions of bulk dichroic couplers, such as that shown in Figure 2-19, that use small lenses and seem to be capable of being made quite compact and possibly rugged. Results of experiments carried out using commerically purchased lenses to test the feasiblity of this approach are reported in Section 7.

[2] K. Kobayashi, R. Ishilcawa, K. Mincainura, and S. Sugimoto to be published.

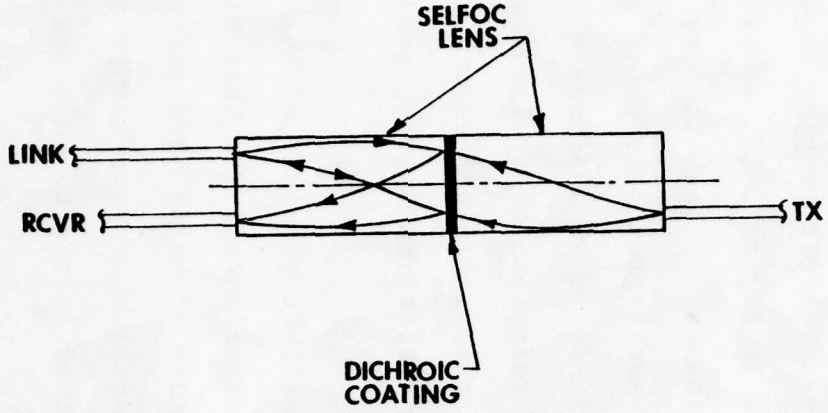

BI-DIRECTIONAL COUPLER USING SELFOC® LENSES

Figure 2-18

302 10330

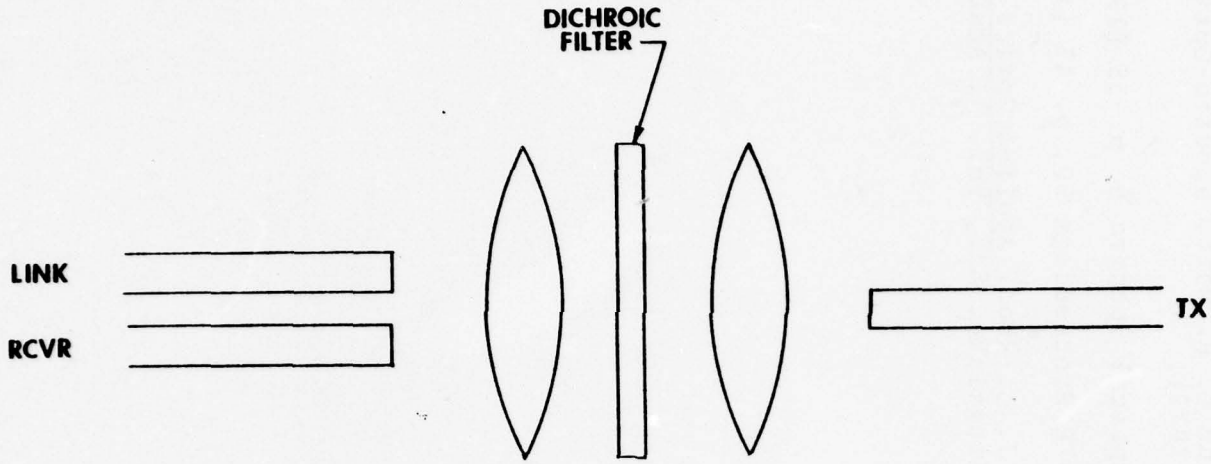

COMPACT BI-DIRECTIONAL COUPLER USING LENSES

Figure 2-19

302 10329

REFERENCES

1. H. E. Bennett and J. M. Bennett, Physics of Thin Films, G. Hass and R. Thun, Eds., Vol. 4, Academic Press, 1967.

2. J. S. Matteucci and L. P. Mott, Electro-Optical Design 4, p. 30 (1972).

3. G. F. Marshall Optical Spectra 6, p. 35 (1972).

4. J. M. Eastman, SPIE Proceedings 50, p. 43 (1974).

5. N. J. Kreidl and J. L. Rood, Applied Optics and Optical Engineering, R. Kingslake, Ed., Vol. 1, Academic Press, 1965.

3.0 FIBER DICHROIC COUPLER

The principal device development under this effort for implementing bi-directional transmission is the fiber dichroic coupler, illustrated in Figure 3-1. The basic construction technique and operation of the coupler is straightforward. A fiber of any all-glass type (that is, not plastic clad fused silica) is cut at an appropriate angle and both halves are polished. On one half a multilayer dielectric coating with dichroic properties is then evapaorated, so that the light of one wavelength range, e.g. .82-.86 μm, is transmitted and another appropriate range, 1.04-1.06 μm, is reflected. The two coupler halves are then reassembled using micropositioners and a transparent epoxy to form a permanent joint. Finally, a third port tap is added to the coupler in such a manner as to receive the light reflected from the dichroic. This tap may be either a detector or another fiber.

The construction and operation described above is a general procedure that has been modified and improved upon during the course of this effort. The original beamsplitter couplers were made by stripping the outer plastic jacket from a central portion of a length of fiber, and then placing the fiber in the center of an epoxy mold. The mold was filled with epoxy and then cured.

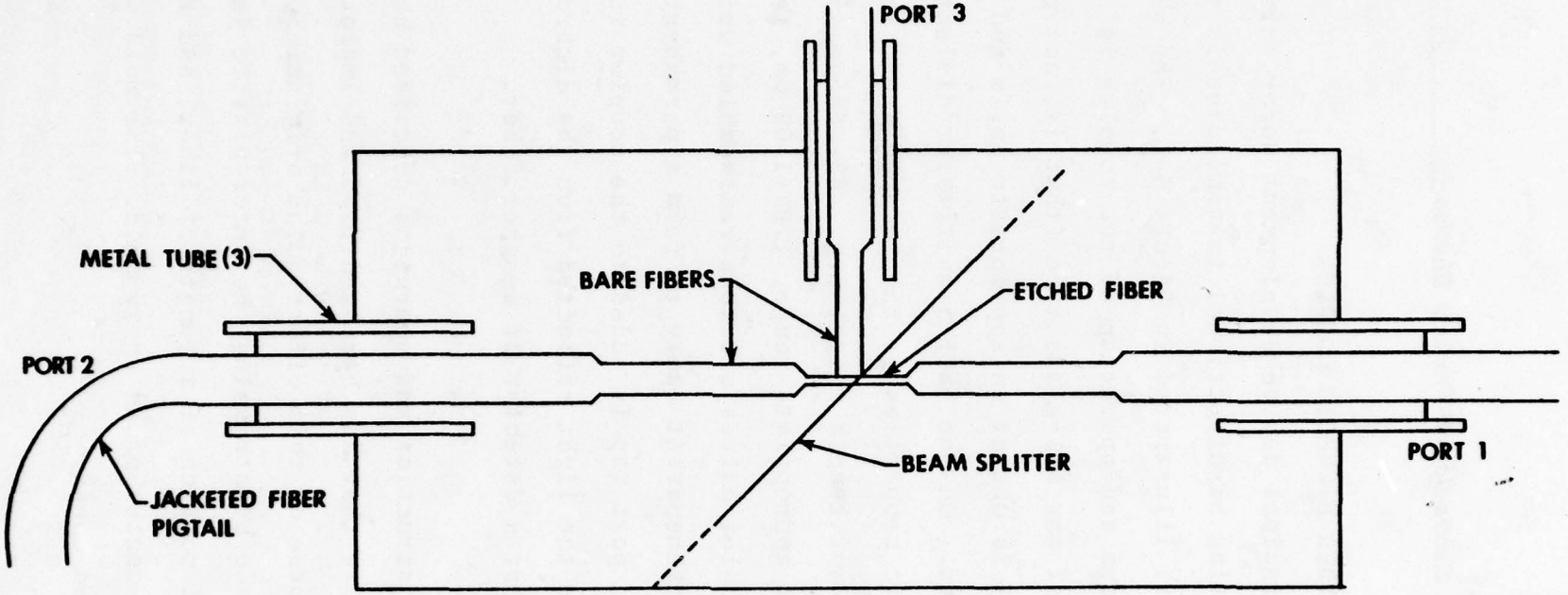

FIBER DICHROIC BEAM SPLITTER

302 10794

Figure 3-1

This solid block of epoxy containing the fiber was next cut in half at a 45° angle, coated, and then reassembled as previously described. The third port access was obtained by drilling or grinding out the epoxy down to the fiber.

While the above procedure yields a rugged, compact coupler, the device has a very limited temperature range due to the widely different thermal expansion coefficients of the fiber and the epoxy. Investigation of other beamsplitter type couplers revealed a failure mechanism caused by the large thermal expansion of the epoxy pulling the fibers apart, resulting in an air (or vacuum) gap forming between the two fibers. Since the fibers are at an angle of 45° in the 1st version of the coupler, an air gap causes total internal reflection of the light for a large angular range of the incident light with the result that most of the light is reflected regardless of wavelength. 'These failures occured for temperatures as low as 30° to 40°C.

A new technique for fabricating the couplers was developed to improve upon the observed temperature characteristics. In this procedure, each fiber half is "sandwiched" between two pieces of glass with a very thin coat of epoxy. Then both halves are individually ground and polished at an angle and assembled as shown in Figure 3-1. One of the halves can be

modified by using a short piece of glass to leave an opening for a third port fiber as shown in the figure. By eliminating most of the epoxy component, the temperature range of the couplers has been increased upward to 40 to 50°C, and additional modifications in the future should be able to extend this range further.

Another modification to the original beamsplitter design was the change in coupler angle from 45° to 25°, illustrated also in Figure 3-1. This modification was found to be necessary due to the inability to produce good dichroic coatings at 45° with unpolarized incident light. This problem, due mainly to Brewster's angle polarization effects, resulted in additional coatings on couplers ground and polished at 25°, as will be explained in more detail in the later sections. In the next section, the results obtained at 45° incidence will be described.

3.1 Phase I Couplers

3.1.1 Short Wave Pass Coatings

The two wavelength regions chosen for this system are .82 to .86 μm (using AlGaAs laser source) and 1.04 to 1.08 μm LED source (using a GaInAsP LED source). For a symmetrical bidirectional

link, two complimentary dichroic couplers are required: a short wave pass (SWP) that transmit .82 to .86 μm and reflects 1.04 to 1.08 μm and a long wave pass (LWP) that transmits 1.04 to 1.08 μm and reflects .82 to .86 μm.

Both SWP and LWP coatings for the Phase I effort (45° angle of incidence) were performed by Corion Corporation using a "cold" and therefore "soft" coating. A brief attempt was made to use a hot deposition in order to obtain a more durable, hard coating, but this effort met with failure due to either outgassing of the epoxy or the differential expansion coefficients of the epoxy and the fiber. The final coating that was obtained for Phase I was soft and slightly hygroscopic, but the adherence was adequate for assembly of the bidirectional coupler halves.

The transmission of the final Phase I SWP coating is shown in Figures 3-2 and 3-3 for the coating witness sample and for an assembled fiber dichroic coupler. The witness sample is a piece of glass placed in the evaporation chamber and coated along with the coupler halves. This glass reference can then be measured to test the applied coating. In this case, the testing must be done with the witness sample placed between two 45° glass prisms, as in Figure 3-3 , in order to simulate the performance of the coating in the fiber dichroic coupler. The difference in performance between the witness sample

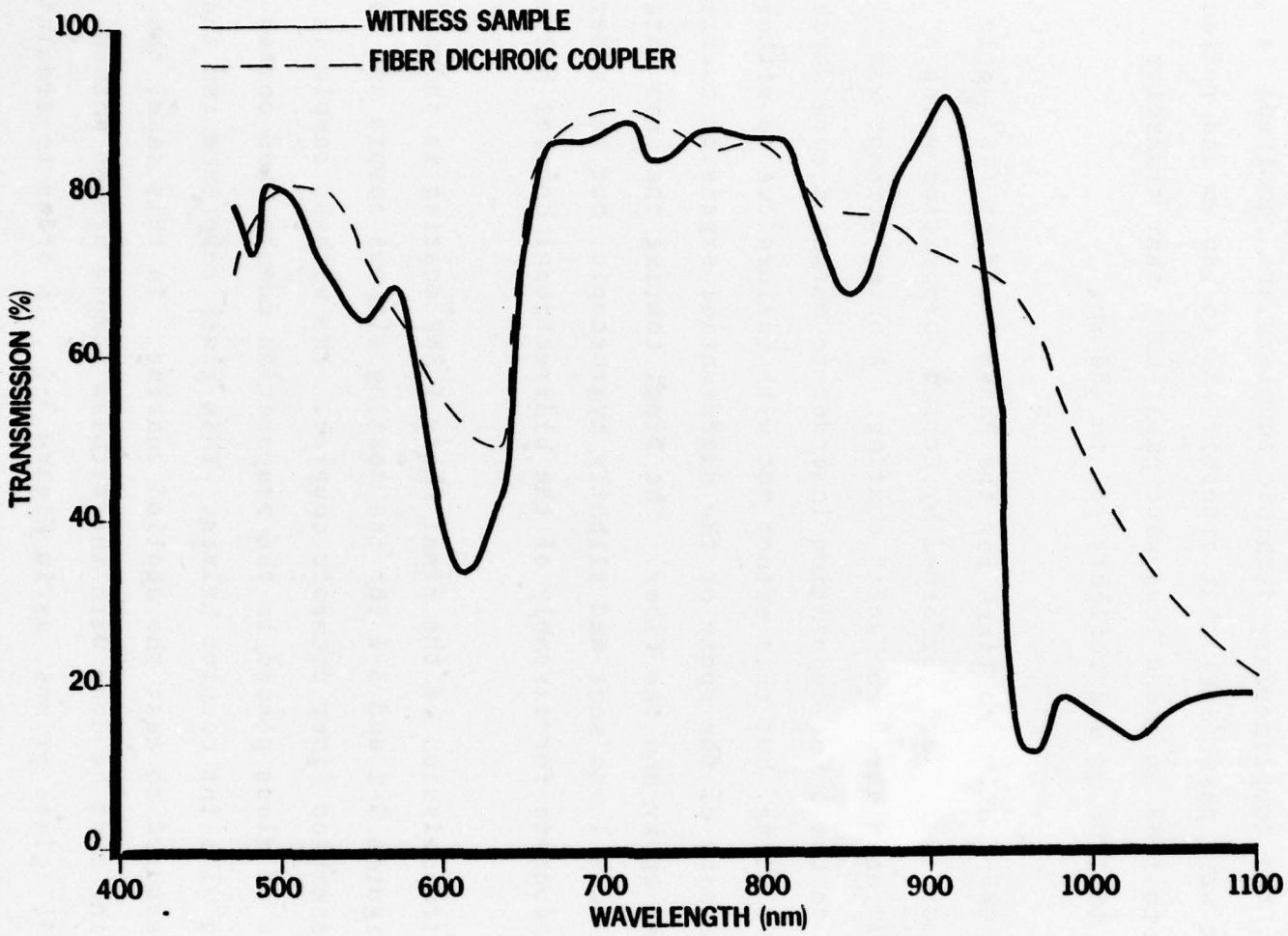

SWP COATING - 3rd COATING RUN

Figure 3-2

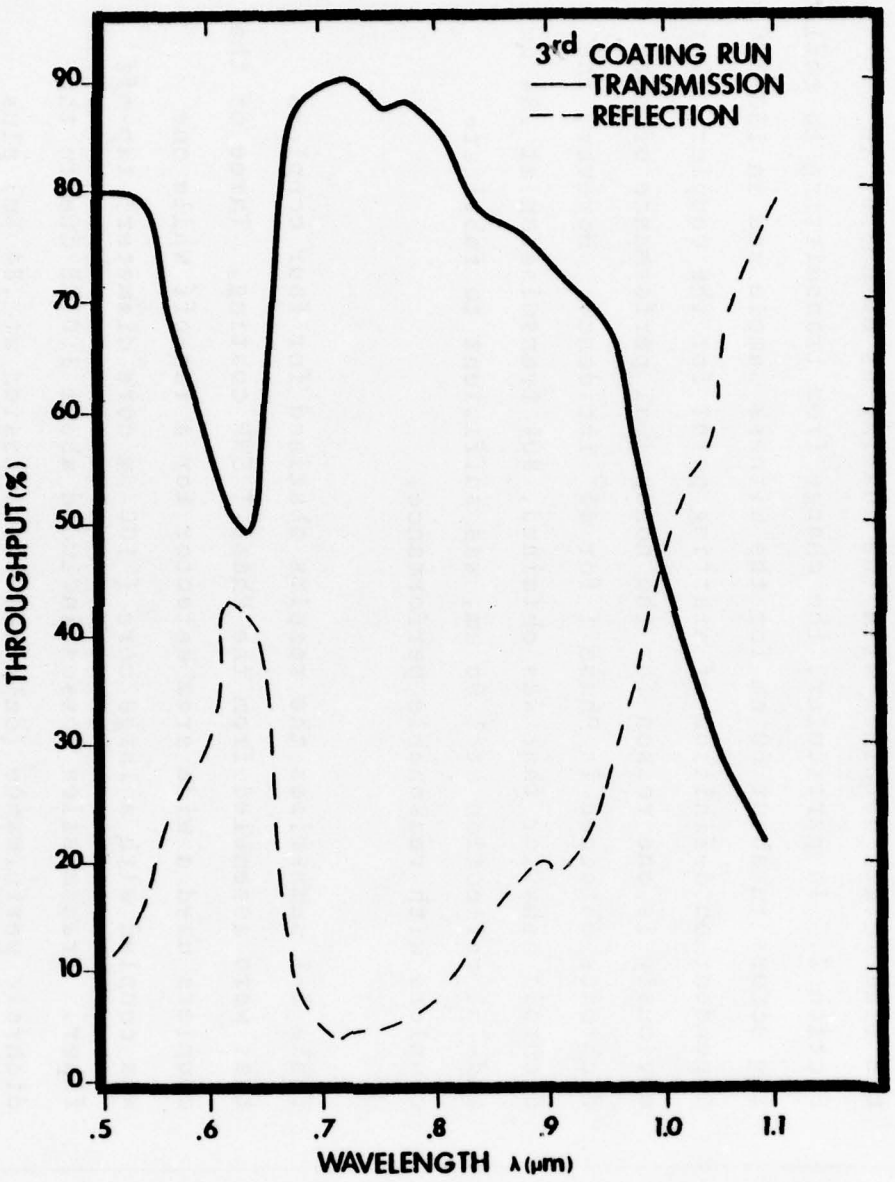

FIBER DICHROIC COUPLER - SWP

302 10255

Figure 3-3

and the coupler is due to the fact that the witness sample was measured with collimated light and the coupler used a .25 NA injection. The wide angle incidence causes a smoothing of the fine detail obtained with the coating as discussed in Section 2. In particular, the change from transmitting to reflecting occurs in about 60 nm for the witness sample and in 150-300 nm dependent on definition of starting point for the coupler. This obviously is one reason for the nonoptimal performance of the dichroics obtained in Phase I for 45^{o} incidence. However, the dichroic behavior that was obtained, 80% transmission at .84 μm and 75% reflection at 1.06 μm, was sufficient to fabricate couplers with reasonable performance.

Table 3-1 summarizes the results obatined for four couplers that were assembled from the Phase I SWP coating. Three of the couplers used a wide area detector for a tap-off while one was coupled with a large core (100 μm core diameter) tap-off fiber. Transmission losses included about 1.0 dB due to the dichroic performance (only 80% transmission at .84 μm) plus an additional loss due to misalignment, so that the total loss ranged from 1.1 to 3.0 dB. Reflection losses were slightly higher, 1.7 to 4.2 dB. The backscatter discrimination, which is the reflection coupling loss at .84 μm for the SWP couplers, average 10 dB. Thus the couplers provide an additional 10 dB of isolation from crosstalk that originates as light back-

Table 3-1

SWP COUPLERS

Coupler	Trans Loss (.84 μm)	Refl. Loss (1.06 μm)	Backscatter Discrim (.84 μm)
1*	1.9 dB	2.7 dB	10 dB
2*	3.0 dB	2.4 dB	10 dB
3*	1.1 dB	1.7 dB	9 dB
4	2.3 dB	4.2 dB	10^{+} dB

*Coupled with Detector Tap only

$^{+}$Includes Undetermined Tapoff Loss

scattered down the fiber.

3.1.2 Long Wave Pass Coatings

The transmission versus wavelength for the long wave pass witness sample is shown in Figure 3-4 and for an assmbled coupler in Figure 3-5. The dichroic characteristics of this coating are significantly poorer than for the SWP coating. In Table 3-2, the performance for two assembled couplers is summarized. These losses are significantly higher than for the SWP couplers, and the backscatter discrimination is only 7 dB.

The main difficulty with the LWP coating is the inability to generate a strong reflected wave, and this is directly related to the fact that the angle of incidence at 45^{o} is close to the Brewster's angle which is the angle for which the reflected wave of the in-plane polarization goes to zero for the coating materials used. In Figure 3-6 the transmission of the LWP witness sample is plotted for the two possible incident polarizations. For the out-of-plane polarization the dichroic performance is quite reasonable, ranging from over 90% transmission to 10% transmission. However, the in-plane polarization transmission never goes below 40%. Thus, for an unpolarized incident wave the transmission is the average of the two polarizations, and the transmission does not decrease to less than 30 or 40%.

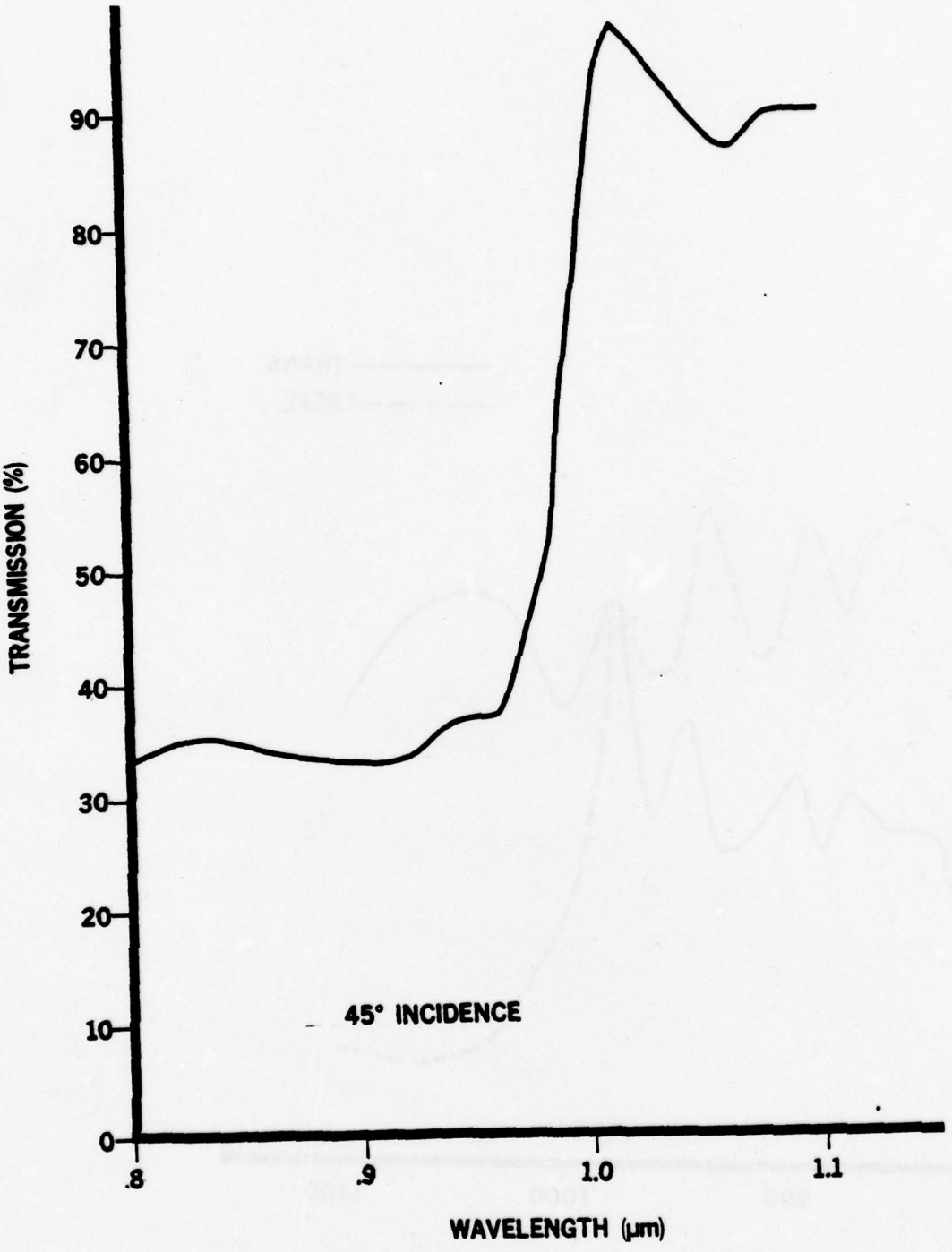

LWP DICHROIC COATING

Figure 3-4

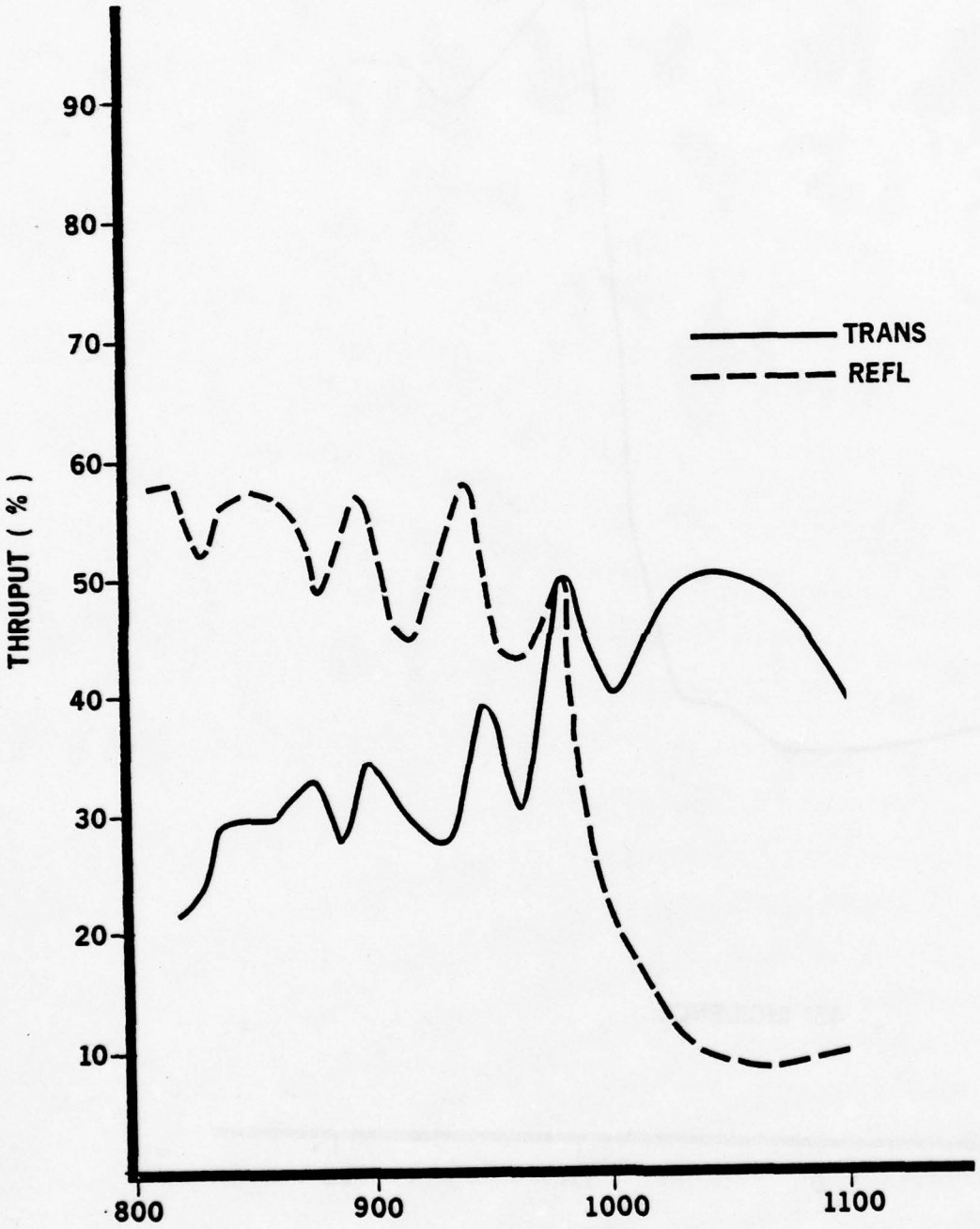

LWP - FDC

302 12058

Figure 3-5

Table 3-2

LWP Couplers

Coupler	Trans. Loss (1.06 μm)	Refl. Loss (.84 μm)	Backscatter Discrim (1.06 μm)
1*	2.5 dB	2.4 dB	7.4 dB
2	3 dB	3.6 dB	7+ dB

*Coupled with Detector Tap Only

+Includes Undetermined Tapoff Coupling Loss

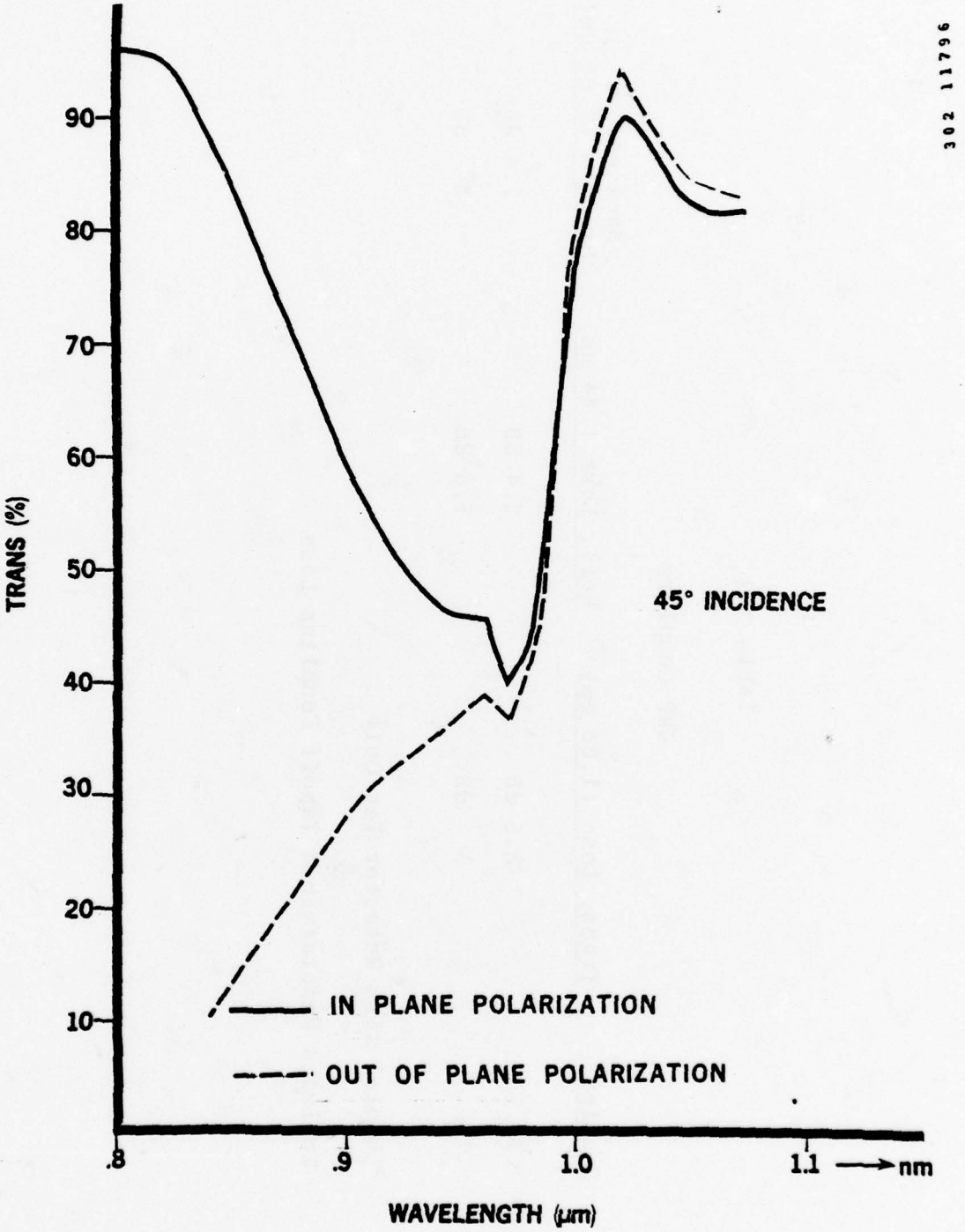

LWP DICHROIC

Figure 3-6

3.2 Phase II Couplers

In order to improve the performance of the dichroic coatings obtained under Phase I, the couplers were redesigned to use a 25° angle of incidence. This avoids Brewster's angle for the entire 25 ±10° incident light cone and gives the coating designers the ability to design for strong reflected wave.

Witness sample runs for the SWP coating, evaportated by OCLI, and the LWP dichroic, made by Corion Corp., are shown in Figure 3-7 and 3-8, respectively. For comparison purposes, it should be noted that the LWP graph includes an 8% Fresnel reflection loss encountered with the measurement prisms, while the SWP graph does not include this loss. Thus both coatings are quite similar in their results, showing over 90% transmission in the pass band and over 95% reflection in the reflection region.

Another problem arose, however, with the SWP coating evaporated by OCLI. In this case, the substrates (coupler halves including fibers) were heated to over 200°C during the deposition in order to obtain a hard coating. Apparently the dichroic layers did adhere very strongly to both the glass fiber and the thin coating of epoxy surrounding the fiber end face, but upon cooling the difference in the thermal

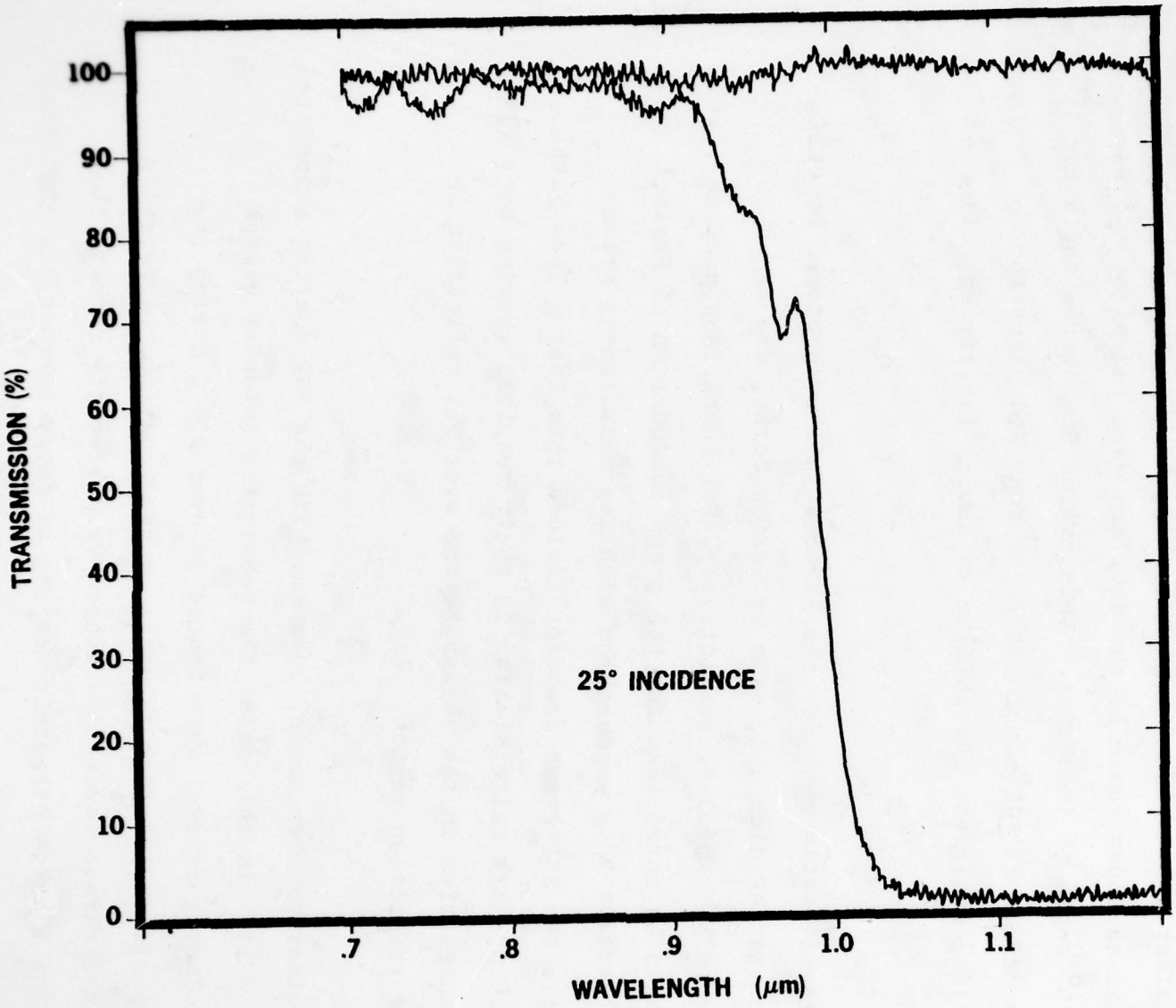

SWP DICHROIC COATING

302 11801

Figure 3-7

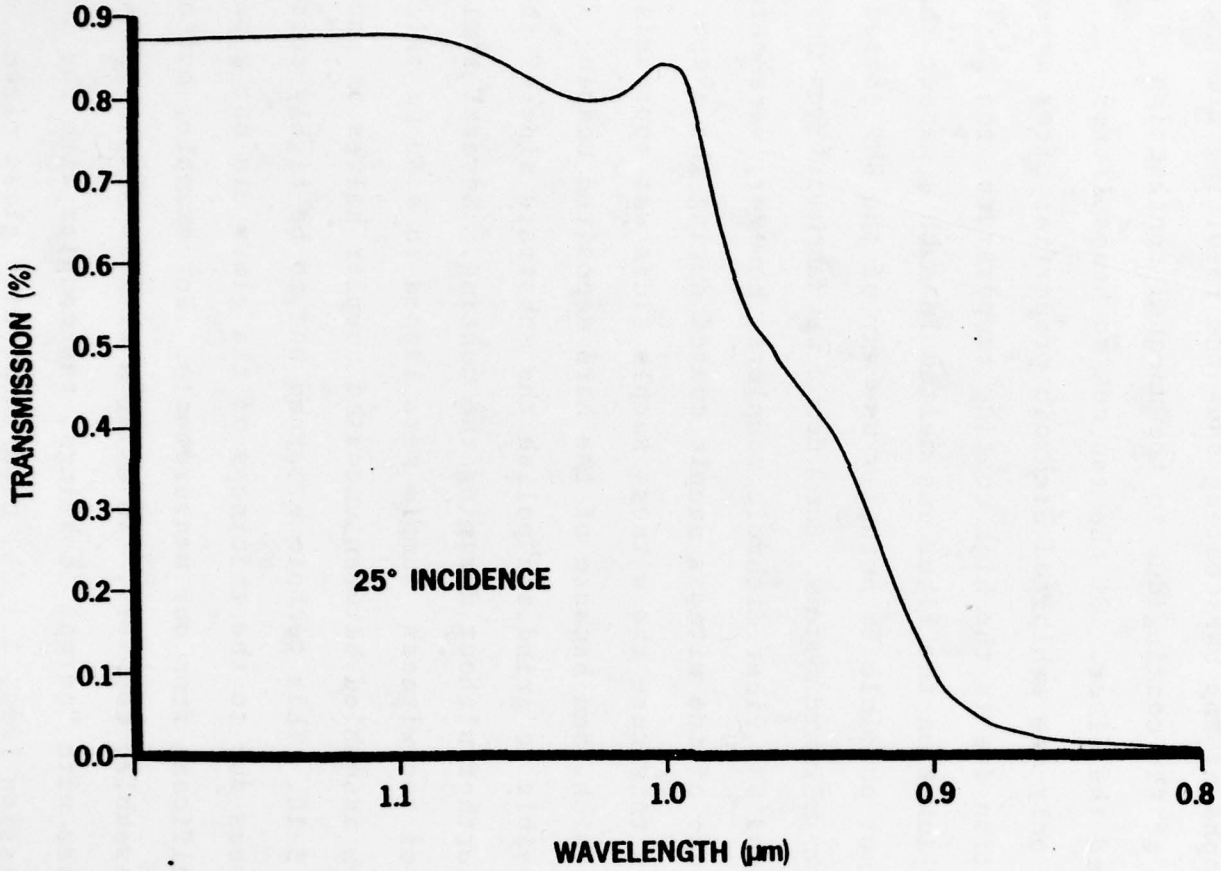

LWP DICHROIC COATING

Figure 3-8

expansion coefficients caused large stresses at the fiber epoxy interface. In Figure 3-9, a series of end face photographs of the SWP coating show the resulting flaking and peeling of the coating due to the unequal contraction of the epoxy and the fiber. Of the ten coated beamsplitter halves, only one exhibited dichroic properties after assembly. In addition due to the high coating temperature, the plastic hytrel jacket on the fiber was melted in such a manner that it was not possible to actually use any of the SWP coated halves in the two delivered systems. But a device was fabricated from this coating run. Good SWP fiber dichroic couplers, however, were obtained by making use of the witness sample coated during the evaporation run. In this case the witness sample glass was approxmiately 150 μm thick, and because of the hard deposited coating it was possible to grind and polish the substrate side of the glass further without damaging the coating. Several small pieces of the witness sample were lapped to a 50 μm thickness and then assembled between uncoated coupler halves as shown in Figure 3-10. This technique turned out to be highly successful and losses due to the thickness of the glass did not appear to be significant from our measurements. For example, out of five assembled couplers, two using a witness sample glass and three with "normal" coatings, the coupler with the lowest transmission loss, 1.1 dB, used the coated glass piece.

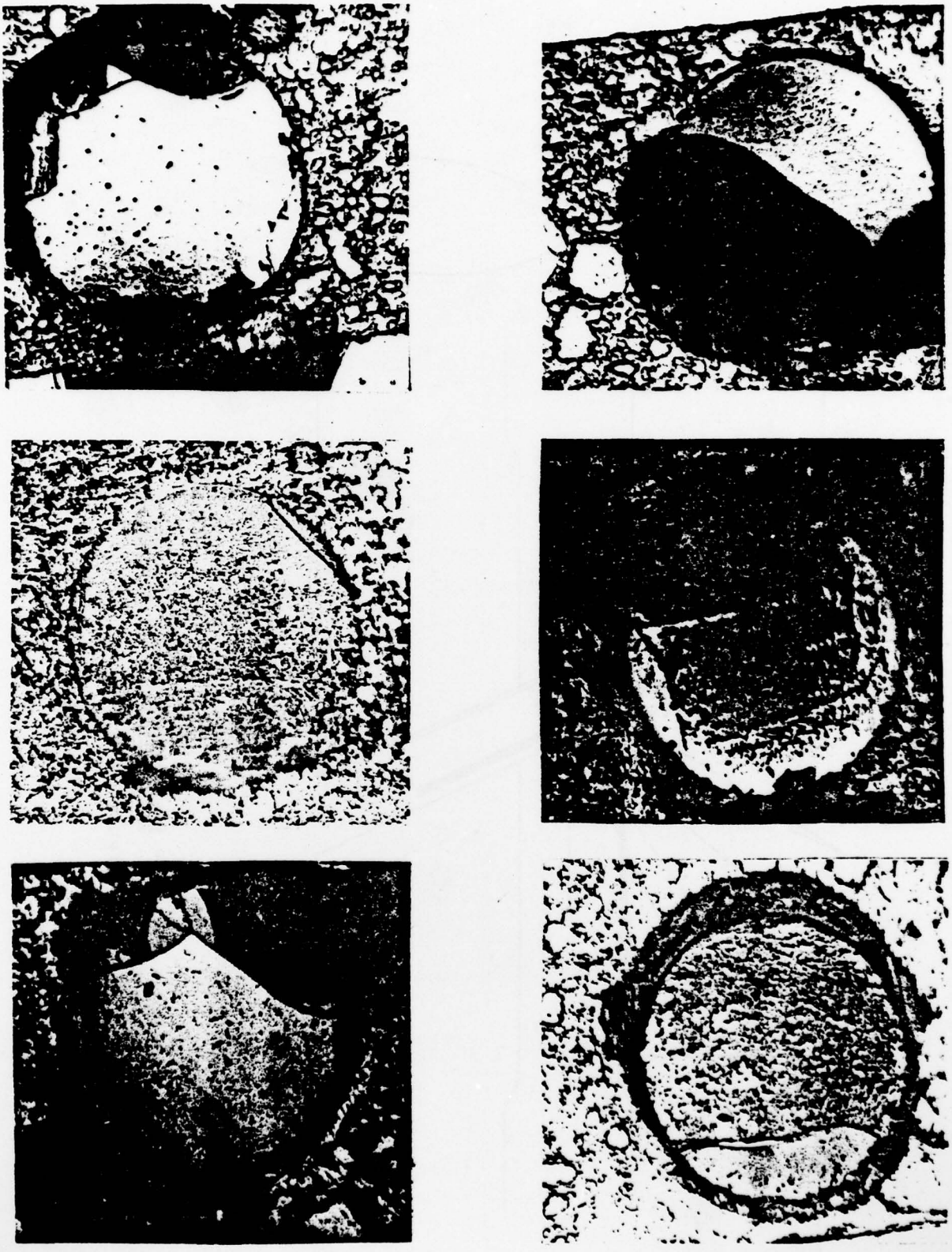

Figure 3-9.

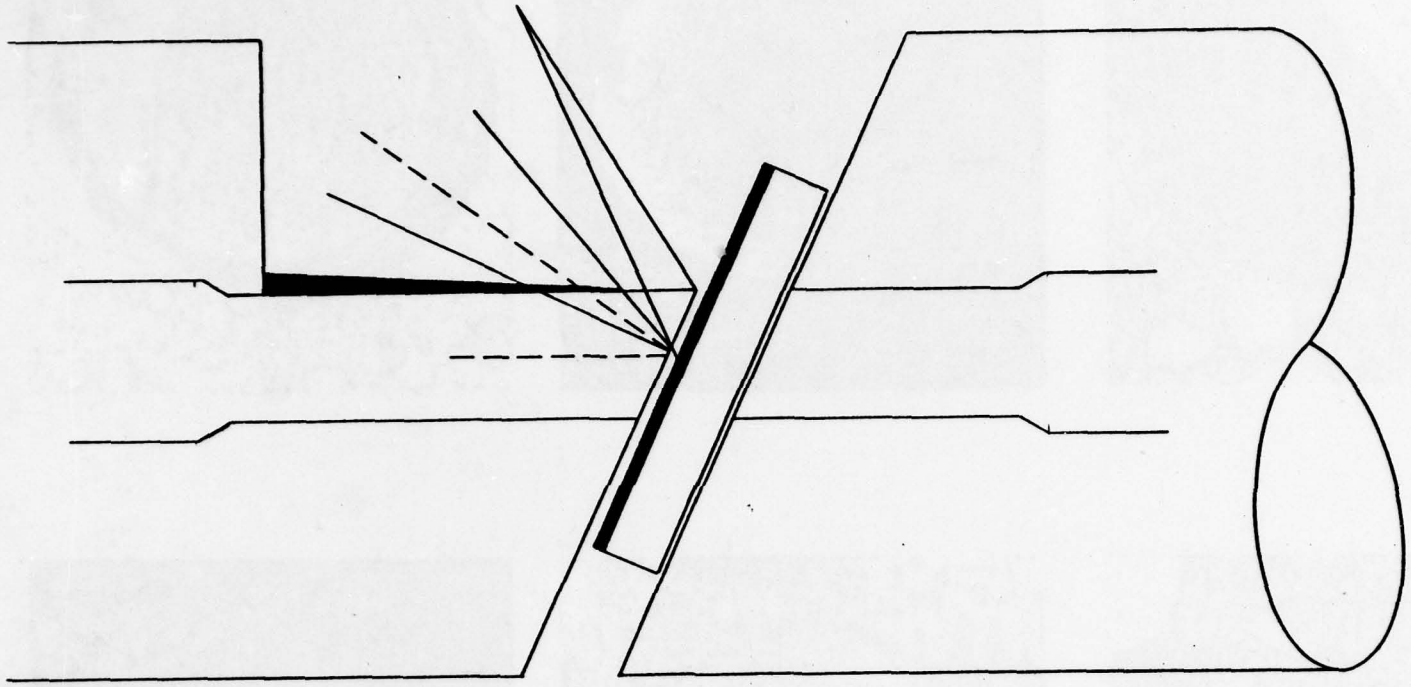

FDWC @ 25° INTERNAL INCIDENCE

Figure 3-10

302 11799

This technique would appear to be very important in improving the construction procedure for future couplers. Coated glass slides, which can then be diced into small pieces will greatly simplify fabrication time and cost for large coupler quantities. In addition, this procedure allows increased flexibility in coupler construction, since any fiber type may be used to make the coupler half followed by epoxying a standard glass dichroic to the face of the fiber. In the future it is likely that most couplers will be constructed in this manner.

The transmission as a function of wavelength for the SWP coupler (using a witness glass piece) and a LWP coupler are shown in Figures 3-11 and 3-12, respectively. The LWP couplers did not use the witness sample since the "cold" coatings from Corion adhered very well for the epoxying operation. In general, all the couplers have similar performance, and coupling technique improvements should eventually lead to lower losses.

A summary of the important results for the five couplers that were assembled are given in Table 3-3. The notation FDWC refers to a fiber dichroic coupler using a dichroic wafer as opposed to the standard fiber dichroic coupler (FDC). Transmission losses for four of the five couplers are less than

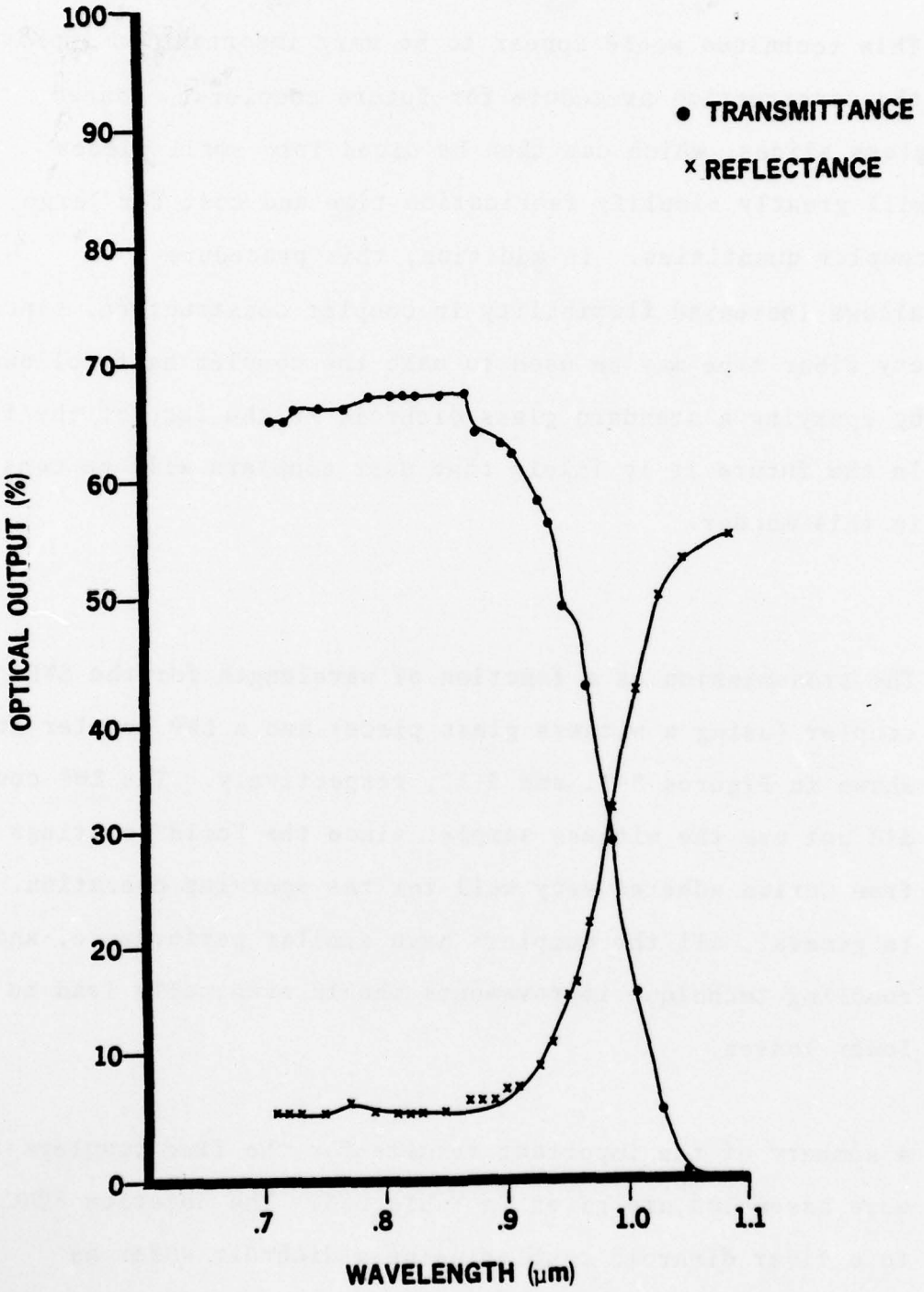

FDWC - SWP

Figure 3-11

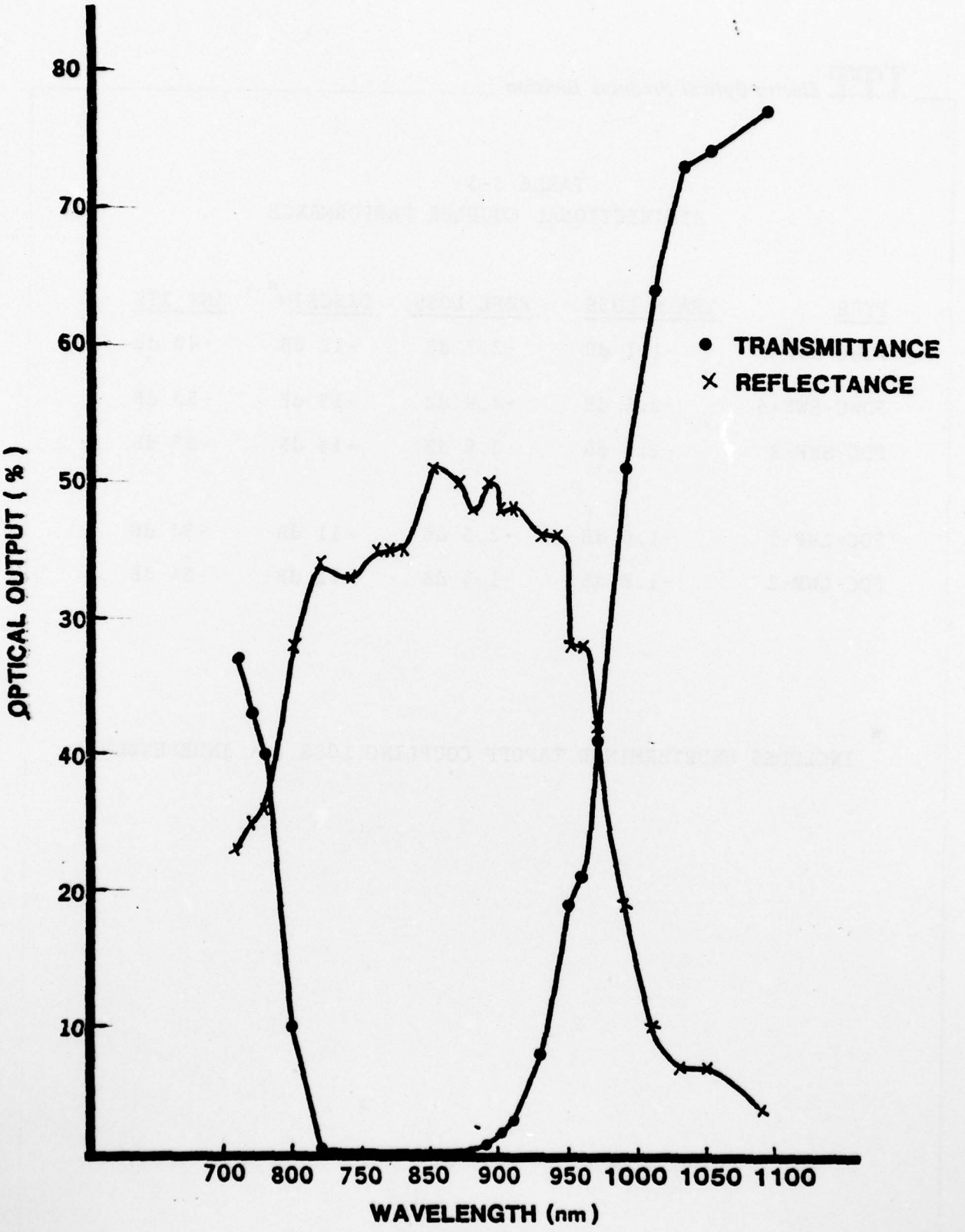

FDC-LWP-1

NA INJECTION = 0.243

302 12066

FIGURE 3-12

TABLE 3-3
BIDIRECTIONAL COUPLER PERFORMANCE

TYPE	TRANS LOSS	REFL LOSS	DISCRIM*	INT XTK
FDWC-SWP-5	-1.1 dB	-2.7 dB	-12 dB	-40 dB
FDWC-SWP-6	-2.5 dB	-4.9 dB	-15 dB	-53 dB
FDC-SWP-8	-1.6 dB	-3.9 dB	-13 dB	-33 dB
FDC-LWP-1	-1.6 dB	-2.3 dB	-11 dB	-34 dB
FDC-LWP-2	-1.8 dB	-1.4 dB	-11 dB	-34 dB

* INCLUDES UNDETERMINED TAPOFF COUPLING LOSS (λ INDEPENDENT)

1.8 dB, while reflection losses are somewhat higher, although still less than 2.7 dB for three of the five couplers. The reflected wave coupling was performed in the manner shown in Figure 3-13a, and some improvement might occur if the fiber was polished at an angle as in Figure 3-13b. The coupling for these two cases was computed previously in the Second Quarterly Report and the results are shown in Figure 3-14 for the two techniques. However, this calculation is for all fibers having 55 μm core, 125 μm o.d.
For the current couplers, the link and transmitter fibers are 55 μm core, 125 μm o.d., graded index, and the receiver tap-off fiber is 100 μm core, 140 μm o.d. step index in order to maximize the coupling. Thus, since the receiver fiber is step index and large, the coupling losses should be much lower than indicated in Figure 3-14. However, in the future it would be useful to attempt the coupling using the technique of Figure 3-13 (b) in order to maximize device performance.

The discrimination against backscattered light (coupler reflection loss at the transmission wavelength) ranges from 11 to 15 dB as opposed to the 7-10 dB obtained for the Phase I couplers. This simply reflects the higher quality of the newer coatings. Higher backscatter discrimination (over 20 dB for the couplers) can be obtained by interchanging the transmitter

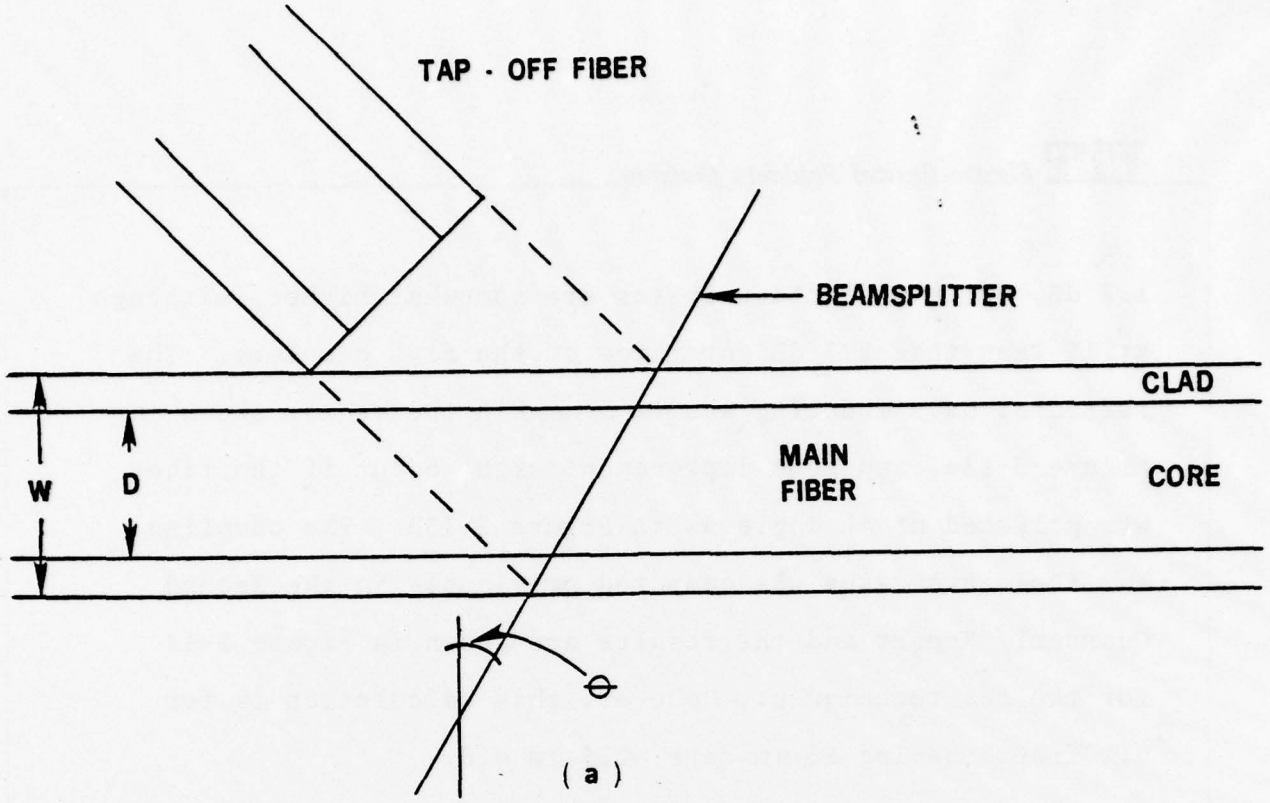

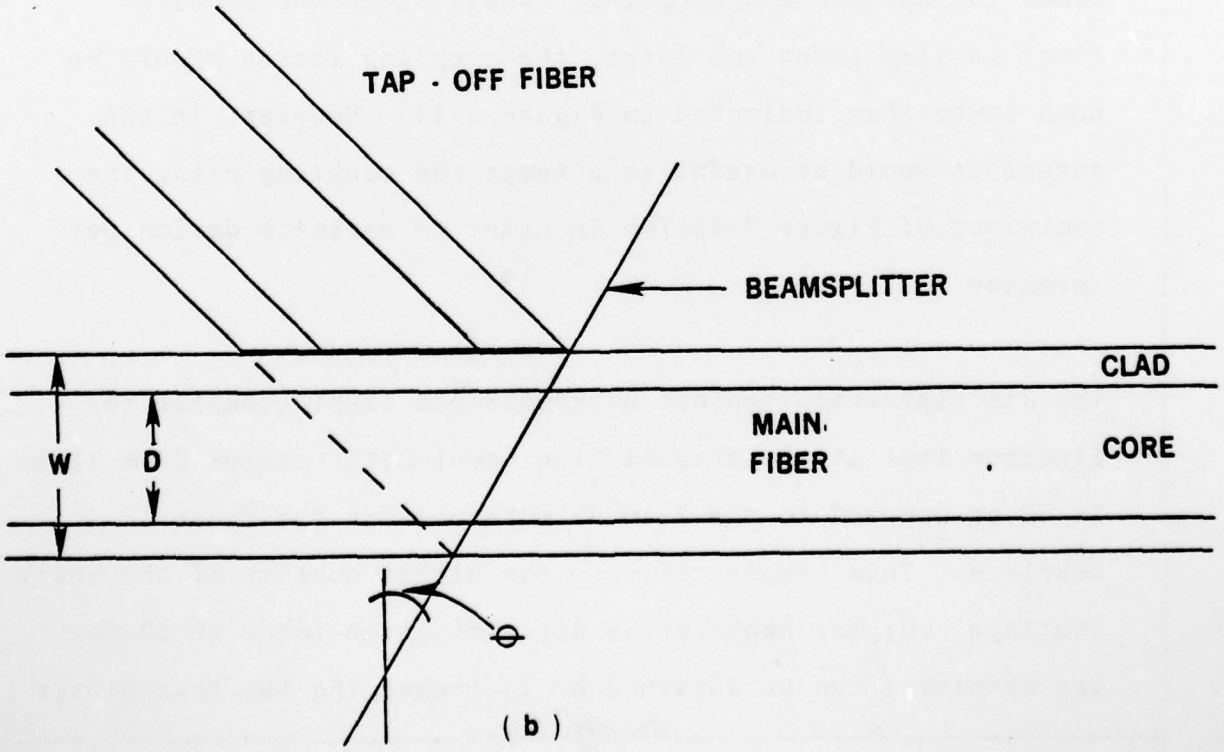

302 12063

Figure-3-13

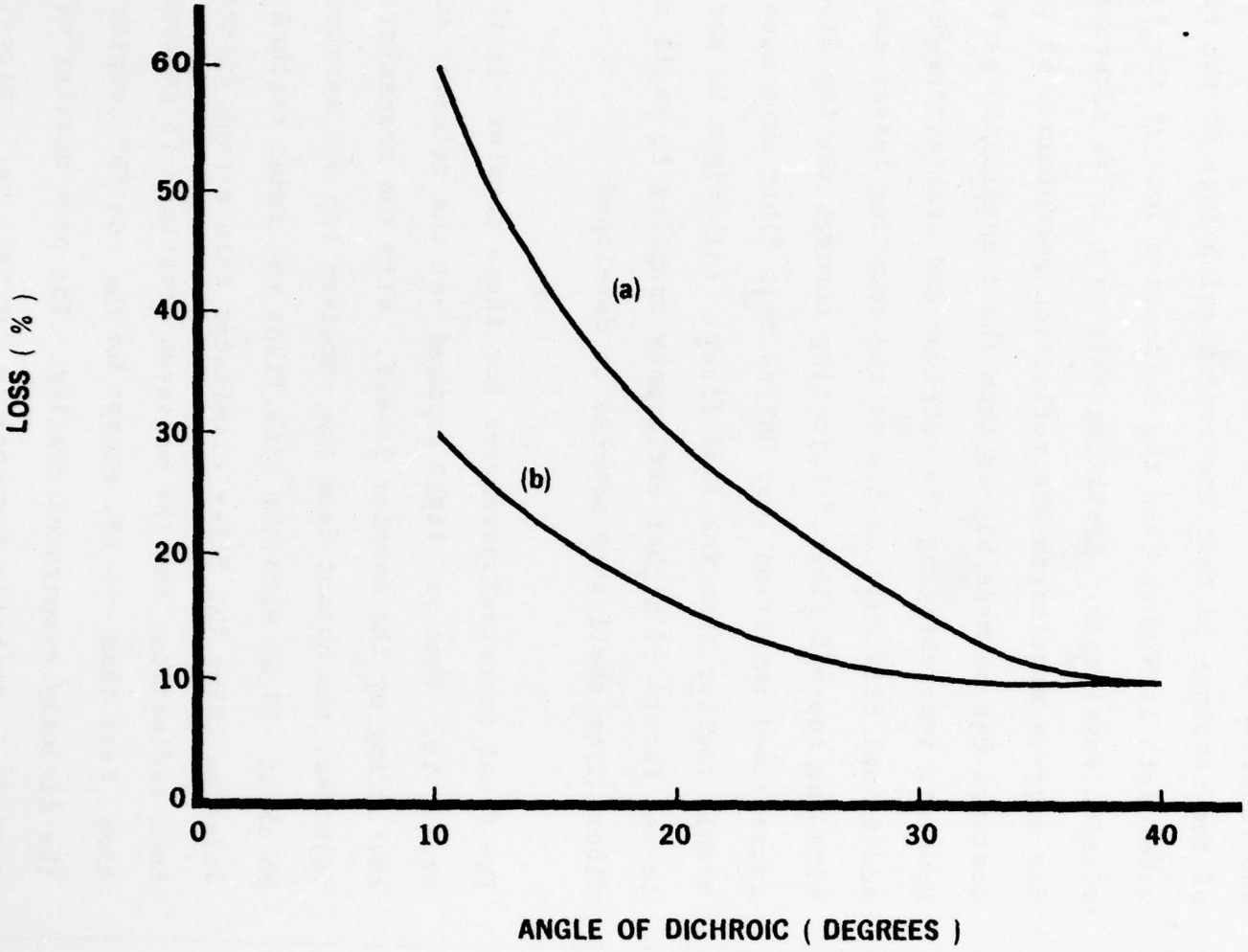

FIBER DICHROIC COUPLER

Figure 3-14

and receiver ports on the couplers. This is due to the nature of the coatings in that the transmission loss at the reflection wavelength is higher than the reflection loss at the transmission wavelength. Restating this fact in an alternate manner, for a given wavelength the reflection performance of the coatings can be made higher than the transmission performance. However, interchanging the receiver and transmitter would cause additional difficulties due to the coupling losses encountered with the tap-off fiber. Injecting through the tap fiber would cause added insertion loss unless this fiber were made considerably smaller than the link fiber. This might be accomplished in the future if higher efficiency coupling to small core fibers from small area sources is developed.

The final important parameter for these couplers is the internal crosstalk, that is, light captured at the receiver due to scattering by the coupler itself. With the transmitter fiber injected, the output from the receiver tap was measured to be about -30 dB with the link fiber not index matched. Index matching the fiber eliminates this strong discrete back reflection, and the measured crosstalk is generally then less than -40 dB, except for the one SWP coupler using the directly evaporated coating. The poor quality of this coating is probably responsible for this performance. One SWP coupler using the glass dichroic measured less than -50 dB crosstalk, and it should be possible to select couplers with

similar performance in the future. A complete summary of the coupler measurements is given in Table 3-4.

The fiber dichroic coupler can be made quite compact and rugged. The size of the coupler itself excluding pigtails is less than ¼" x ¼" x 1" long. To provide additional support, an inner aluminum package, 3/4" x 3/4 " x 1¼", was developed. Finally, this package was mounted in an external case about 2" x 2" x 3", in order to provide complete protection for the fiber leads during the handling and testing that was required. A photograph of this package is shown in Figure 3-15. Environmental tests have not been carried out on these devices, but they are designed to survive normal handling encountered in the laboratory.

Four of the five couplers that were assembled (FDWC-SWP-5, FDWC-SWP-6, FDC-LWP-1, and FDC-LWP-2) were used with transmitter and receiver modules and several kilometers of fiber in testing the system performance of these devices. Detailed measurements of crosstalk and BER were carried out and are reported in Section 6.0. The additional system components that were used are first described in Sections 4.0 and 5.0.

AD-A075 467 ITT ELECTRO-OPTICAL PRODUCTS DIV ROANOKE VA F/G 20/6
BIDIRECTIONAL COUPLER FOR FULL DUPLEX TRANSMISSION ON A SINGLE --ETC(U)
AUG 79 A R NELSON, G A GASPARIAN, G W BICKEL DAAB07-77-C-1798
UNCLASSIFIED CORADCOM-77-1798-F NL

2 OF 2
AD
A075467

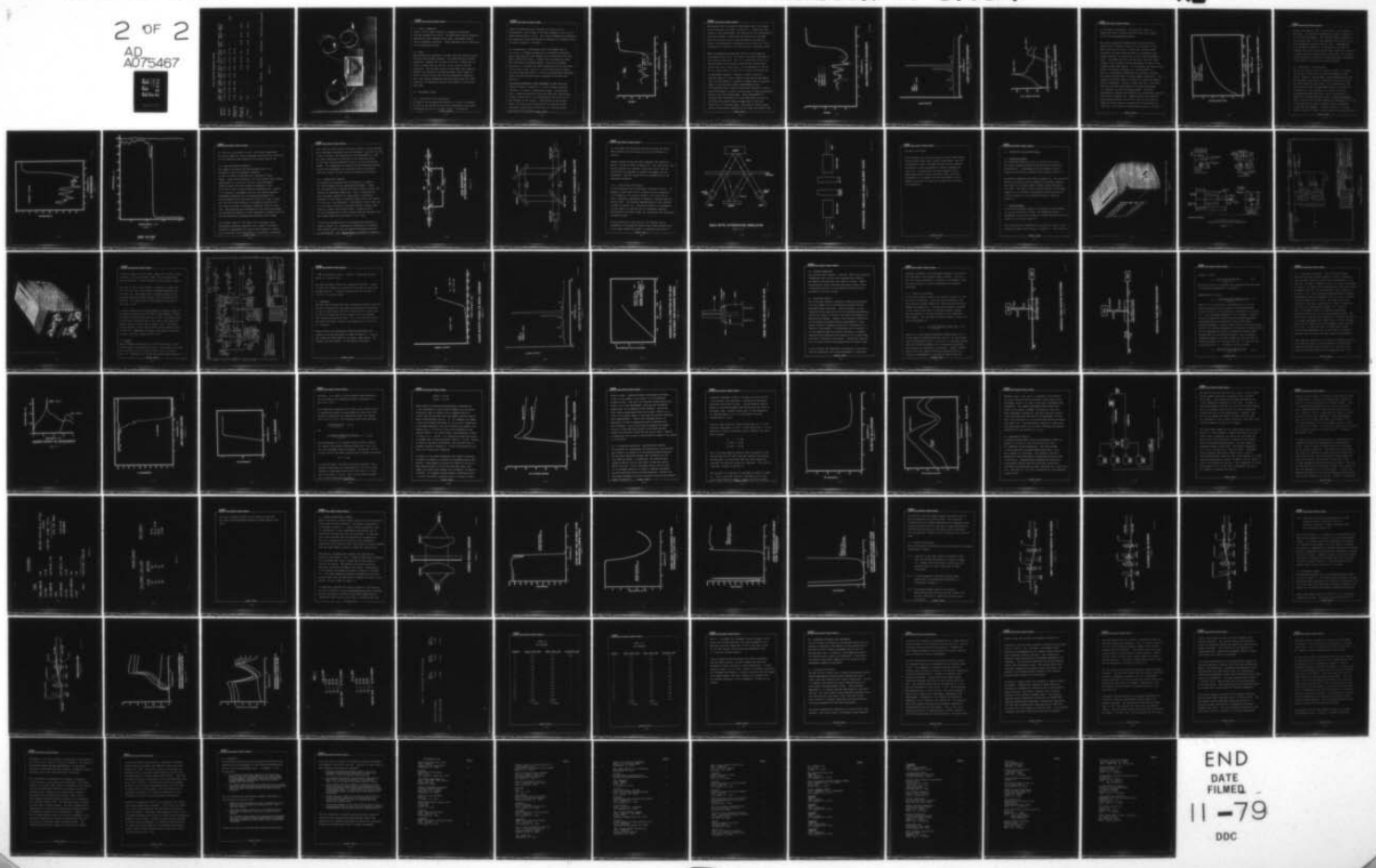

END
DATE FILMED
11-79
DDC

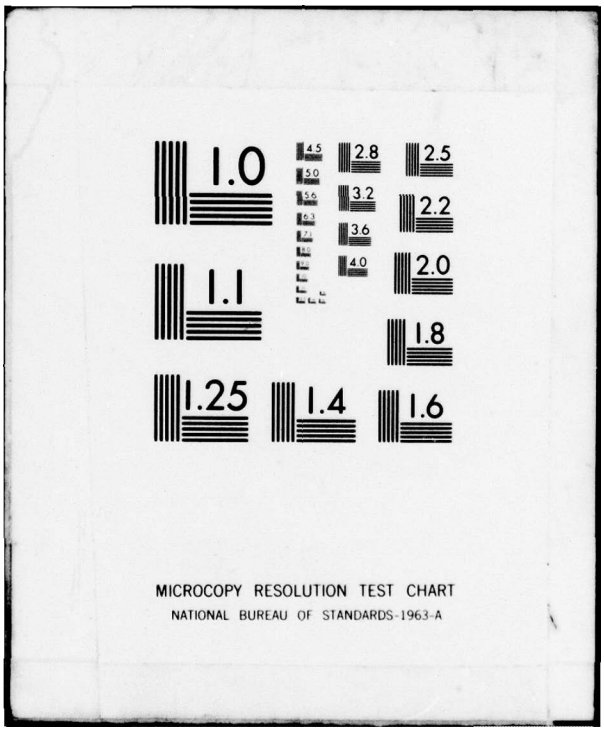
1.0
1.1
1.25
1.4
1.6
1.8
2.0
2.2
2.5
2.8
3.2
3.6
4.0
4.5
5.0
5.6
6.3
7.1
MICROCOPY RESOLUTION TEST CHART
NATIONAL BUREAU OF STANDARDS-1963-A

OPTICAL EVALUATION BIDIRECTIONAL COUPLERS

Coupler ID	850 nm $\alpha_T^{L\rightarrow XM}$	850 nm $\alpha_T^{XM\rightarrow L}$	850 nm $\alpha_R^{XM\rightarrow RC}$	850 nm $*\alpha_R^{XM\rightarrow RC}$	850 nm $\alpha_R^{L\rightarrow RC}$	1060 nm $\alpha_R^{L\rightarrow RC}$	1060 nm $\alpha_T^{L\rightarrow XM}$	1060 nm $\alpha_T^{XM\rightarrow L}$	1060 nm $\alpha_R^{XM\rightarrow RC}$	1060 nm $*\alpha_R^{XM\rightarrow RC}$	
FDWC SWP-5	-1.2 dB	-1.1 dB	-27 dB	-40 dB	-12 dB	-2.7 dB	-13 dB	---	---	---	
FDC-SWP-8	-1.5 dB	-1.6 dB	-29 dB	-33 dB	-13 dB	-3.9 dB	-11.2 dB	---	---	---	SPARE
[FDWC-SWP-6 SWP-6]	-1.4 dB	-2.5 dB	-38 dB	-53 dB	-15 dB	-4.9 dB	-13.5 dB	---	---	---	
[FDC-LWP-1 LWP-1]	-22 dB	---	---	---	-2.3 dB	-11.1 dB	-1 dB	-1.6 dB	-29 dB	<-34 dB	
FDC-LWP-2	-20 dB	---	---	---	-1.4 dB	-11 dB	-1.8 dB	-1.8 dB	-30 dB	<-34 dB	

Legend: L=Link XM=Transmitter RC=Receiver R=Reflectance T=Transmittance *=XTR=Crosstalk (Index Matched)

Table 3-4

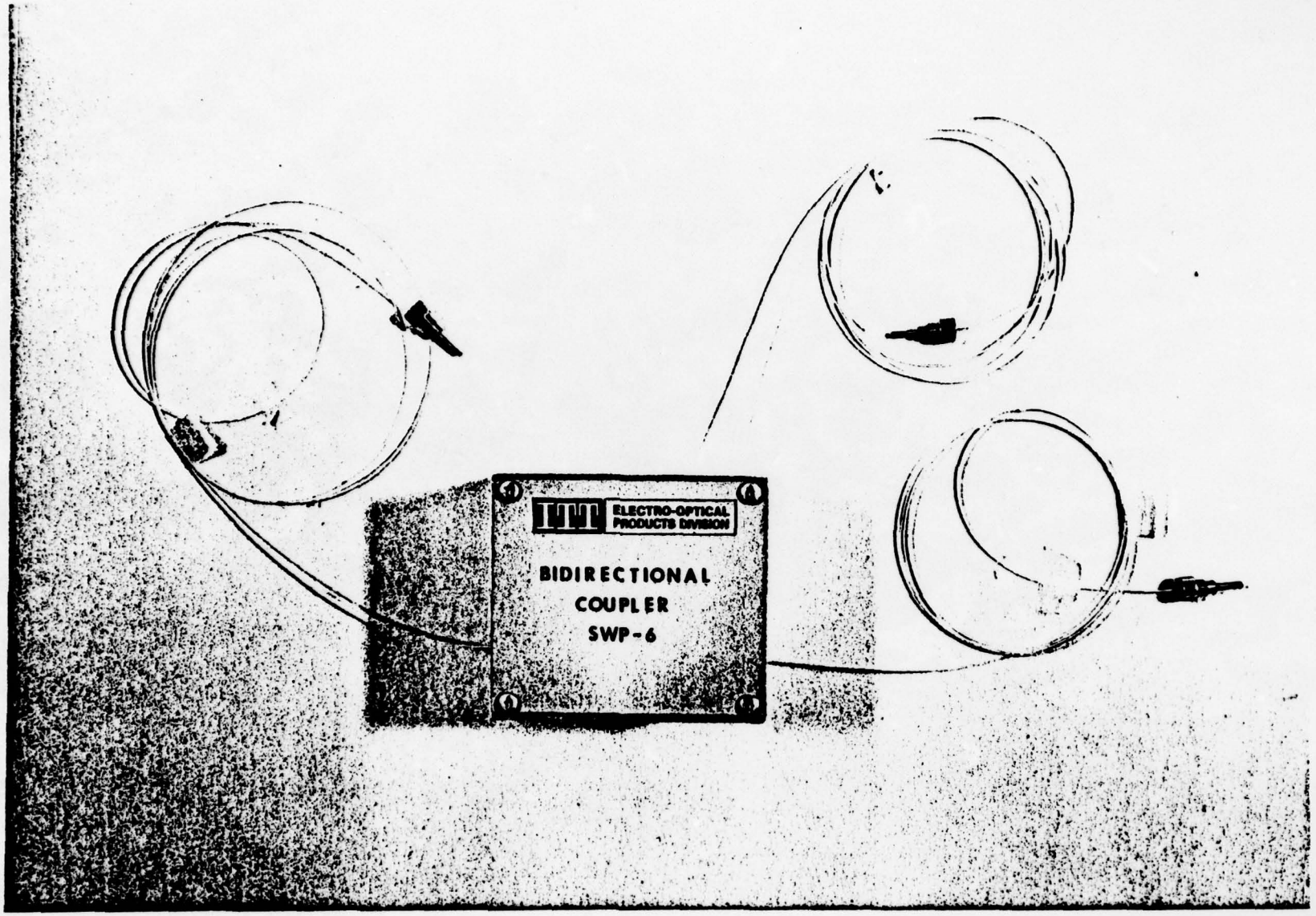
ITT
ELECTRO-OPTICAL
PRODUCTS DIVISION
BIDIRECTIONAL
COUPLER
SWP-6

Figure 3-15

4.0 Optical Components

As part of the coupler testing, a complete bidirectional link was assembled and tested. The additional optical components required for this testing are the fiber, wavelength filters and an attenuation simulator. These components will be described in the following sections.

4.1 Fiber

Approximately one kilometer of optical fiber has been delivered with the bidirectional couplers. The fiber has the following properties: nominal 125 μm clad, 59 μm core, 6 dB/km loss at .85 μm, 4 dB/km loss at 1.06 μm, .28 N.A. and 1.6 nsec/km dispersion. Two 250 meter spools of the fiber with connector ferrules are included in the one kilometer total length, in order to assist in the link test and attenuation simulation. Also, the couplers themselves have been made using this fiber, except for the third port tap-off fiber which is 100 μm core, step index.

4.2 Wavelength Filters

4.2.1 LWP Filter (1.06 μm Receiver)

As shown in the discussion of Section 6, a filter is required on the 1.06 μm receiver to block fiber backscatter and coupler scattering from the .84 μm laser source. An effective

method of performing this filtering is to use a III-IV semiconductor, such as GaAs or InP that transmits in the 1.06 μm region and absorbs at .84 μm. For a direct bandgap semi-conductor, the transition from transmitting to absorbing is extremely sharp, as shown in Figure 4-1 for GaAs.

The transmission at wavelengths above the bandgap such as at 1.06 μm, is limited essentially by the Fresnel reflection. These reflections are the dominant loss contributions and total about 3 dB for both faces. However, an ar coating can reduce this reflection loss substantially. For an air interface, SiO with n = 1.9 lowers the total reflection loss for both faces to less than 1.0 dB. TiO_2 (n = 2.3) has been used to reduce the total reflection loss to .7 dB for two epoxy/GaAs interfaces, since in actual use the filter is epoxied to the fiber and detector.

The theoretical absorption at short wavelengths, as shown by the curve labeled "theory" in Figure 4-1, is very strong, exceeding -100 dB at .87 μm for a 432μm thick sample. The measured curve, produced using white light and 100A wide interference filters, levels off at -40 dB attenuation due to the out of band leakage of the filters. Fluctuations in the results below .8 μm result from variations in the quality of the individual interference filters and, to a smaller extent, from noise in the system.

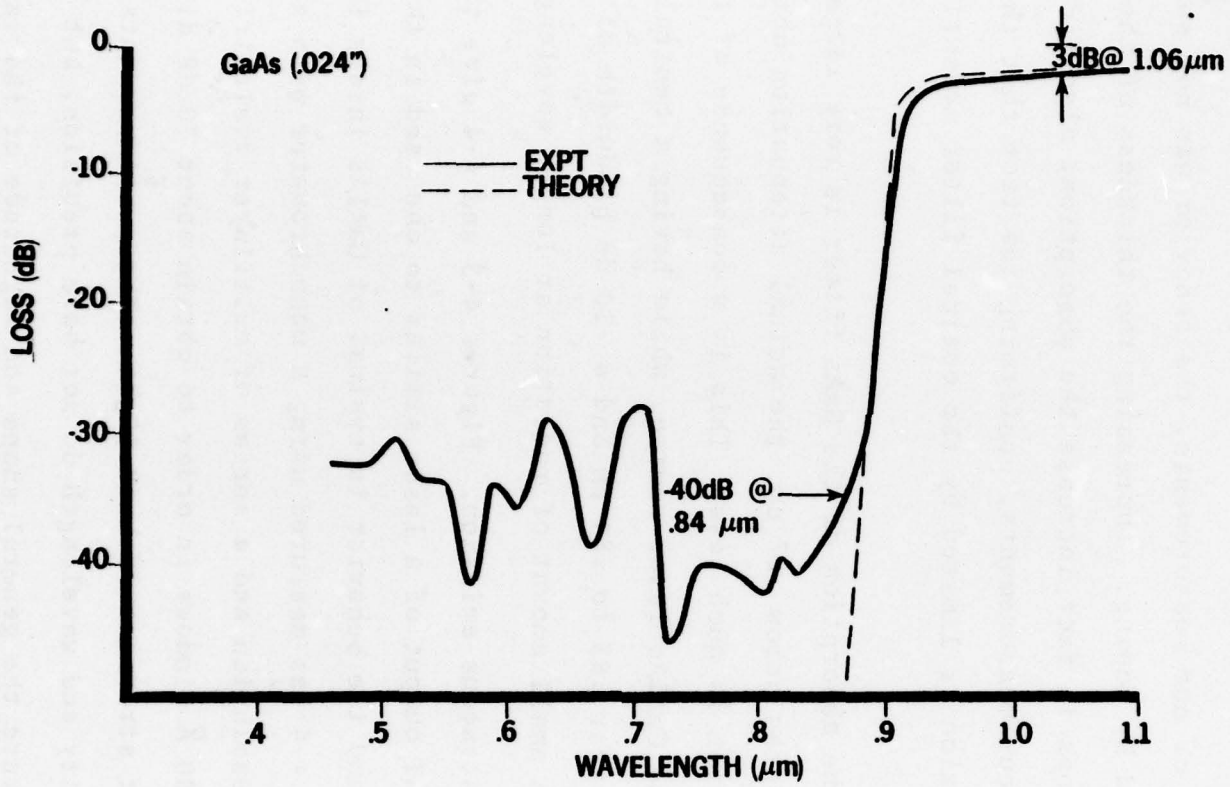

GaAs ATTENUATION VS WAVELENGTH

Figure 4-1

302 10261

Measurements were also made of GaAs doped with Cr and larger crystal thickness, as shown in Figure 4-2. Within the limitations of our measurements, the behavior was not substantially affected by doping. Increasing the thickness of the GaAs, which does in fact increase the absorption, also did not affect our measurements, confirming the fact that the -40 dB attenuation is limited by the optical filter measuring system.

While the absorption of the GaAs filter is very large for wavelengths below .87 μm, the actual attenuation obtained in the system is much less. This is a consequence of the fact that the GaAlAs laser source, while having a central wavelength near .83 to .84 μm and a -10 dB bandwidth of .001 μm, emits a small amount of radiation at longer wavelengths due to spontaneous emission. Figures 4-3 and 4-4 give the spectral output of a laser similar to one used in the duplex link, and the behavior is typical of GaAlAs lasers in general. Figure 4-4 was measured using a monochromator with a 10 Å resolution and a series of multilayer dielectric filters with 100 Å windows in order to obtain about 70 dB discrimination against stray out-of-band light. These measurements of intensity and wavelength do not have precision, but they do illustrate the general shape and magnitude of the laser output over a six decade range. The output is fairly unsymmetrical with greater radiation at the longer wavelengths than

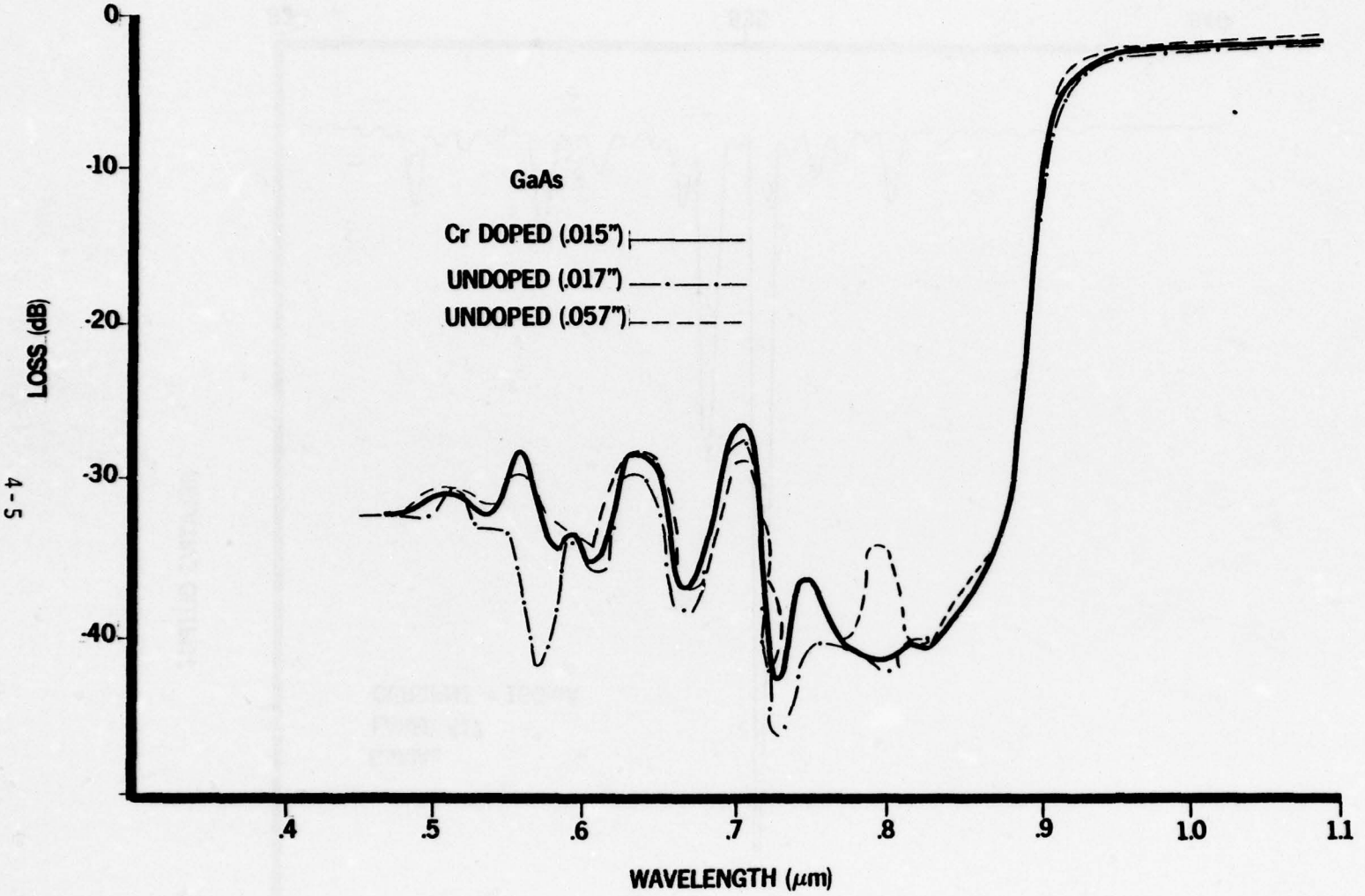

GaAs ATTENUATION VS WAVELENGTH

Figure 4-2

902 10259

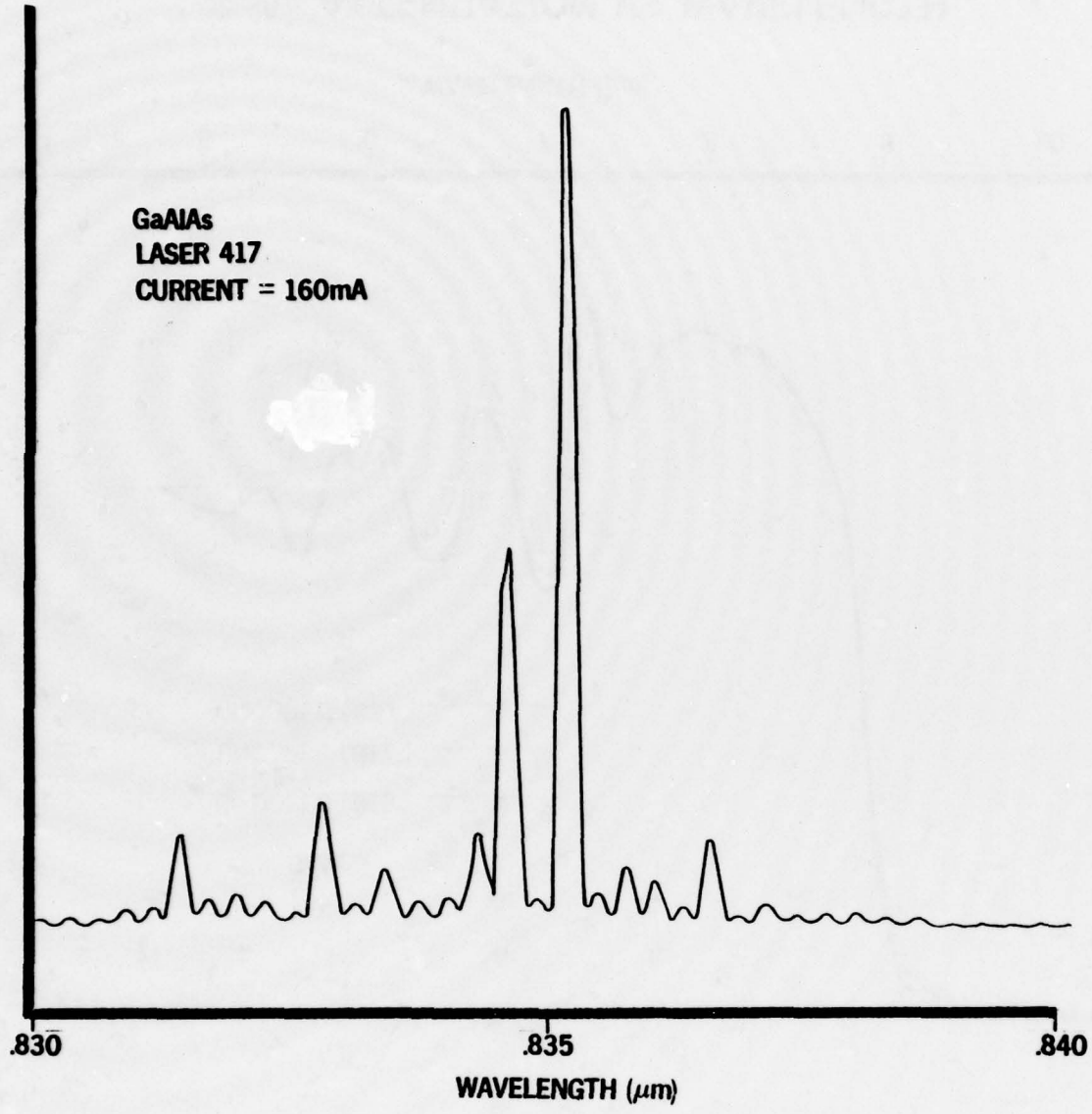

LASER OUTPUT VS WAVELENGTH

302 10249

Figure 4-3

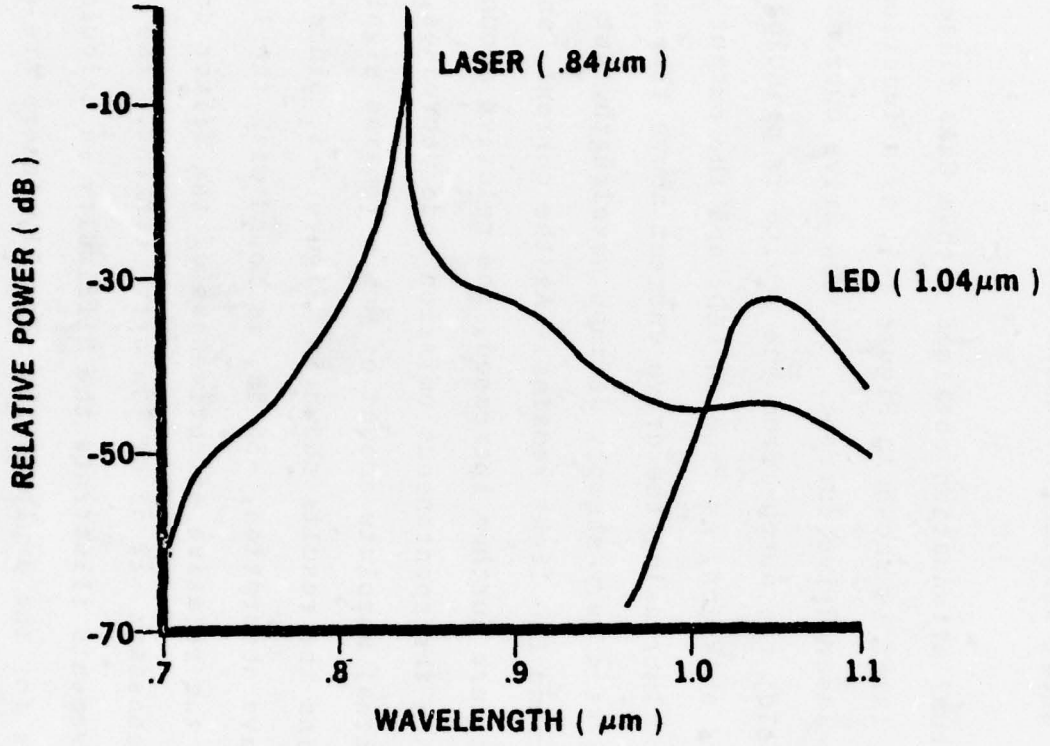

SOURCE OUTPUT VS. WAVELENGTH

Figure 4-4

at the shorter wavelengths. In particular there is a significant amount of power emitted at the 1.06 μm region of the short wavelength laserdiode.

The actual attenuation obtained with a GaAs filter and a GaA1As laser is shown in Figure 4-5, as a function of the GaA1As laser drive current. At low drive current (below threshold) the output from the device is principally spontaneous emission, as from an LED, and the output bandwidth is large. Increasing the drive current above threshold causes lasing at a very sharply defined wavelength, but much of the background LED light remains. As the current, and optical power output, are further increased, the relative amount of power in the spontaneous emission mode decreases, although the actual absolute amount of power remains significant. This explains the results shown in Figure 4-5, since the largest relative absorption, -36 dB, is found with the 1.2 mW output, while the relative effectiveness of the filter decreases to a constant -22 dB at low drive current. The above measurements illustrate the difficulty in calculating crosstalk levels for the duplex link. Usually lasers are considered monochromatic sources, but for this case the full spectral range of emission must be considered in all calculations of crosstalk. This problem is discussed more fully in Section 6.

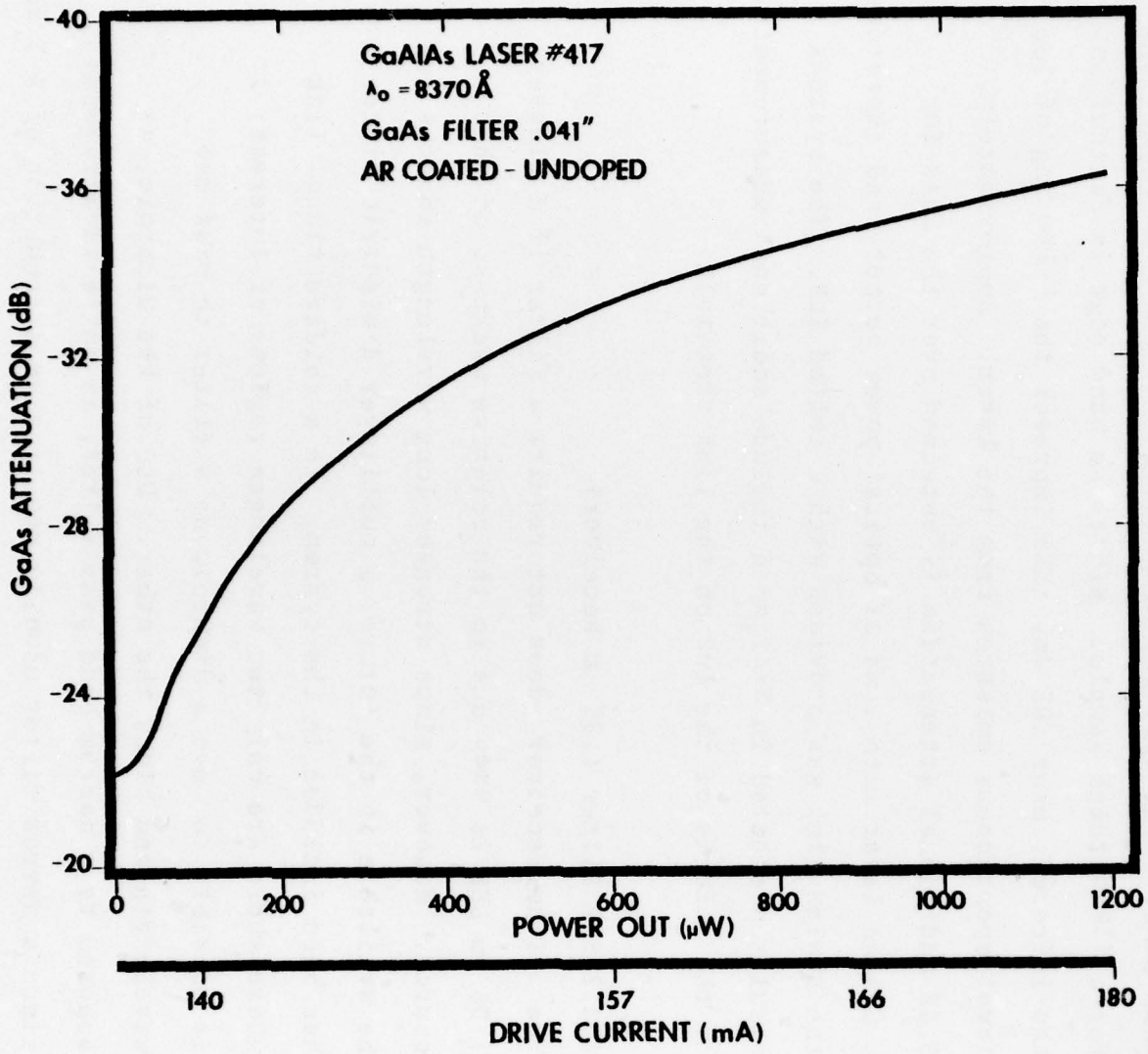

ATTENUATION OF FILTER VS. LASER POWER OUTPUT 302 10252

Figure 4-5

Another semiconductor InP, is more useful for our purposes than GaAs. The spectral transmission is shown in Figure 4-6 for a 330μm thick sample. Since the band edge is farther in the infrared, near .95 μm, this improves the filtering of low level spontaneous emission from the laser. Approximately, 5 dB additional attenuation is obtained over the GaAs for a GaA1As laser with 1 mW of optical power output, and therefore, the duplex link was provided with a coated InP. The systems results presented in Section 6 include additional measurements on the effects of the InP on the link crosstalk.

4.2.2 SWP Filter (.85 μm Receiver)

The .85 μm receiver does not require a filter if a Plessey 1.06 μm LED is used due to the relative weakness of that source. However, since stronger long wavelength sources may be available in the future, a multilayer dielectric filter has been included in the system. In a bidirectional link where there are only two wavelength regions of interest, it is possible to use a dichroic as a filter to pass one wavelength and block the other. Use of the dichroic, as opposed to a narrow band pass filter, is quite advantageous, since a narrow filter usually requires an attenuation of 2-3 dB in the pass band in order to obtain 40 dB of attenuation at all other wavelengths. As shown in Figure 4-7 for the dichroic used as a filter in this system, the transmission loss

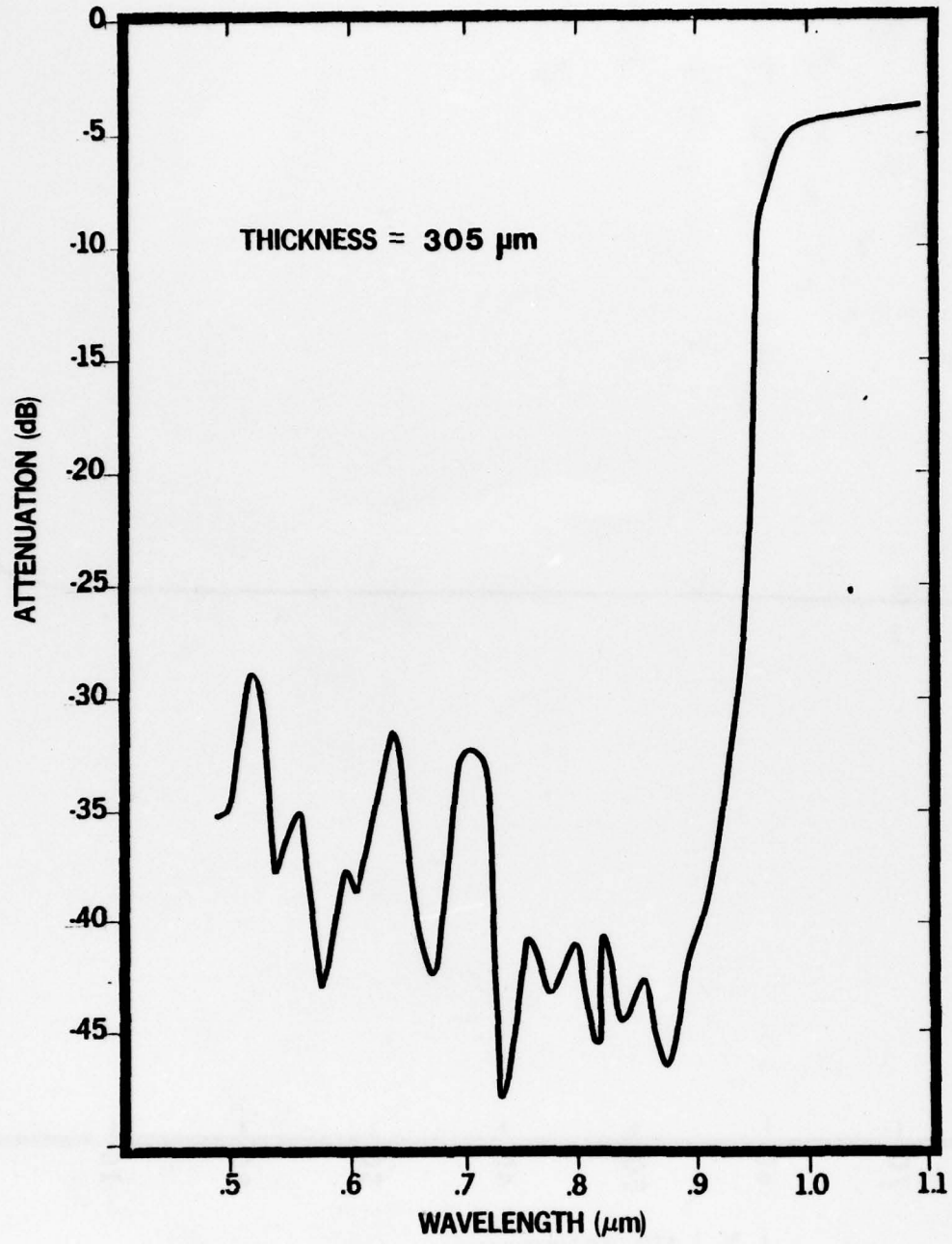

InP TRANSMISSION

302 10266

Figure 4-6

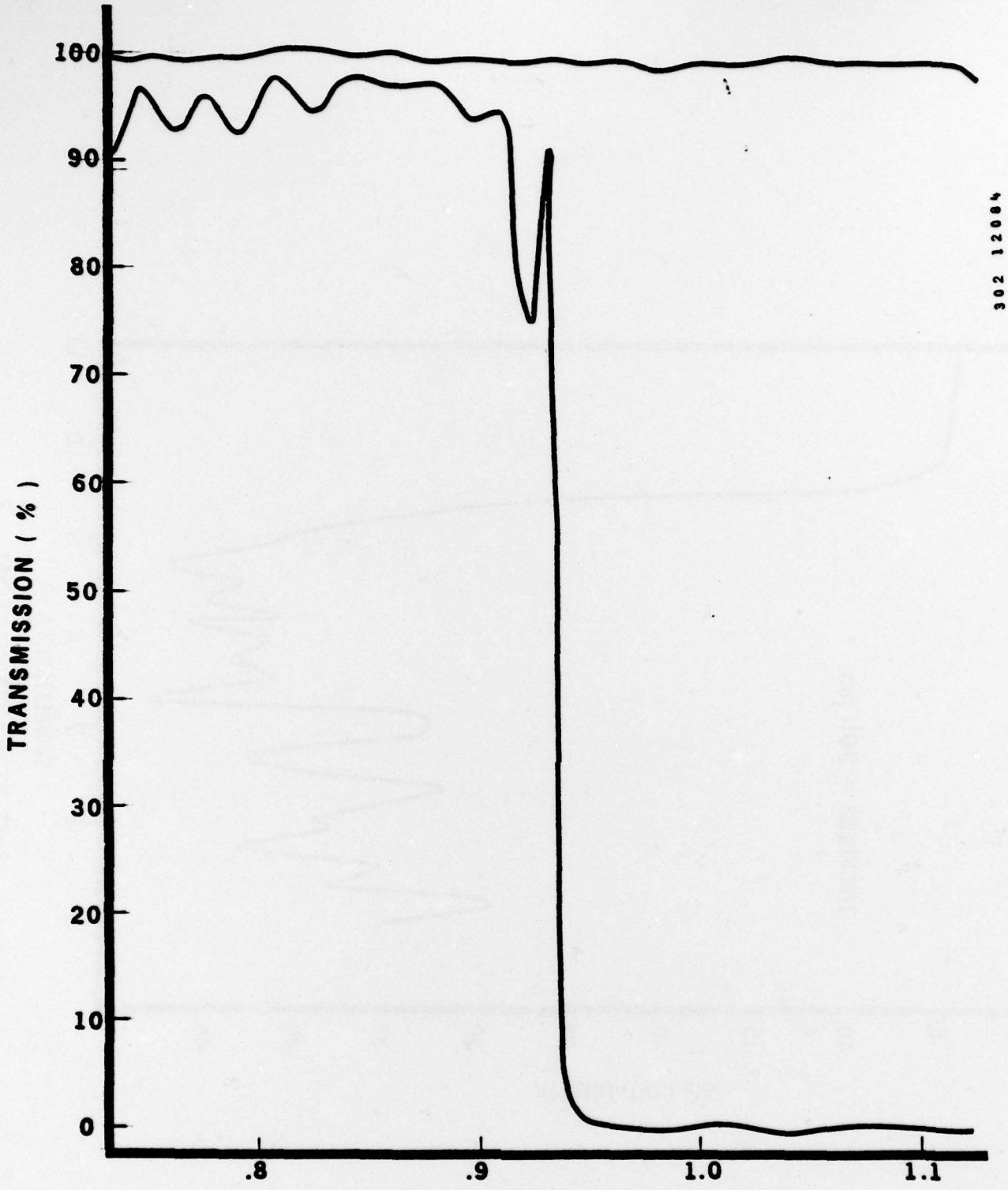

FIGURE 4-7

SWP FILTER

at .84 μm is a few tenths of a dB. The actual transmission at 1.06 μm cannot be read on the graph, but the filter rejection in this region has been measured to be greater than 40 dB.

4.3 Fiber Attenuation Simulator

For complete testing of the bidirectional link, it is desirable to use an attenuation simulator in order to measure performance as a function of fiber length. Since the attenuation of low loss optical fiber differs significantly at .84 μm and 1.06 μm, a dual wavelength simulator would allow for testing of parameters, such as bit error rate, in both directions simultaneously. However, it is possible to thoroughly test the link using wavelength independent simulated loss by measuring performance for one wavelength and one direction of travel at a time. During this test the source sending in the opposite direction will also operate in order to provide a realistic source of cross-talk. When measuring the performance of the second wavelength, the attenuation simulator is then readjusted to simulate the loss for that particular wavelength and the given fiber length.

The original intent of this effort was to develop a dual wavelength attenuation simulator, and a number of different designs for implementing this device were analyzed. However, due to excessive losses encountered in preliminary experiments

and a lack of time to pursue the matter further, a final working dual wavelength attentuator was not developed. Link loss for the tests in Section 6 was simulated for one wavelength at a time by simply separating the distance of two connecting fibers in the link, and this appeared to work in a very satsifactory manner. For completeness we describe in the following sections several dual wavelength loss simulators that were analyzed under this effort and that could be developed in the future.

4.3.1 Beamsplitter Approach

The beamsplitter approach uses two dichroics to separate and then recombine the two operating wavelengths. Figure 4-8 illustrates this simulator with fiber dichroic coupler performing the wavelength separation. Loss is controlled for each wavelength separately by using either a calibrated separation of two fibers or neutral density filters and lenses for each leg of the attenuator. This method is quite lossy due to the present structure of the fiber dichroic couplers that requires a large core receiver fiber. Insertion losses for one wavelength due to the injection from the tap fiber into the coupler would be of the order of 5 to 10 dB.

A bulk optic implementation of the beamsplitter approach is shown in Figure 4-9. Attenuation is performed by calibrated bulk filters placed in the two separate wavelength branches of the simulator. This version of the attenuator is feasible

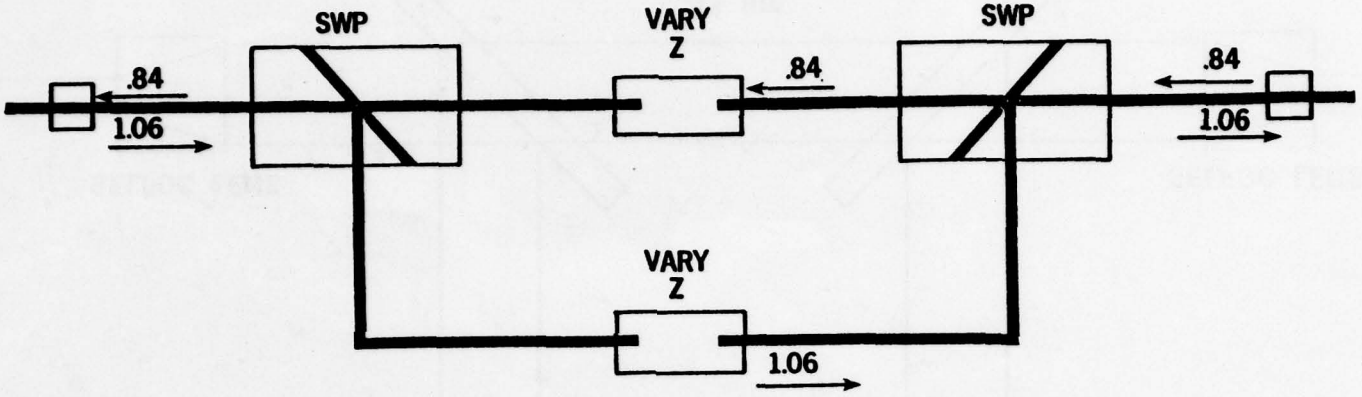

DUAL WAVELENGTH ATTENUATION SIMULATOR

Figure 4-8

302 10264

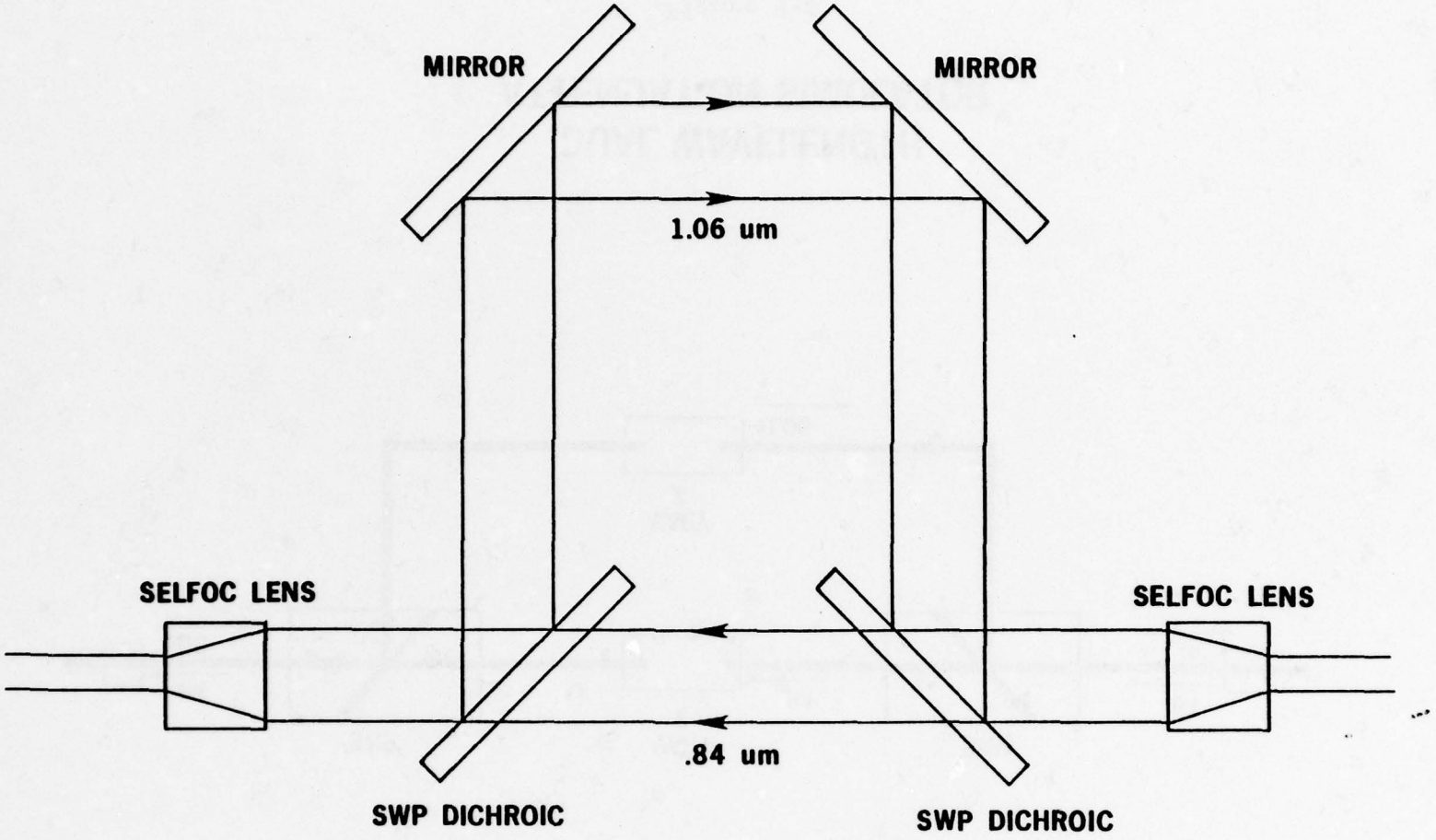

BULK OPTIC ATTENUATER SIMULATOR

FIGURE 4-9

but the number of adjustments required to align the device made operation with low insertion loss very difficult to achieve.

Another version of the bulk optic approach that should be easier to align is shown in Figure 4-10. One fiber with a lens and the dichroic are initially fixed and a mirror and the second fiber are adjusted to maximize throughput for one wavelength. Then the second mirror is manipulated for the remaining wavelength.

4.3.2 Colored Glass Plus Lenses

A second approach uses colored glass absorption filters. For example, a glass such as BG 14 (Schott) has an attenuation of 3.5 dB/mm at 1.06 μm and 6 dB/mm at .85 μm and can be used in different thicknesses to simulate a varying length of optical fiber. One possible implementation of this approach is shown in Figure 4-11. The link is broken at the midpoint and the fibers are inserted into an attenuator simulator consisting of two Selfoc lenses for collimation and refocussing and glass fitlers.

A back reflection in the link from the simulator may be prevented by ar coating the lenses using index matching fluid in the space between the lenses, or epoxying clear glass to

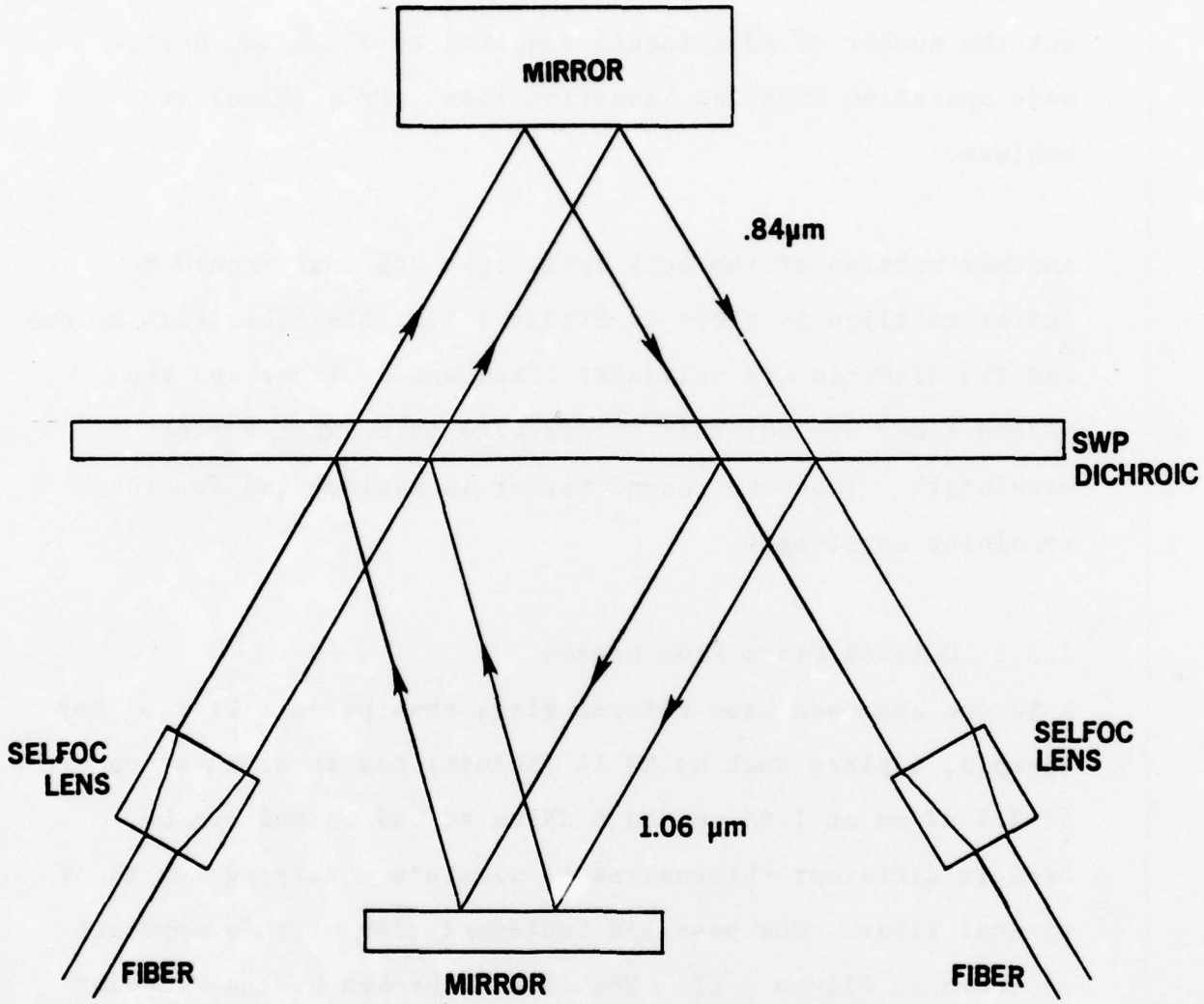

BULK OPTIC ATTENUATION SIMULATOR

Figure 4-10

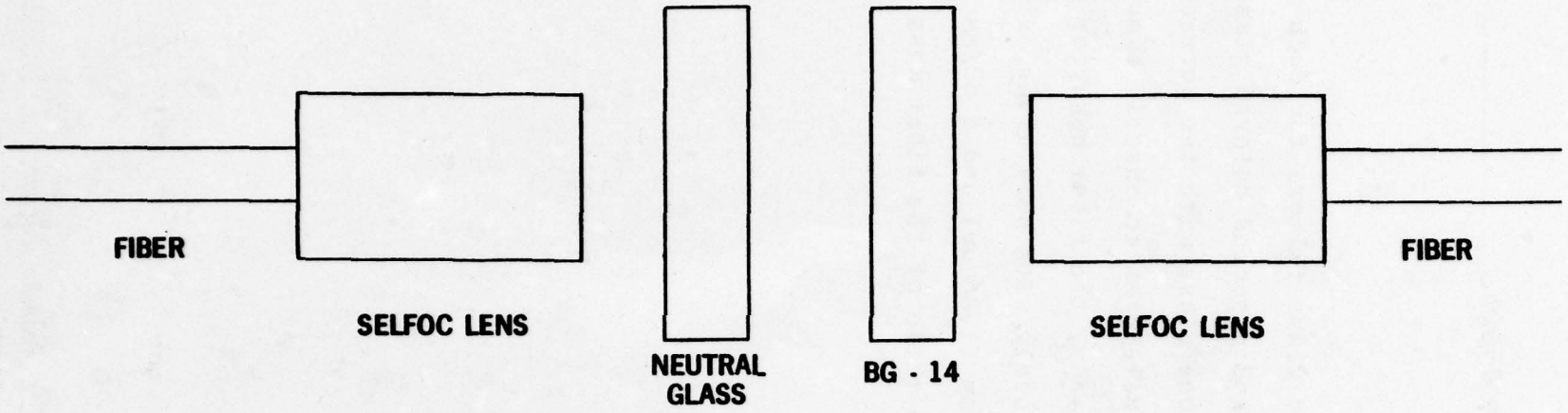

ATTENUATION SIMULATOR USING COLORED GLASS

Figure 4-11

the end of the lenses.

The attenuator uses two glass filters for each fiber length, neutral density glass and a second colored glass, since it is difficult to find one glass with the correct spectral attenuation at both wavelengths to exactly simulate the fiber loss. Alternatively, the fiber behavior can be approximated fairly closely with BG14 alone, since the attenuation of 3.5 dB/mm (1.06 μm) and 6 dB/mm (.85 μm) compares well with the ratio of the fiber loss for those two wavelengths.

5.0 TRANSMITTER AND RECEIVER MODULE

5.1 Transmitter Module

The transmitter module for both .84 μm and 1.06 μm uses previously developed hardware which has proven performance specifications. A photograph of the transmitter module as viewed from the optical connector end is shown in Figure 5-1.

The physical dimensions are shown in Figure 5.2. The electrical inputs are located on the end opposite the optical connector and consist of the power supply (+5Vdc), ground and digital data input. The case is highly conductive and is sufficiently rugged so as to withstand considerable vibration during use. A circuit diagram of the transmitter module is shown in Figure 5-3.

5.2 Receiver Module

As with the transmitter module, the proposed receiver module is a proven electrical, optical, and mechanical design. A photograph of the receiver module as viewed from the electrical output end is shown in Figure 5-4.

The outside physical dimensions are identical to those of the transmitter module shown earlier in Figure 5-2. The electrical

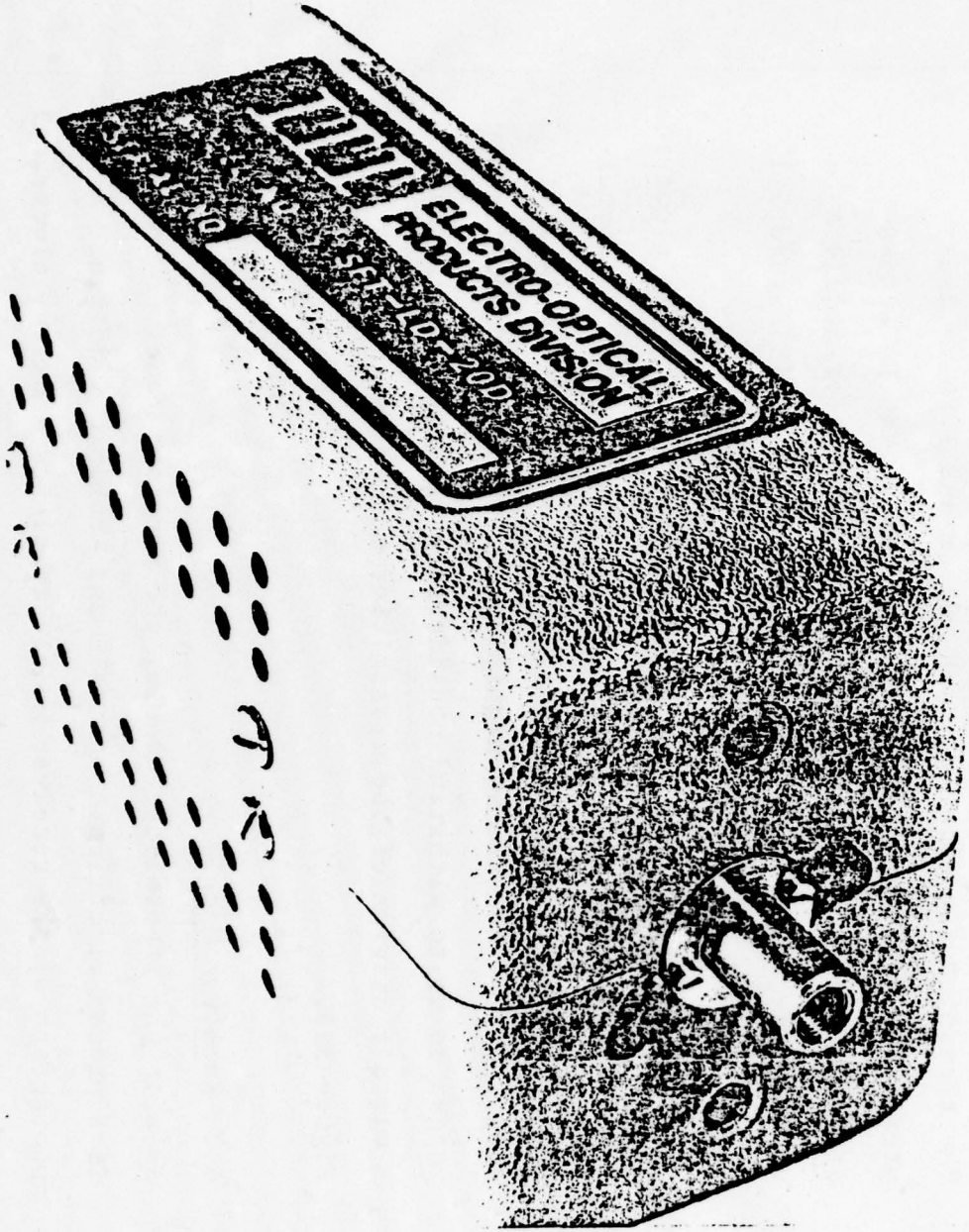

Transmitter Module (Optical Connector View)

Figure 5-1

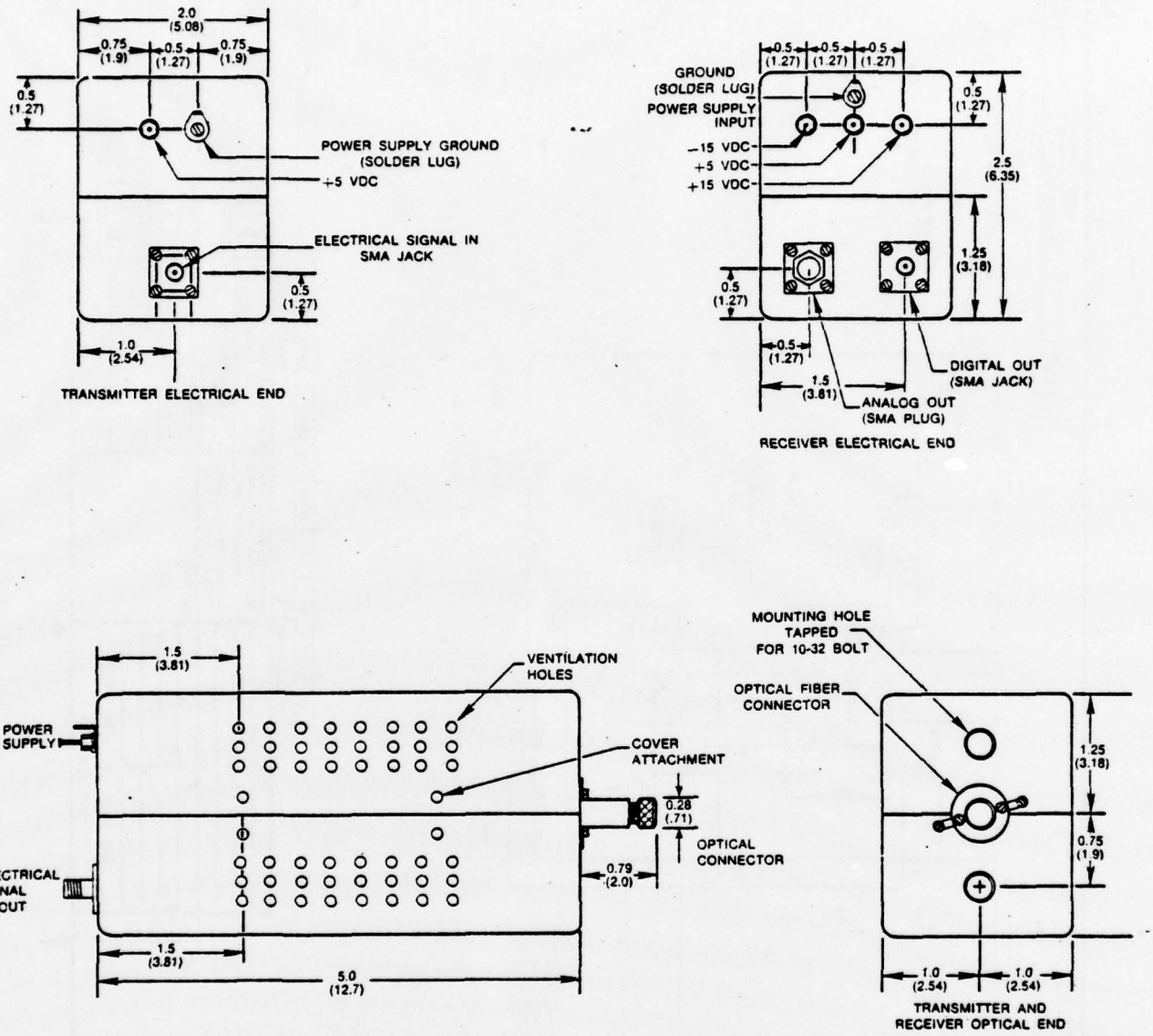

All dimensions in inches (centimeters)

TRANSMITTER/RECEIVER MODULE DIMENSIONS

Figure 5-2

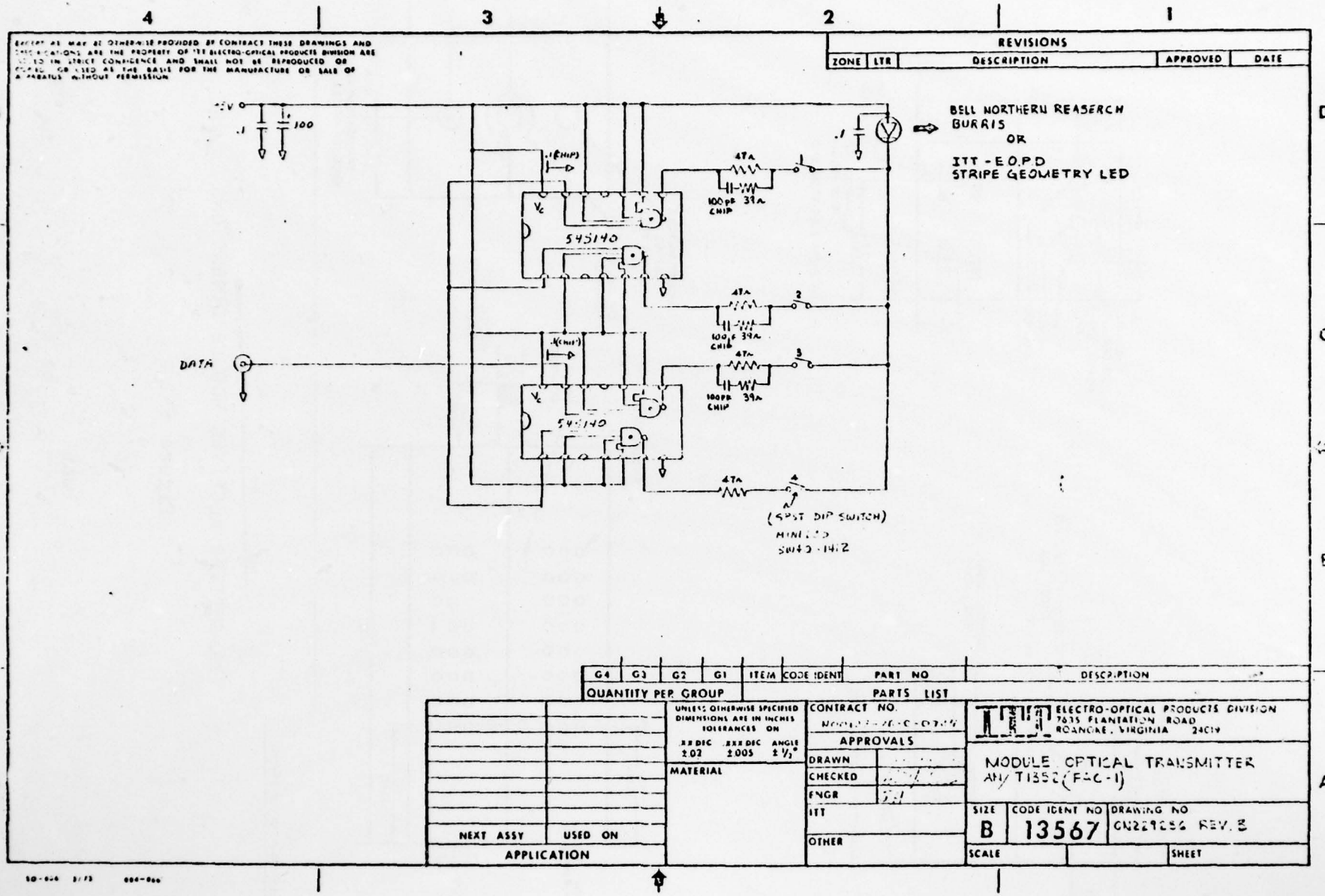

Figure 5-3

TRANSMITTER SCHEMATIC DRAWING

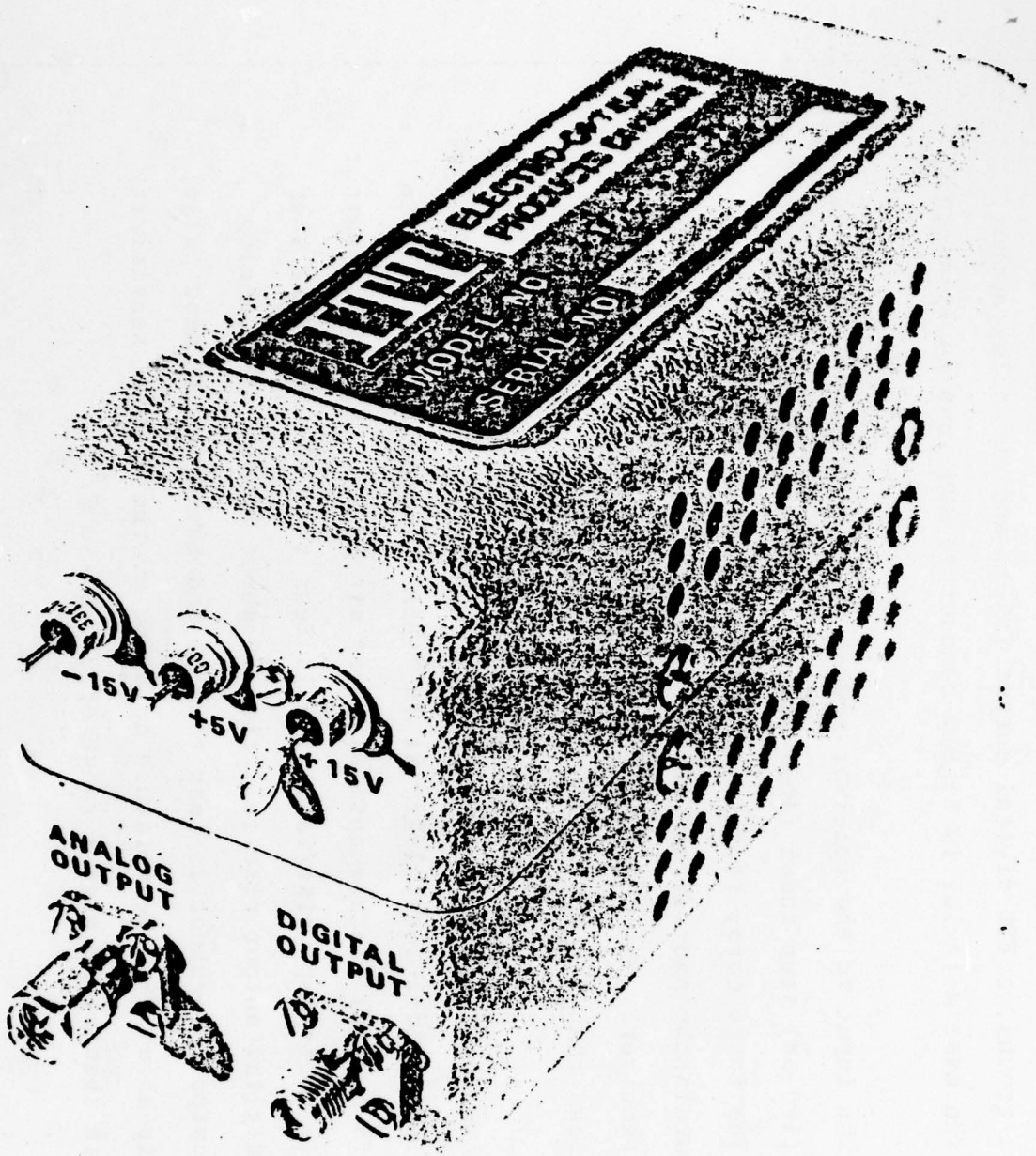

Figure 5-4
RECEIVER MODULE (ELECTRICAL CONNECTOR VIEW)

interfaces consist of three power supply lines (±15Vdc, +5Vdc), a ground, a TTL digital output (NRZ), and an analog output. The case material is highly conductive and inherently rugged.

The input to the receiver module is coupled to a large core (100 μm) step index fiber within a bulkhead mountable jack. The large core, step index fiber is pigtail coupled to an avalanche photodiode (APD) located in the front-end of the receiver. The coupling loss of the pigtail to the APD is less than 0.5 dB.

A circuit design of the receiver module is shown in Figure 5.5. The optical sensitivity at 10^{-8} BER is approximately -53 dBm (5 nwatts) average optical power at .84 μm. The analog output (3 volts p-p) rise/fall time is less than 18 nsec while the digital output rise/fall time is about 5 nsec. The analog output overshoot is less than 5% and the droop (50 nsec pulse) is about 9%. Temperature derating of the optical sensitivity is about 1 dB over a range of 0^{o} to $+50^{o}$C.

5.3 Sources

Short wavelength transmitters for the bidirectional link use ITT-EOPD double heterostructure lasers. The output power versus drive current for one of the delivered lasers is shown in Fig. 5-6. Threshold is at 100 mA and a peak coupled output of

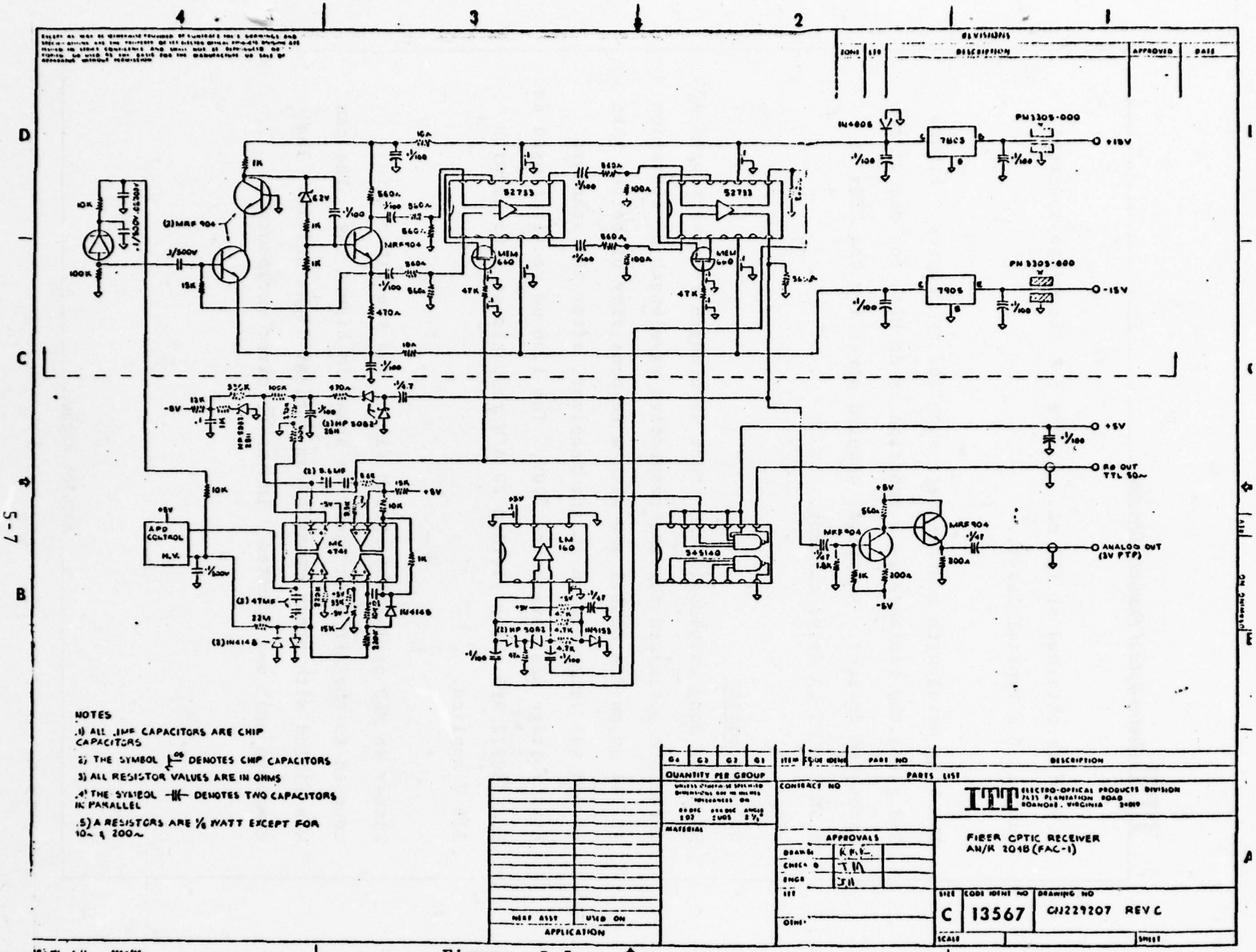

Figure 5-5
RECEIVER SCHEMATIC DRAWING

1.9 mW is obtained at 134 mA. Figure 5-7 shows the spectral output of a typical laser.

The long wavelength sources were supplied by Plessey. Figure 5-8 gives the radiance as a function of dc bias for one of the uncoupled devices. A typical coupled power for the LEDs is 5 μW for 75 μA drive current.

5.4 Detectors

Both the long wavelength and short wavelength receivers used APD detectors optimized for the respective wavelength of operation. At .84 μm an RCA C30921 APD with a responsivity of better than 65 A/W was incorporated in the receiver, after the standard bias voltage was lowered to 200V. The 1.06 μm receiver used an RCA C30922 APD which yielded 20 A/W response at 1.06 μm with 325 V applied.

Either an MLD or InP absorption filter and the fiber were coupled to the APD with epoxy as shown in Figure 5-9. The can was filled with black epoxy as an ambient light shield. The complete unit was mounted in the receiver enclosure.

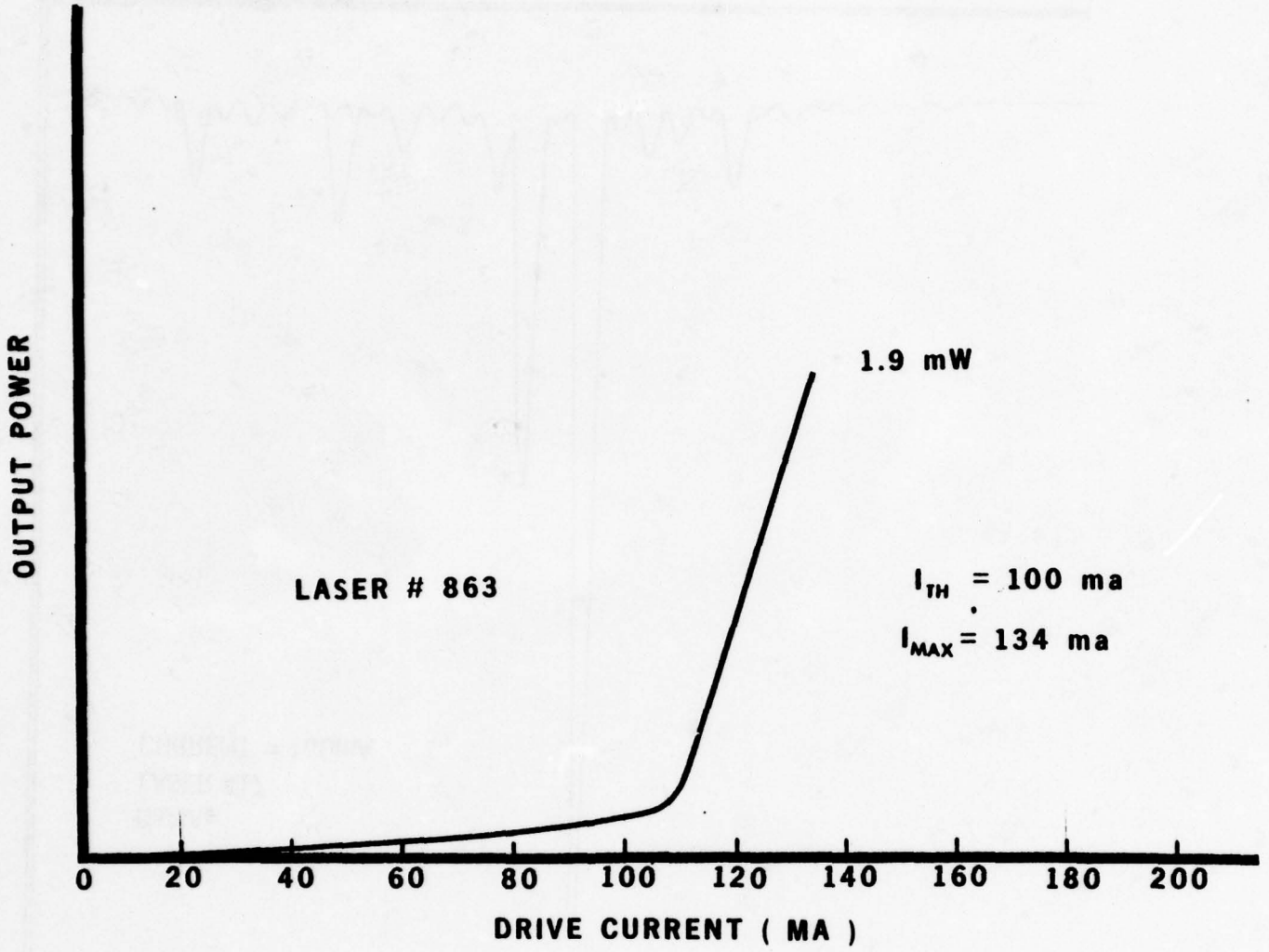

LASER OUTPUT POWER VS DRIVE CURRENT

FIGURE 5-6

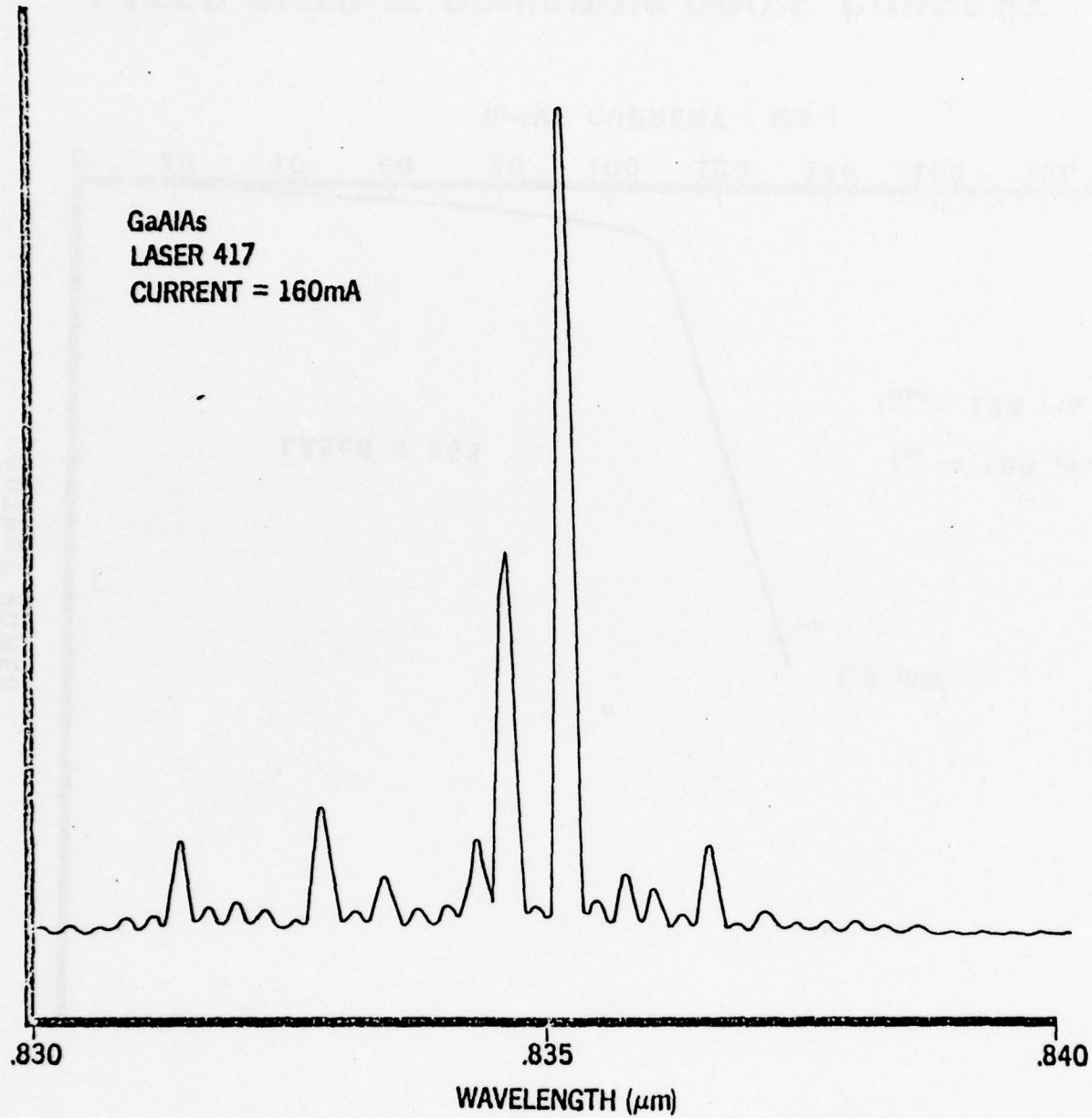

LASER OUTPUT VS WAVELENGTH

FIGURE 5-7

302 10249

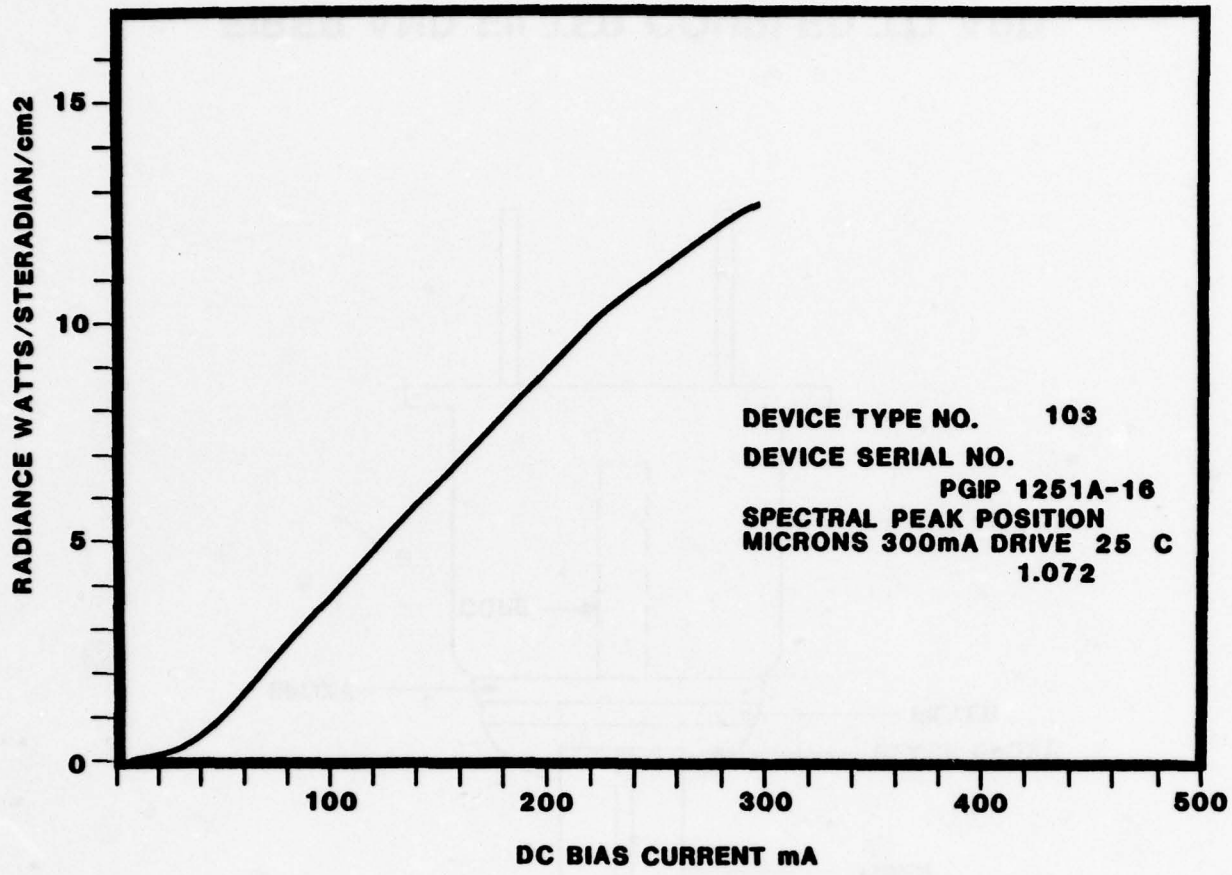

RADIANCE AS A FUNCTION OF DC BIAS FOR PLESSEY HIGH RADIANCE DIODES

302 12083

FIGURE 5-8

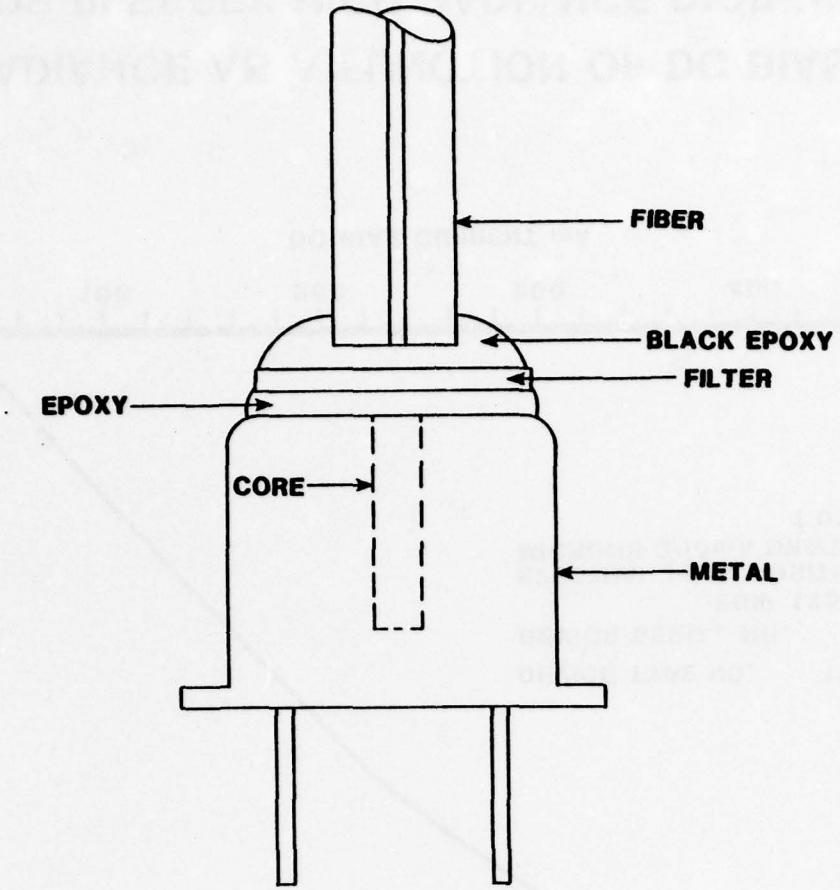

FIBER AND FILTER COUPLED TO APD

FIGURE 5-9

302 12082

6.0 SYSTEMS INTEGRATION

Four bidirectional couplers (2 SWP and 2 LWP) with associated transmitters and receivers were assembled and tested in two separate bidirectional data links at 20 Mb/s. Before discussing the results obtained from these systems trials, a theoretical analysis of the expected crosstalk will be presented in the next section.

6.1 Crosstalk Analysis

One of the most important parameters affecting performance of a full duplex link is the optical crosstalk from the wavelength duplex operation. Initial estimate of this crosstalk can be made quite easily by assuming monochromatic sources and values for dichroic and filter performance at a particular wavelength. However, more accurate calculations of the expected crosstalk require measurements of laser output, dichroic transmission and filter attenuation as a function of wavelength. In performing such an analysis, it is soon apparent that the receiver isolation is severely limited by the relatively small amount of out of band radiation that is emitted by the sources. Significant radiation at 1.06 μm has actually been measured for the GaAlAs laser.

In this section, the individual contributions to the crosstalk are identified, and using measurements of individual

component performance and intelligent estimates, calculations have been made of the expected total crosstalk. The crosstalk is further described as a function of wavelength so that the steps required to improve performance can be easily identified.

6.1.1 Sources of Crosstalk

In the fiber dichroic coupler, two distinct sources of crosstalk may be identified: crosstalk from scattering in the fiber dichroic coupler (Figure 6-1) and crosstalk from fiber backscatter (Figure 6-2). The optical crosstalk is defined in this study as the ratio of the optical power incident upon the detector to the optical power in the transmitter fiber pigtail. For the case of coupler scatter, we then find for the crosstalk, C_1,

$$C_1 = \frac{\int T\ (\lambda) \cdot CS\ (\lambda) \cdot F\ (\lambda) \cdot d\lambda}{\int T\ (\lambda)\ d\lambda} \qquad (6\text{-}1)$$

where $T(\lambda)$ is the coupled transmitter optical power, $CS\ (\lambda)$ is the coupler scattering function, and $F\ (\lambda)$ is the attenuation of the detector filter. In Eq. 6-1, it has been assumed that all relevant parameters are a function of wavelength, and therefore an integration is necessary. However, measurements of CS, the coupler scattering, indicate that it is relatively independent of λ and may be removed from the

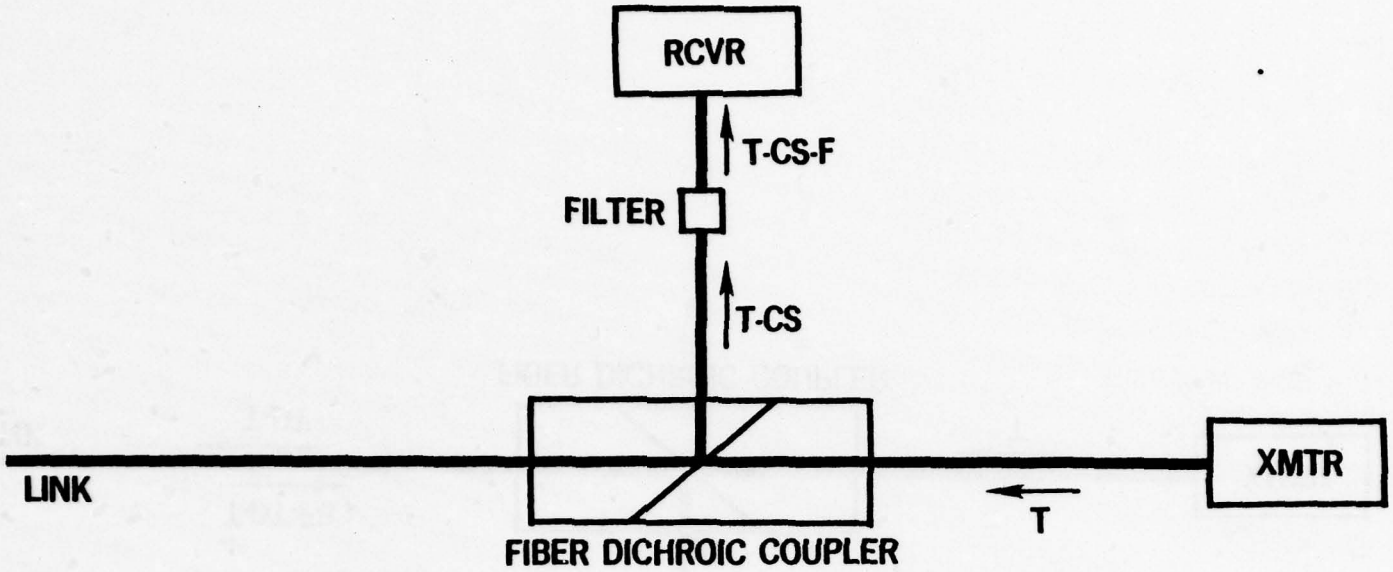

CROSSTALK FROM COUPLER SCATTERING

Figure 6-1

302 10247

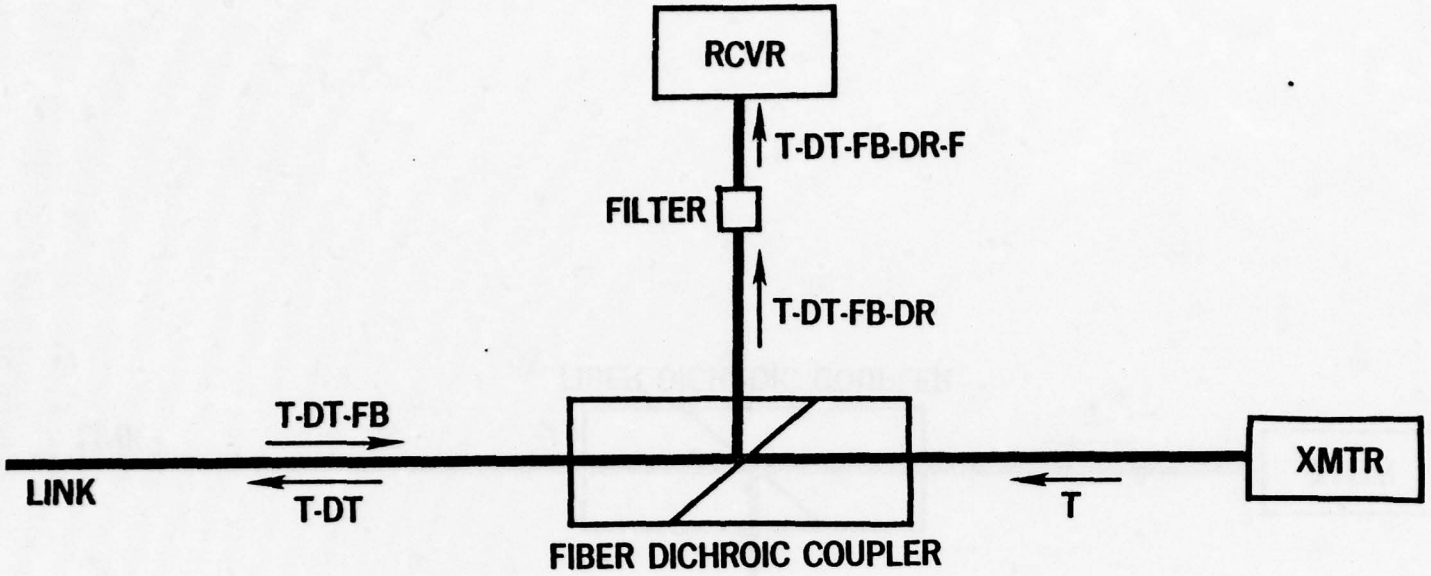

CROSSTALK FROM FIBER BACKSCATTER

Figure 6-2

302 10248

integral, so that

$$C_1 = \frac{CS \int T(\lambda) \cdot F(\lambda)\, d\lambda}{\int T(\lambda)\, d\lambda} \qquad (6\text{-}2)$$

The second source of crosstalk, back scattering from the fiber, is illustrated schematically in Figure 6-2.

Mathematically, we have

$$C_2 = \frac{\int T(\lambda) \cdot DT(\lambda) \cdot FB(\lambda) \cdot DR(\lambda) \cdot F(\lambda)\, d\lambda}{\int T(\lambda)\, d\lambda} \qquad (6\text{-}3)$$

where DT (λ) is the dichroic transmission, FB (λ) is the fiber backscatter from all sources, both distributed and discrete, and DR (λ) is the dichroic reflection as a function of λ. The wavelength dependence of FB is unknown. Discrete sources of backscatter should yield wavelength independent scattering while the distributed scatter should have a Rayleigh dependence. However, these effects are further complicated by the wavelength dependence of the fiber attenuation which will be important for sources of backscatter that are some distance down the link from the coupler. This wavelength dependence appears to be quite complicated and will vary for different systems, but for most cases, FB (λ) should be only a weak function of λ. Therefore, we shall assume:

$$C_2 = \frac{FB \int T(\lambda) \cdot DT \cdot (\lambda) \cdot DR(\lambda) \cdot F(\lambda)\, d\lambda}{\int T(\lambda)\, d\lambda} \qquad (6\text{-}4)$$

6.1.2 Crosstalk Calculation - Short Wave Pass Coating

The short wave pass dichroic coupler is used in conjunction with the AlGaAs laser and a GaAs filter blocking the 1.06 μm receiver. In order to compute C_1 and C_2, as shown in equations 6-2 and 6-4, we require the output spectrum of the laser versus wavelength up to the cut-off wavelength of the Si detector, or about 1.1 μm. This spectrum was measured using a grating monochromater and 100 Å bandpass filters in order to decrease the stray light level to -70 dB. The output for a laser operated at 1 mW total coupled power is shown in comparison with the 1.06 μm LED output in Figure 6-3. As can be seen in the figure, there is significant spontaneous emission from the laser in the long wavelength region. The GaAlAs laser output was also measured in a separate experiment at a longer wavelength with a GaAs filter, to block the major portion of the output, and a 100 Å bandpass filter centered at 1.05 μm. In this case with 1 mW total laser output, the measured transmission was -55 dBm, which is in general agreement with the values obtained using the monochromater.

Other functions required are the dichroic transmission (DT(λ)) and reflection (DR(λ)), shown in Figure 6-4, and the GaAs absorption spectrum given in Figure 6-5. The GaAs curve comes from handbook values for the absorption for a .5 mm

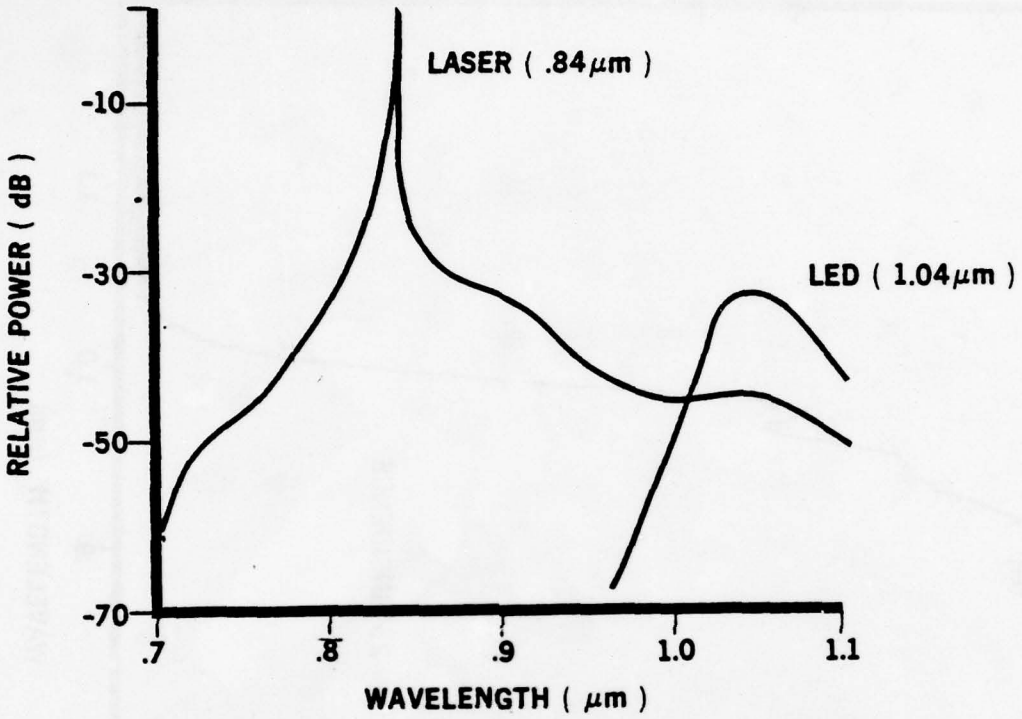

SOURCE OUTPUT VS. WAVELENGTH

Figure 6-3

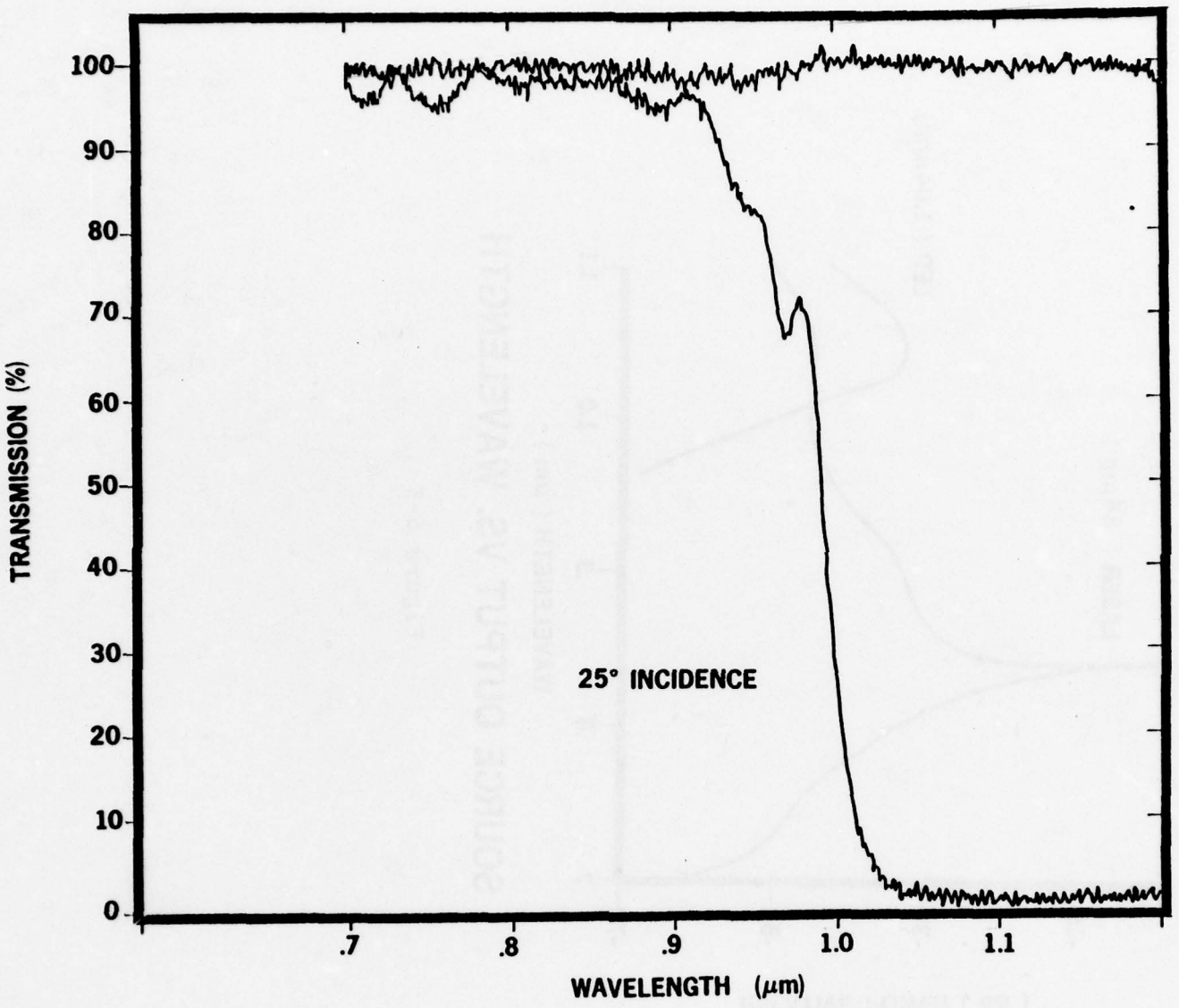

SWP DICHROIC COATING

302 11801

Figure 6-4

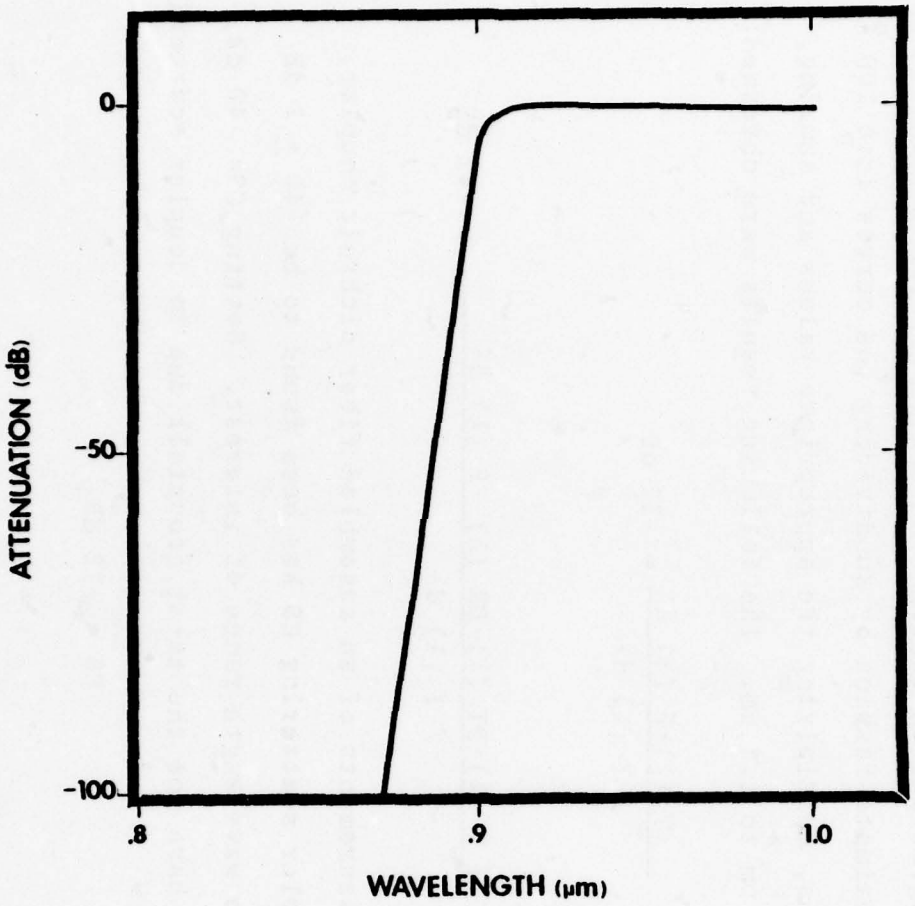

GaAs ATTENUATION

302 10256

Figure 6-5

thickness. As a result of this extremely high absorption, we can terminate the integrations shown in equations 6-2 and 6-4 at .8 μm.

The integrations indicated for C_1 and C_2 were carried out in an approximate fashion by subdividing the curves into 100 Å intervals, multiplying the appropriate values and summing, from .8 μm to 1.1 μm. The following results were obtained:

$$\frac{\int T(\lambda) \cdot F(\lambda)\, d\lambda}{\int T(\lambda)\, d\lambda} = -32 \text{ dB}$$

and

$$\frac{\int T(\lambda) \cdot DT(\lambda) \cdot DR(\lambda) \cdot F(\lambda)\, d\lambda}{\int T(\lambda)\, d\lambda} = -42 \text{ dB}$$

From measurements of an assembled fiber dichroic coupler, the coupler scattering CS has been found to be -40 ± 2 dB over the wavelength range of interest. Setting CS= -40 dB, we then have for the total crosstalk due to coupler scattering:

$$CS = -72 \text{ dB}.$$

As described above, the fiber backscatter parameter, FB is somewhat complicated, but measurements at ITT and by others indicate an approximate value for FB (dc level) is -20 dB and FB (ac level) = -40 dB. Thus, for the total crosstalk due to fiber backscatter, we have:

$C_2(dc) = -62$ dB

$C_2(ac) = -82$ dB.

These values of crosstalk obtained from a consideration of the performance of each coupler element over the entire wavelength range of interest can be compared with the results that are obtained with the simpler analysis usually made of monochromatic sources. If, for examples, we assume a laser with central wavelength at .86 μm and no significant out-of-band radiation, then the crosstalk from coupler scatterming (C_1) is -40 dB for CS plus the attenuaton of the receiver filter. For a GaAs filter, the attenation is about -100 dB_1 or C_1 = -140 dB. If a multilayer dielectric filter is assumed with -40 dB attenuation, then C_1 = -80 dB. However, as shown by the above calculations, the crosstalk level is actually limited to around C_1 = -72 dB by scattering of low level out-of-band laser radiation.

In Figure 6-6 the fiber backscatter and coupler scattering crosstalk are shown as a function of wavelength before integration. These graphs illustrate the effect of the out-of-band radiation above .9 μm on the crosstalk level, and suggest the areas where changes will be helpful in lowering crosstalk. For example, better dichroic performance below .9 μm will not affect crosstalk levels, so long as a GaAs

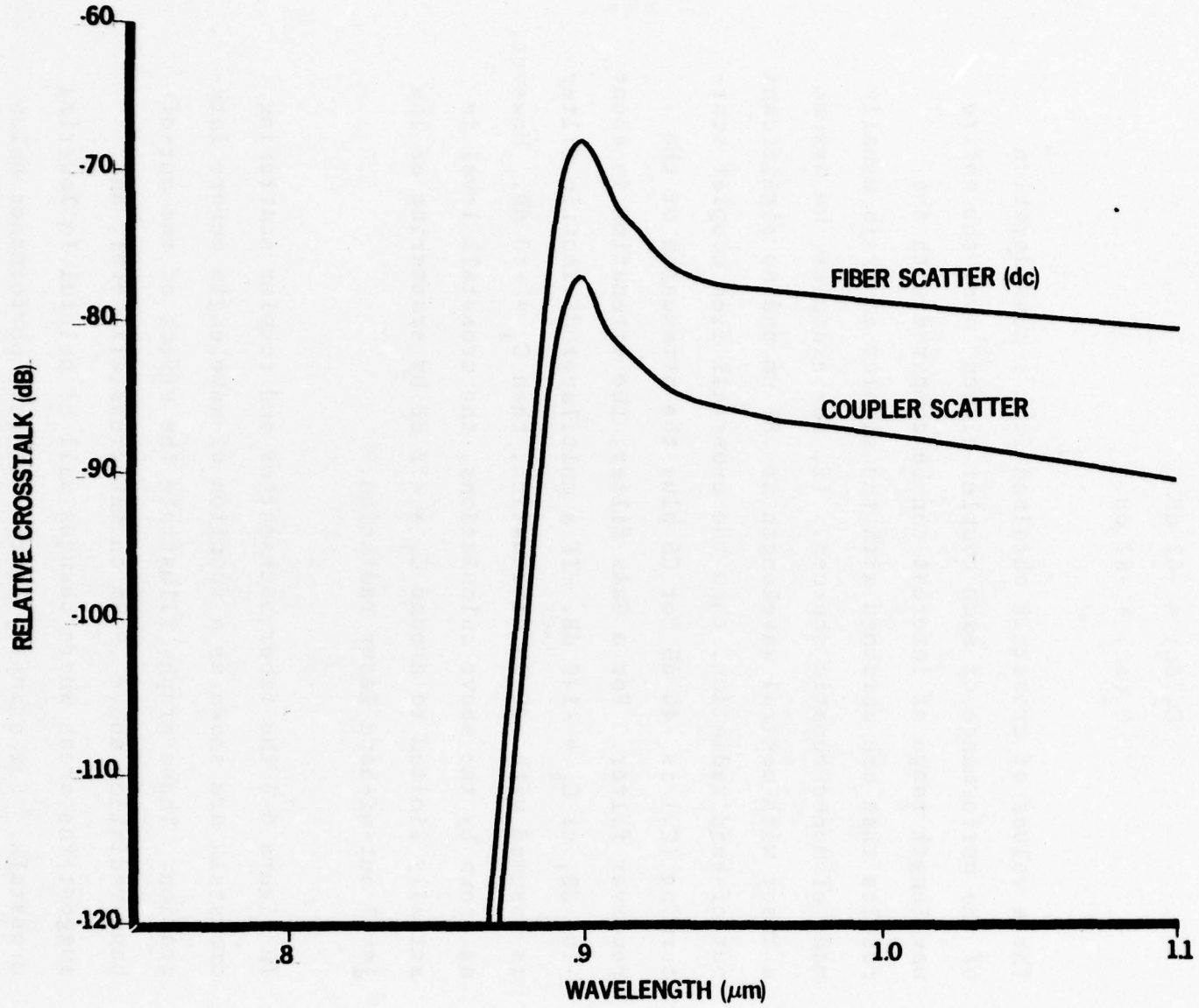

CROSSTALK VS. WAVELENGTH - 1.06μm RECEIVER

302 10260

Figure 6-6

filter is used. Improved dichroic discrimination between .9 and 1.0 μm, however, will yield 5 to 10 dB improved crosstalk level. The use of InP instead of GaAs should also yield a 5 to 10 dB improvement, since the InP absorption begins about .05 μm farther in the infrared. One of the most effective improvements that can be made, however, is a filter on the laser output to drop that out-of-band radiation level significantly. Using a well designed filter, an additional -40 dB of attenuation could be obtained with this procedure. This filter could be designed for evaporation on a fiber end face similar to the fiber dichroic coupler and inserted in-line with the source fiber. However, an additional loss of one to two dB would be added to the system by this filter.

6.1.3 Crosstalk Calculation - Long Wave Pass Coating

The procedure for calculating the crosstalk for the long wave pass dichroic is identical to the previous method indicated for the short wave pass coating, but the details for the two cases do differ. In particular, our analysis will assume an LED at 1.06 μm, since that is what the current duplex link uses. Due to the weaker output form the LED, it is extremely difficult to obtain a complete wavelength spectrum measuring the out-of-band radiation. Instead, the wavelength dependence has been estimated using the measurements shown in Figure 6-3.

A material analogous to GaAs or InP does not exist for the .85 μm receiver, and therefore, a conventional multilayer dielectric filter must be used. The performance shown in Figure 6-7 has been obtained with filters that were used in the duplex link. Slightly better than -40 dB attenuation was obtained from 1.0 to 1.1 μm with better than 95% transmission at .85 μm.

Using the same values for coupler scattering, CS = -40 dB, and fiber backscatter, FB (dc) = -20 dB and FB (ac) = -40 dB, equations 6-2 and 6-4 have been used to calculate the cross-talk as before:

$$C_1 = -74 \text{ dB}$$
$$C_2 \text{ (dc)} = -63 \text{ dB}$$
$$C_2 \text{ (ac)} = -83 \text{ dB}.$$

Due to the uncertainties involved, this calculation is less accurate than for the short wave pass coating, but because the LED power is so much less than the laser output, the crosstalk for this case is much less important. This will be shown more clearly in Secion 6.2

The crosstalk as a function of wavelength is shown in Figure 6-8. Again, the chief crosstalk contribution is in the out-of-band radiation region. In this case the crosstalk

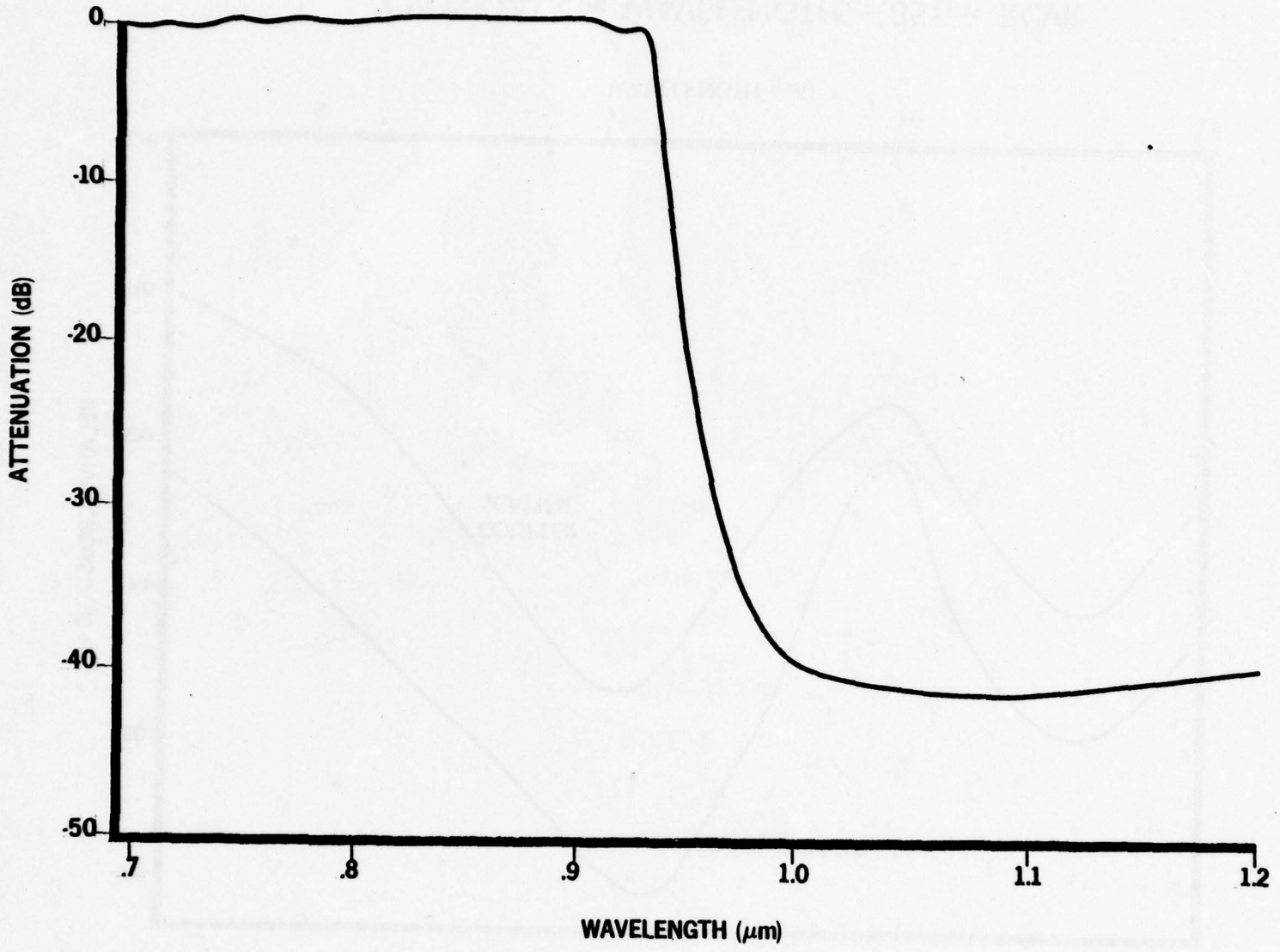

FILTER FOR .85 μm RECEIVER

Figure 6-7

302 10265

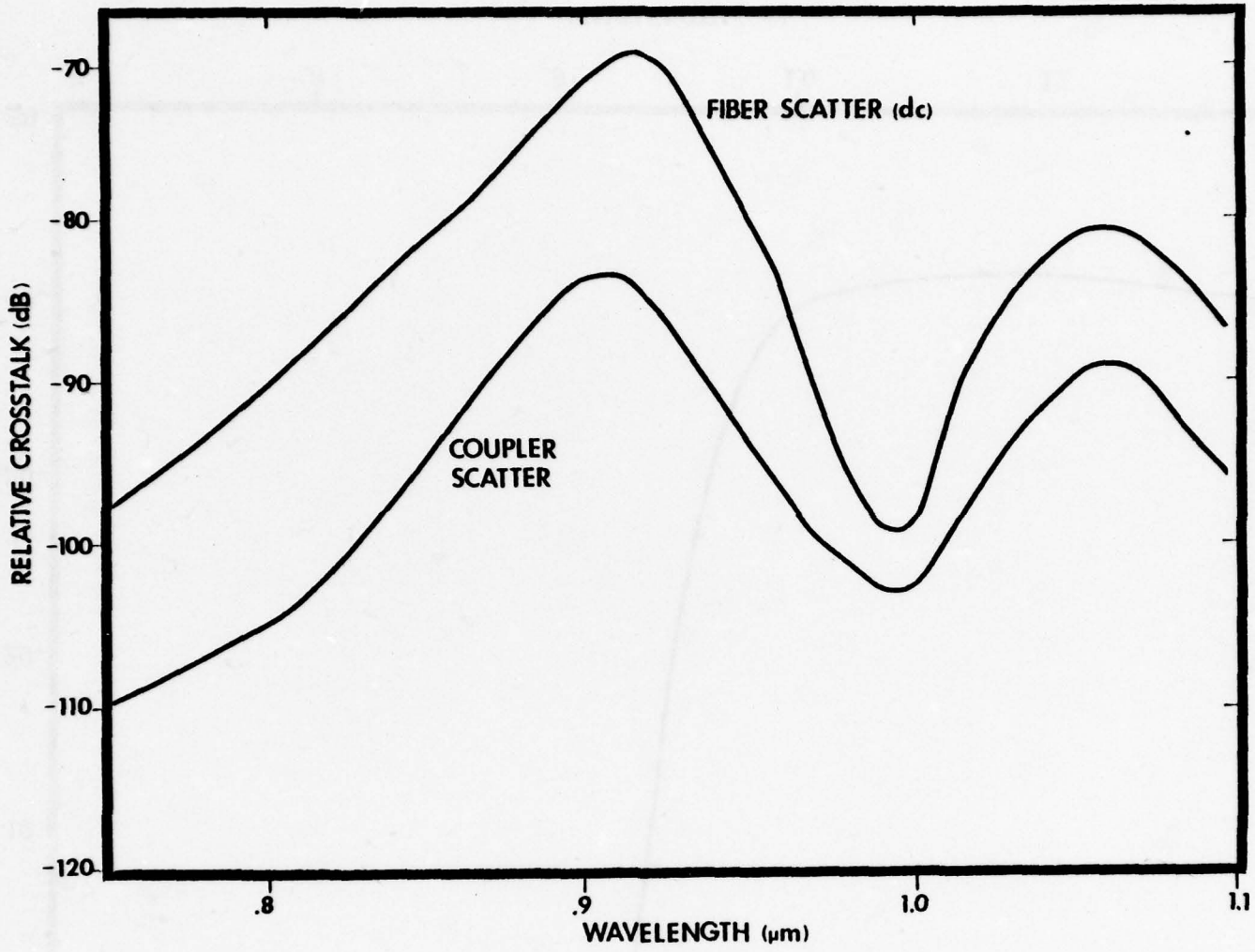

CROSSTALK vs. WAVELENGTH – .85 μm RCVR

302 10254

Figure 6-8

maximum is near .9 μm, and it is doubtful if the dichroic or filter rejection could be improved a great deal at this wavelength, which is so close to the laser wavelength being transmitted. The largest improvement would arise from a filter on the source. However, in contrast to the very large improvement obtained for the short wave pass coupler, source filtering would add only 10 dB improvement for this case, since crosstalk at 1.06 μm would then become noticeable (see Figure 6-8). The most natural steps for a large crosstalk improvement would be both source filtering and improved transmission of the dichroic at 1.06 μm.

6.2 Experimental Results

A complete bidirectional system was assembled as shown in Figure 6-9 in order to test the link bit error rate as a function of link attenuation. The link included a 1.06 μm LED with 8 μm peak coupled power and a .84 μm laser capable of 1 mW output. The receivers used APD's optmized for their wavelength of operation and with an MLD or InP filter. Attenuation was simulated by joining the bidirectional coupler fiber and link fiber using micropositioners and adjusting the fiber separation for a particular loss. Sections 3.0, 4.0, and 5.0 describe the link components in more detail.

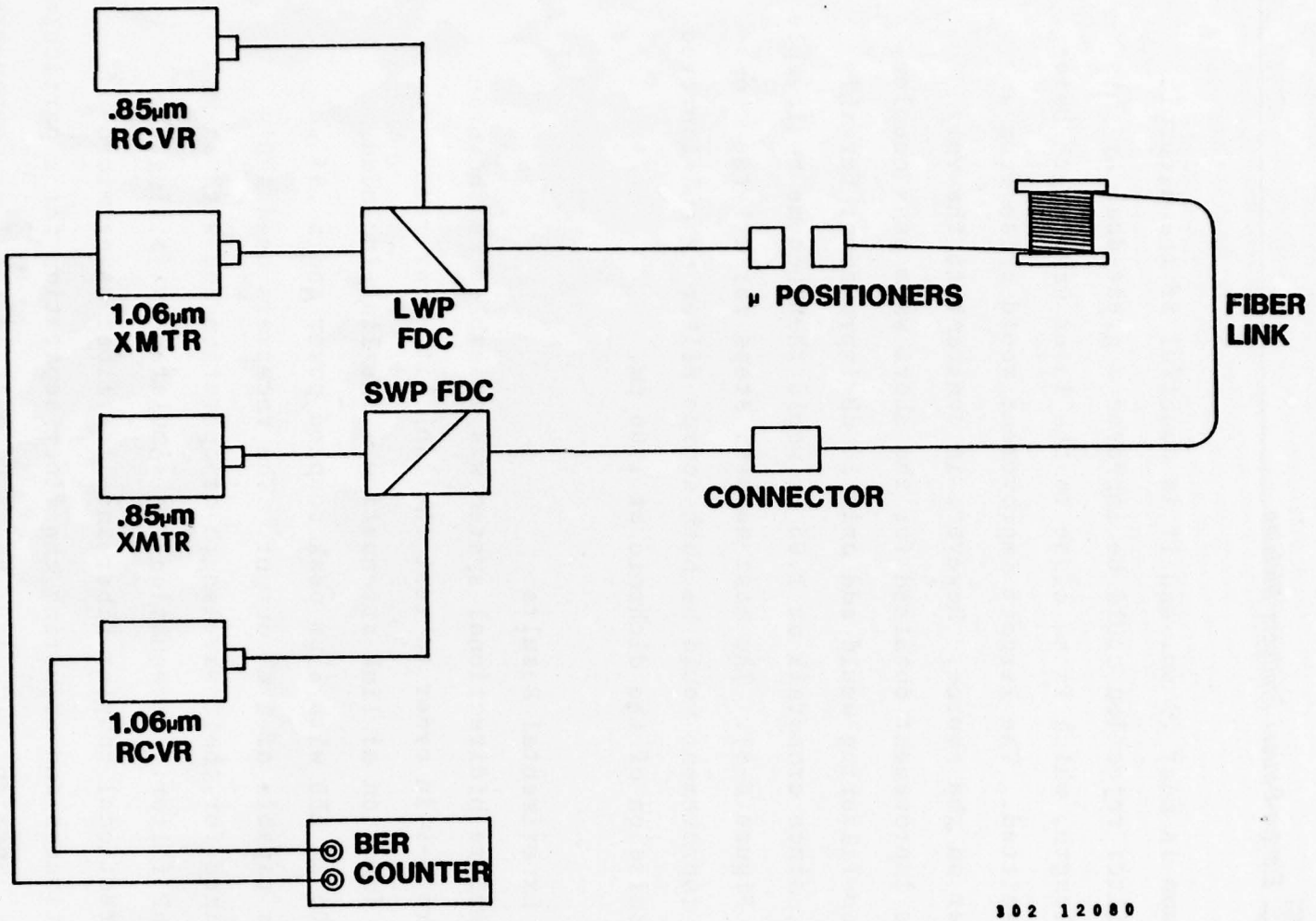

BIDIRECTIONAL SYSTEM EVALUATION

FIGURE 6-9

One problem did occur with the laser source, in that a good digital signal could not be obtained at the 1 mW level and 20 Mb/s. This resulted in poor BER measurements due to the transmitter electronics or the laser. In order to avoid this problem, the laser was run at 100 μW when testing the .84 μm channel, which is still an order of magnitude greater than the 1.06 LED coupled power. However, when the 1.06 μm channel was tested, the power for the laser was increased to 1 mW in order to provide a true test of the crosstalk immunity of the 1.06 μm channel.

The system power budget for the bidirectional link is given in Table 6-1. Total connector, coupler and filter losses are about 13 dB if connectors are used on the link fiber and about 10 dB if the link fiber is spliced to the couplers. For our case using micropositioners, the loss should be somewhere between 10 and 13 dB. The receiver sensitivity at .85 μm is -53 dBm for 10^{-8} BER at 20 Mb/s. Assuming a drop in detector efficiency of about 5 dB at 1.06 μm, the required receiver power for the 1.06 μm channel is -48 dBm. Since the source power is about -24 dBm at 1.06 μm, there is about 24 dB allowed for link loss. This translates to a fiber loss margin of 11 to 14 dB, after allowing for the loss of the couplers, connectors and filters.

Using the link of Figure 6-9 without a link fiber and using micropositioners to connect the bidirectional couplers, a margin of 11 dB was measured of 10^{-8} BER at 20 Mb/s. This is in approximate agreement with the above calculations. Since standard production fibers now have losses of less than 2 dB/km at 1.06 μm, a link length of almost 6 km would be possible using these components. Actual measurements were carried out using a 6 km fiber, and a BER of 10^{-2} to 10^{-4} was measured for the 1.06 μm channel, which is within a few dB of a 10^{-8} BER. A 3 km fiber was also used for testing and the BER was found to be better than 10^{-10}, limited by measurements time.

As predicted from the previous analysis, crosstalk was not a problem affecting link performance for the particular system. Table 6-2 gives the measured values of crosstalk for the system of Figure 6-1. The filter is InP and index match refers to whether the coupler/link fiber connection is index matched or not. With the connector index matched and using an InP filter, the crosstalk is less than -70 dB, in rough agreement with the previous calculations. Since the receiver sensitivity is only about -50 dBm, this isolation is more than adequate for a 1 mW source power. In fact, the measured performance of the link was unaffected even with non-index matched connectors in the link. However, in the future

SYSTEM MARGIN

LOSSES

SOURCE CONNECTOR	2 DB
FDC TRANS	1.5 DB
LINK CONNECTOR	2 DB (SPLICE .5 DB)
FIBER	
LINK CONNECTOR	2 DB (SPLICE .5 DB)
FDC REFL.	2.5 DB
RECEIVER CONNECTOR	2 DB
FILTER	1 DB
TOTAL =	13 DB (10 DB) + FIBER LOSS

REVR SENS = 48 DB (1.06 μM, 10^{-8} BER, 20 MB/s)

SOURCE PWR = -24 DBM (1.06 μM)

24 DB LINK MARGIN

11 DB (14 DB)
FIBER MARGIN

Table 6-1

MEASURED CROSSTALK

.84 μM SOURCE, 1.06 μM RCVR		EXPT'L RESULTS
FILTER	INDEX MATCH	
NO	NO	-32 DB
NO	YES	-40 TO -50 DB
YES	NO	-68 DB
YES	YES	<-70 DB

Table 6-2

the use of stronger sources or more sensitive receivers may require that additional measures be taken against cross-talk.

7.0 LENSED BIDIRECTIONAL COUPLER

Another version of a bidirectional coupler has been constructed using lenses and bulk dichroics. The general configuration is as shown in Figure 7-1. Light from the transmitter fiber is collimated by a lens, reflected by the dichroic and re-focussed by the same lens into the link fiber. At the same time, light incident from the link fiber is collimated by the lens, transmitted by the dichroic, and focussed by a second lens on the receiver fiber, which may be a larger diameter than the other fibers in order to reduce the coupling loss.

High quality, polished glass aspherics are used for the lensing in the coupler. An ar coating of MgF nearly eliminates all reflection loss, since a high index (n=1.89) glass is used for the lenses. The dichroics are state-of-the-art multilayer dielectric coatings on BK-7 glass. Calculations of the dichroic performance are shown in Figures 7-2 through 7-5. The actual measured transmission agreed with the calculations except that the SWP dichroic leakage was around -43 dB, and not -58 dB as shown in Figure 7-3.

As additional component not shown in Figure 7-1 and required to limit crosstalk is a glass anti-reflection piece on the link fiber. Without this glass, a portion of the light imaged from the transmitter fiber onto the link fiber is reflected back onto

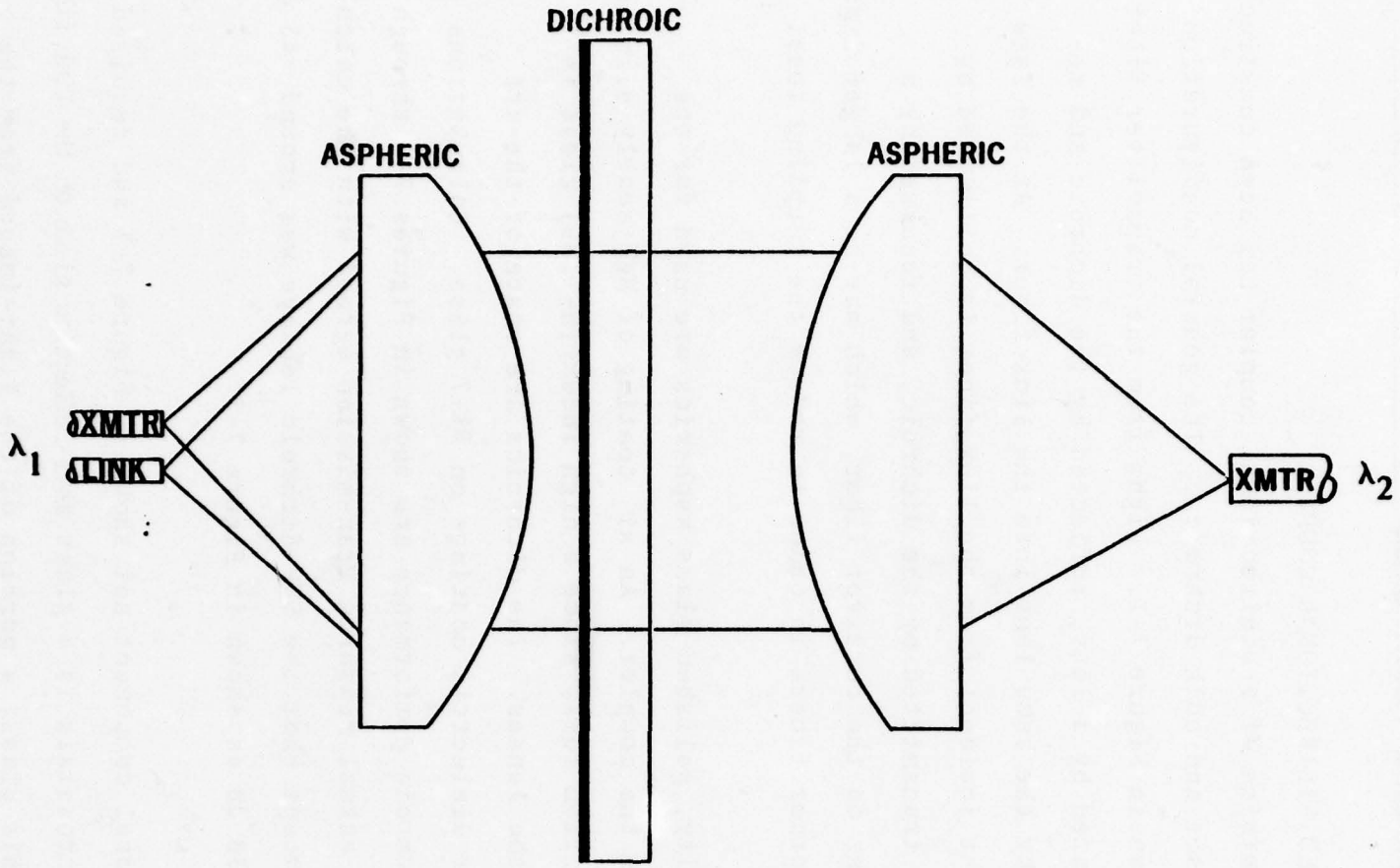

LENSED DUPLEX COUPLER

FIGURE 7-1

302 10801

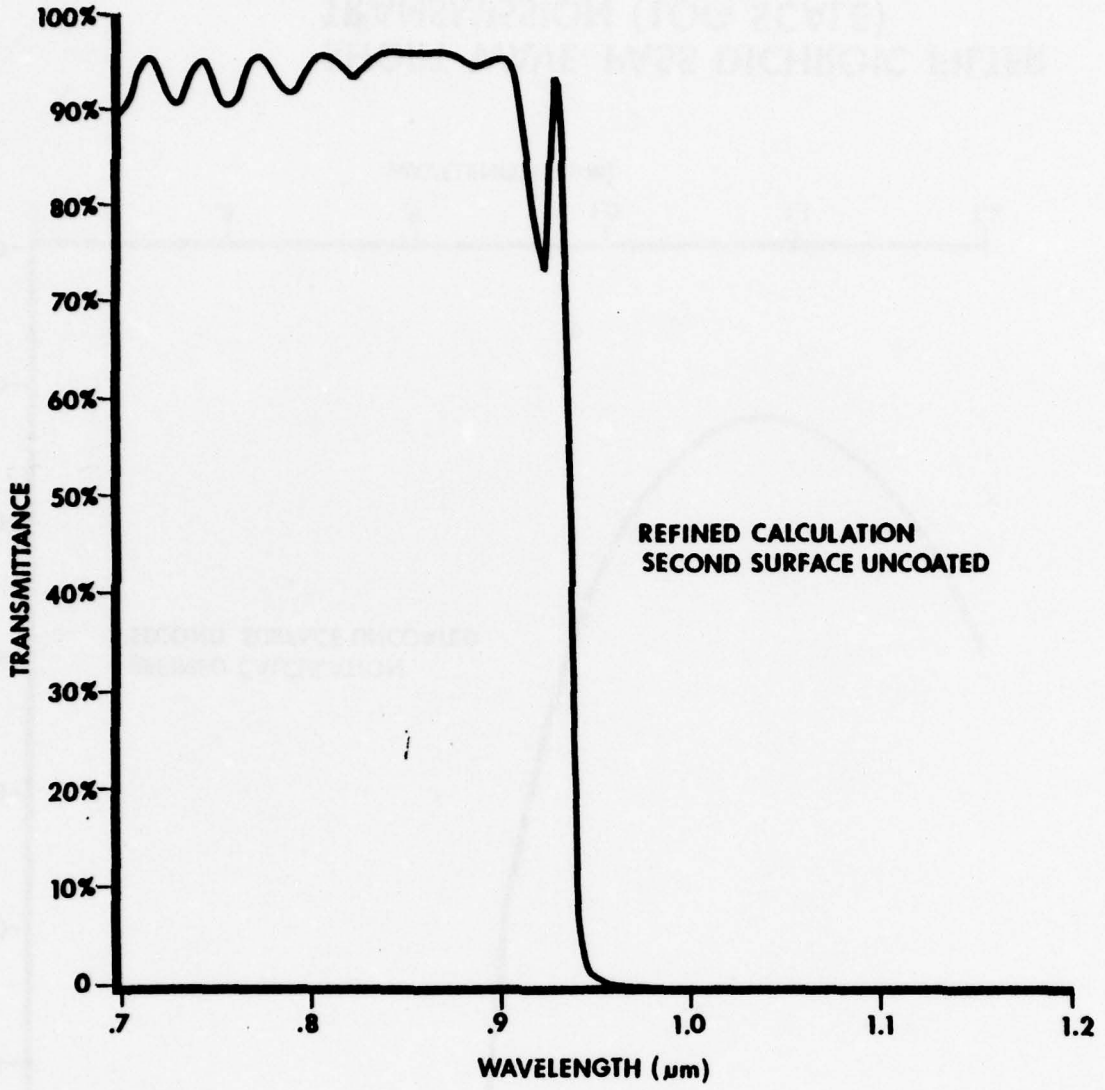

SHORT WAVE PASS DICHROIC FILTER TRANSMISSION (LINEAR SCALE)

Figure 7-2

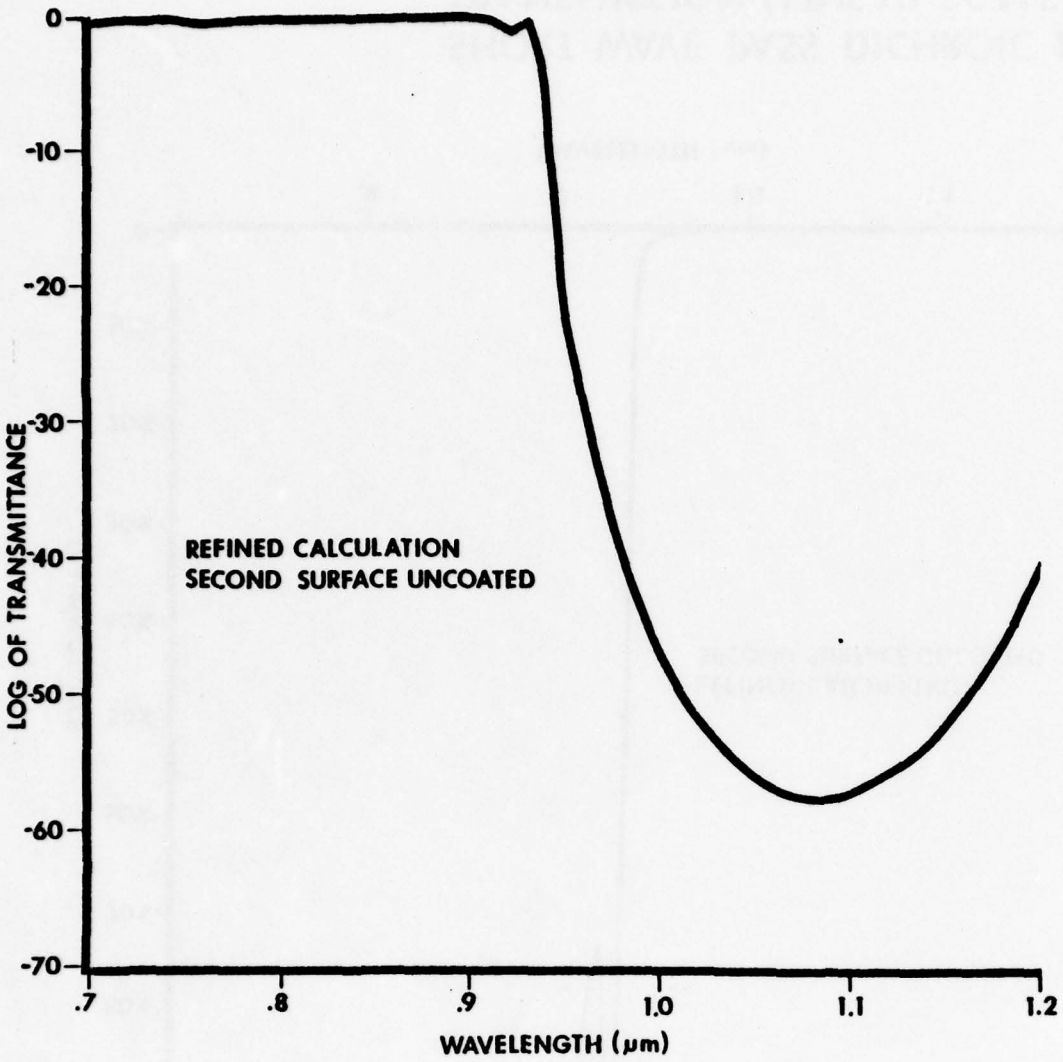

SHORT WAVE PASS DICHROIC FILTER TRANSMISSION (LOG SCALE)

Figure 7-3

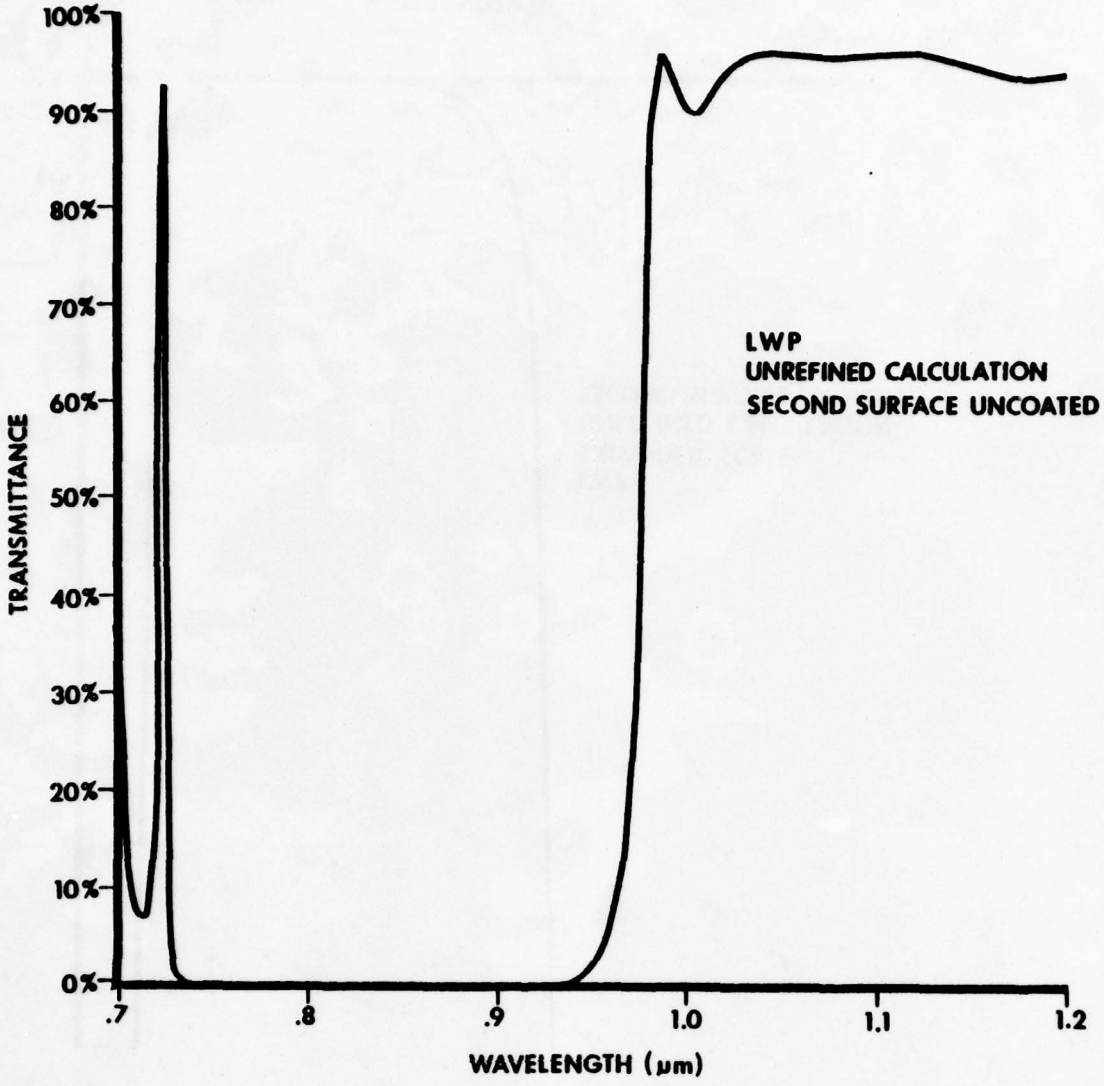

LONG WAVELENGTH PASS DICHROIC FILTER TRANSMISSION

Figure 7-4

302 11124

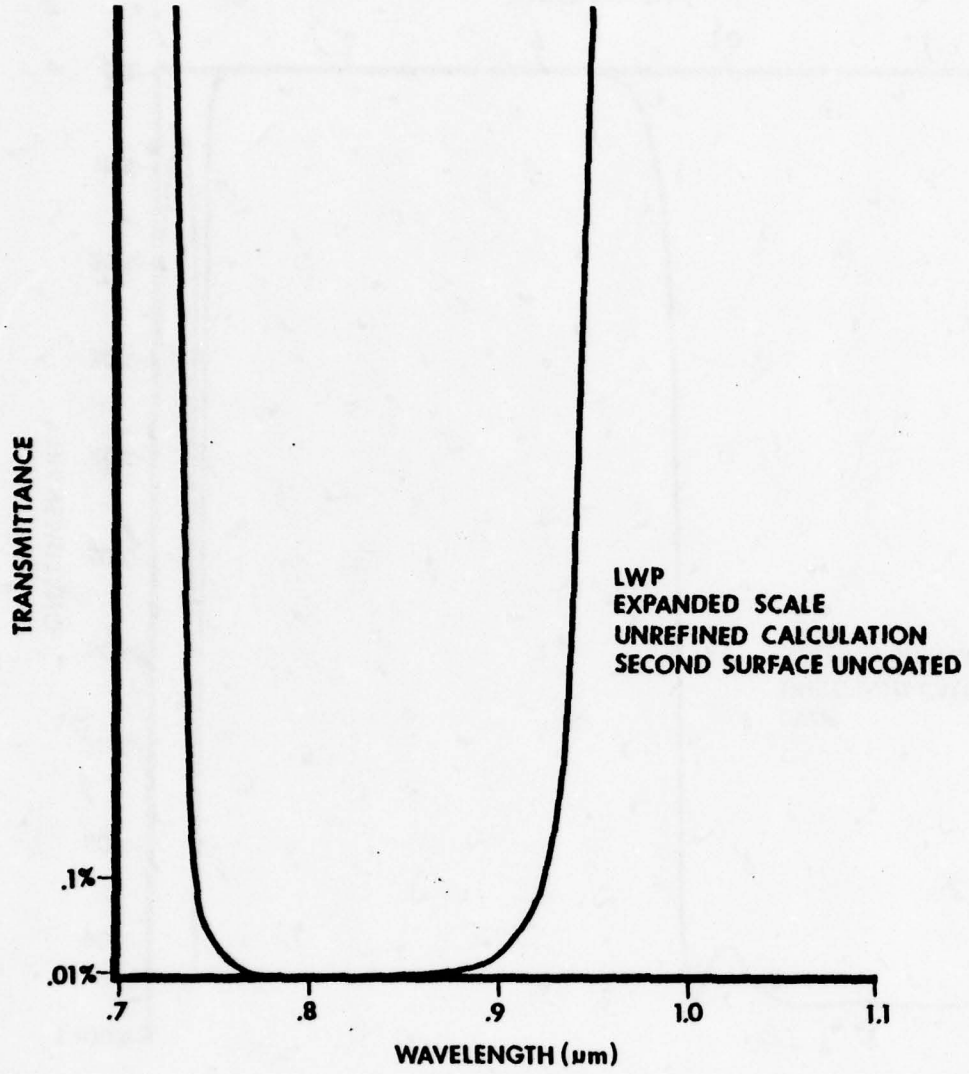

LONG WAVE PASS DICHROIC FILTER TRANSMISSION (EXPANDED SCALE)

302 11125

Figure 7-5

the dichroic, and the leakage through the dichroic will be directly imaged on the receiver fiber. This crosstalk contribution can be lowered significantly by epoxying a piece of glass to the end of the link fiber so that the reflection from the fiber end face is very small, and the reflection from the glass/air interface is not refocused on the receiver fiber.

7.1 Crosstalk Calculation

There are four main contributions to the crosstalk in the lensed bidirectional coupler:

(c-1) A portion of the light from the transmitter fiber will leak through the dichroic, as shown in Figure 7-6. However, this focus spot is offset from the receiver fiber, so only a small part of light is captured.

(c-2) A certain amount of the light from the transmitter fiber is scattered by the dichroic, as illustrated in Figure 7-7.

(c-3) As discussed before light may be directly backscattered from the fiber end face (Figure 7-8) but this reflection is reduced by the glass anti-reflection.

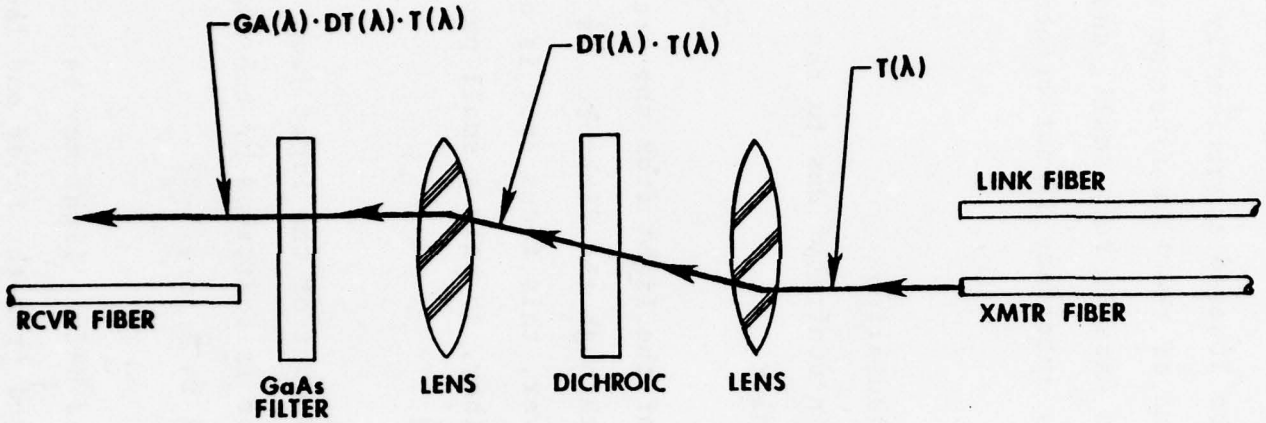

DIRECT TRANSMISSION THROUGH THE DICHROIC

Figure 7-6

302 11116

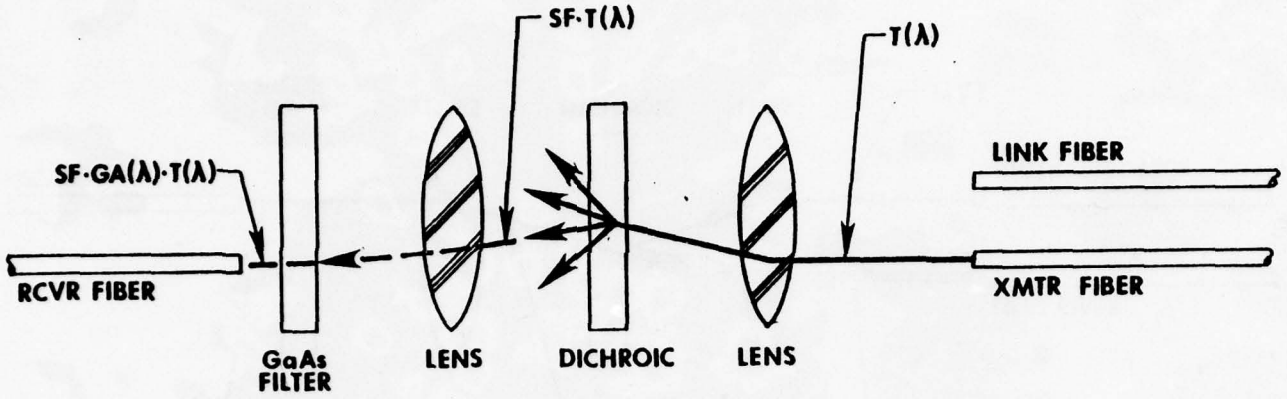

SCATTERING BY THE DICHROIC

Figure 7-7

302 11117

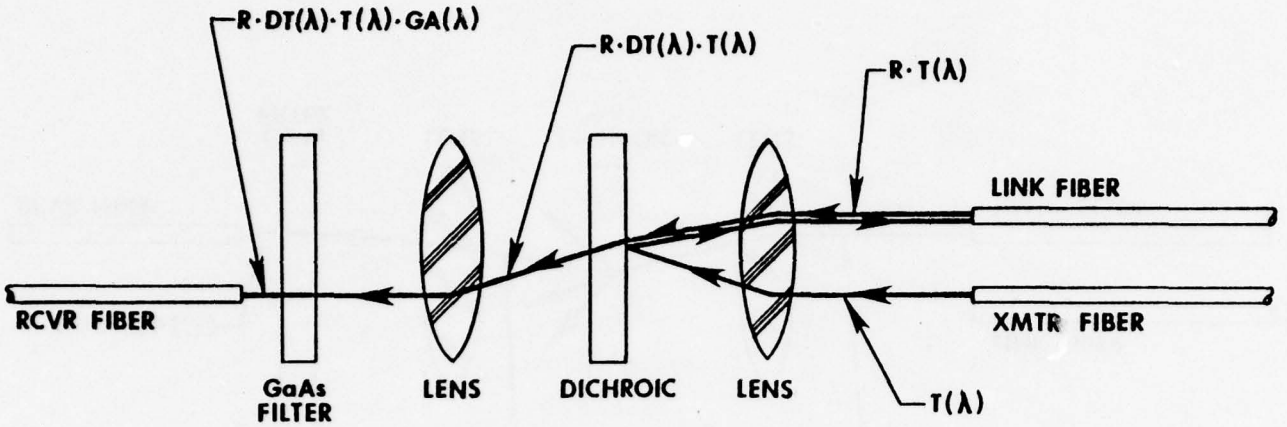

BACK REFLECTION FROM FIBER END FACE

Figure 7-8

302 11118

(c-4) Light may be directly backscattered from either discrete sources in the fiber, such as a connector or splice, or from a continuous fiber back reflection (Figure 7-9).

Each of these factors, c-1 through c-4, is calculated in the same manner discussed in Section 6.1 for the fiber dichroic coupler. The dichroic and filter performance are obtained as a function of wavelength, the source output is measured, and sources of backscatter and component scatter are estimated. Finally, integrations are performed over wavelength to compute the total crosstalk. Figures 7-10 and 7-11 give the computed crosstalk as a function of wavelength and total calculated crosstalk is given in Table 7-1. The calculations do not include using a filter for the .85 μm receiver.

7.2 Performance Summary

The measured crosstalk for the lensed bidirectional coupler is given in Table 7-2. The values actually obtained are somewhat better than predicted by the theoretical calculations, due to the fact that very conservative estimates were made in the theoretical calculation for unknown scattering coefficients.

Twenty-eight lensed couplers, 14 SWP and 14 LWP, have been assembled and tested. The results are given in Table 7-3,

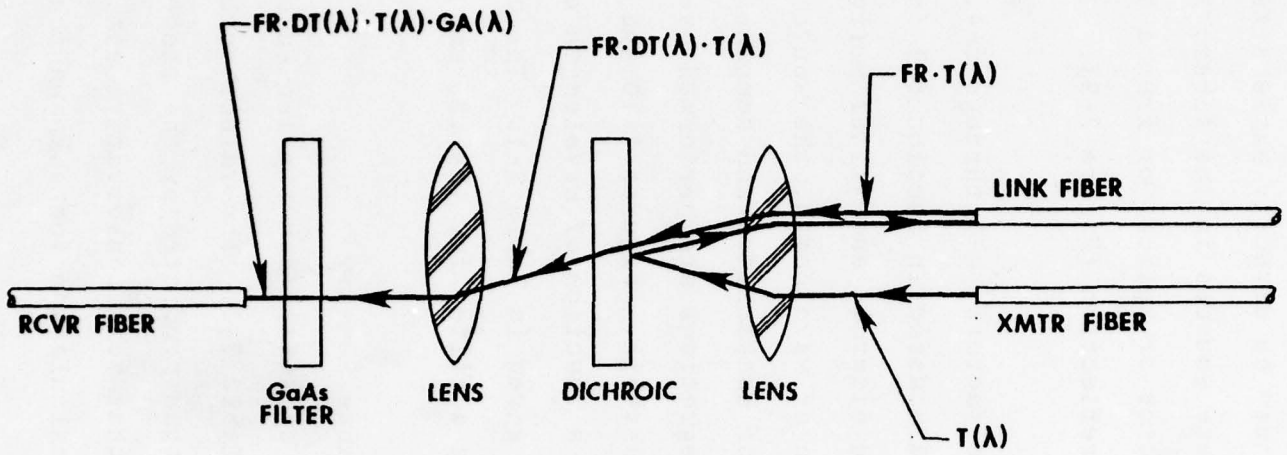

FIBER BACKSCATTER

Figure 7-9

302 11119

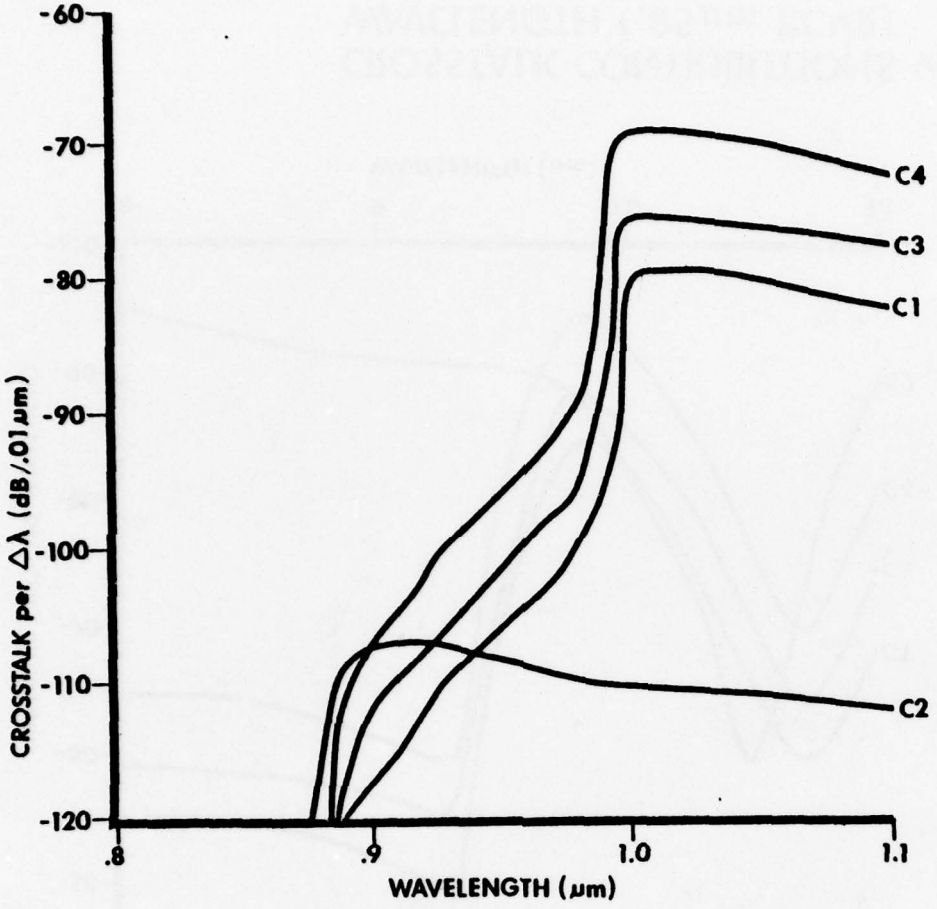

CROSSTALK CONTRIBUTIONS vs. WAVELENGTH (1.06 μm RCVR)

Figure 7-10

302 11115

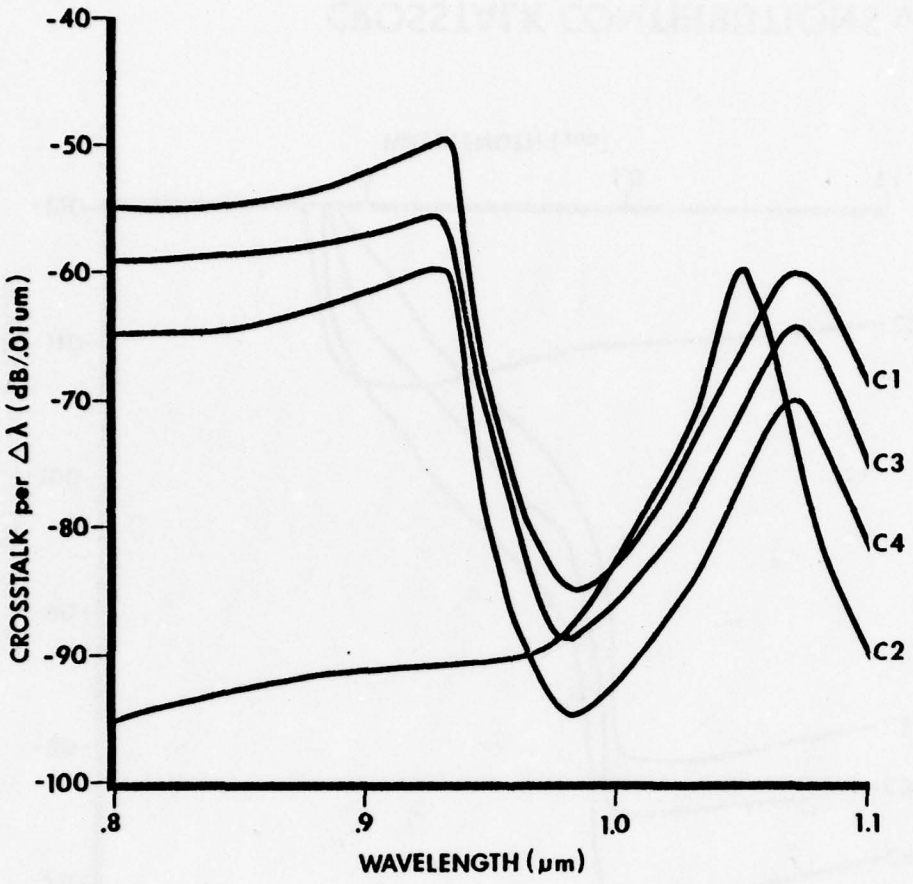

CROSSTALK CONTRIBUTIONS vs. WAVELENGTH (.85μm RCVR)

Figure 7-11

302 11114

TABLE 7-1

	1.06 μM RCVR
C_1	= -75 dB
C_2	= -98 dB
C_3	= -69 dB
C_4	= -65 dB
CROSSTALK TOTAL	= -63 dB ESTIMATED

	.85 μM RCVR
C_1	= -50 dB
C_2	= -57 dB
C_3	= -44 dB
C_4	= -40 dB
CROSSTALK TOTAL	= -38 dB ESTIMATED

Table 7-2. Cross Talk With LWP Lensed Coupler.

	AR No GaAs No	AR Yes GaAs No	AR Yes GaAs Yes
Link Fiber Not Matched	-57 dB	-58 dB	-70 dB
Link Fiber Index Matched	-58 dB	-67 dB	<-70 dB

Table 7-3

SWP COUPLERS

Coupler	Trans. Loss (dB)	Refl. Loss (dB)	Crosstalk (dB)
1	2.3	2.1	<-50
2	1.5	2.8	"
3	2.2	2.7	"
4	1.0	2.3	"
5	2.0	2.3	"
6	1.5	2.2	"
7	1.4	2.5	"
8	.9	2.2	"
9	1.6	2.0	"
10	1.1	2.8	"
11	1.6	2.9	"
12	1.3	2.9	"
13	1.2	2.4	"
14	1.6	3.3	"
	1.5 Avg.	2.5 Avg.	

Table 7-4

LWP COUPLERS

Coupler	Trans. Loss (dB)	Refl. Loss (dB)	Crosstalk (dB)
1	1.1	1.4	-66
2	.5	1.6	-69
3	1.7	1.7	-70
4	1.0	.9	-72
5	2.1	1.4	-78
6	1.8	1.6	-59
7	1.4	1.4	-69
8	1.4	1.3	-75
9	1.0	1.4	-79
10	1.5	1.3	-60
11	1.6	1.1	-82
12	1.9	1.7	-84
13	1.2	1.1	-89
14	2.6	1.2	-87
	1.5 Avg.	1.4 Avg.	

and 7-4. In general the throughput losses averaged 1.5 dB, except for the SWP reflection loss which averaged 2.5 dB. Measured crosstalk ranged from -59 dB to less than -80 dB for the LWP couplers and was below the measurable limit of -50 dB for the SWP couplers.

Since at present the bulk dichroic has better performance than the fiber dichroic, the bulk coupler does have the advantage of better rejection of fiber backscatter, -40 dB as opposed to about -12 to -15 dB. However, the overall crosstalk and throughput performance is similar; and while the bulk coupler can be made compact, the fiber dichroic will probably have the eventual advantage in size, ruggedness, reliability and economy.

8.0 DISCUSSION OF RESULTS AND CONCLUSIONS

In this section a discussion of the detailed results of the program is presented, with emphasis on the capabilities of the Fiber Dichroic Coupler development and its use in a bidirectional link. In addition, some comparison results for lensed dichoric couplers are presented. In Section 8.2 some general conclusions supported by the results of this development program are presented.

8.1 Discussion of Results

The goal of this contract was to identify and examine various coupler approaches to bidirectional transmission over a single fiber and establish their overall limitations. Section 2.0 compares the theoretical optical characteristics for three models using macroscopic lenses. Three potential approaches, i.e., prisms, grating, and dichroics, have been analyzed. All three methods yield comparable characteristics - low insertion loss (less than -2 dB), less than -40 dB cross talk due to internal scattering, and more than 40 dB of rejection against the link fiber backscatter.

The primary experimental appraoch was a fiber dichroic beam splitter. The initial Phase I development program employed

a device with a dichroic coating deposited on a fiber end face having an angle of 45° relative to the optical axis. Several prototypes were constructed and evaluated. Although the basic premise proposed in the contract was correct, physical laws restricted its optical performance.

The main deficiency was that an efficient dichroic coating was extremely difficult to manufacture at an internal angle of 45°. The propagation of unpolarized light near the Brewster angle limited the quality of the optical transmission/reflection characteristics. Section 3.0 contains a more detailed evaluation. The short-wave pass (SWP) coupler exhibited wavelength selection but the rejection ratio was poor. The transmittance at 840 nm was measured at -2.3 dB and the reflectance at 1060 nm was -4.2 dB. The backscatter discrimination was -10 dB at 840 nm. This level includes a tapoff fiber coupling loss (wavelength independent) from misalignment. Consequently, the internal discrimination capability of the coating is less than 10 dB. The long-wave pass (LWP) coupler showed poorer performance (backscatter discrimination) than the SWP coupler. This is due to the increased difficulty in manufacturing a dichroic surface at 45° with the proper optical characteristics. The polarization

effects in the LWP dichroic are examined in Section 3.0.

Essentially, the LWP coupler exhibits a backscatter discrimination of -5 dB to -7 dB. The Phase I development effort resulted in the demonstration of a duplex coupler using the fiber-integrated dichroic reflector. The transmission/reflection coupling efficiency (wavelength independent) was acceptable. The overriding limitation was the polarization effects near the Brewster angle. With present fiber optic technology (unpolarized multimode sources and fiber), the potential for developing duplex couplers at 45^{o} internal incidence angle appears to be restricted.

The Phase II coupler effort was initiated to improve coupler performance. Reducing the internal incidence angle was successful in reducing the limitations due to near Brewster angle operation. The Phase II couplers used a dichroic reflector at 25^{o} internal incidence angle. This allowed improved dichroic properties and the use of a tapoff fiber coupling scheme already developed. Reducing the angle below 25^{o} would have allowed direct coupling from the link fiber into the core of the tapoff (or receiver) fiber. As the program continued, additional fabrication technique developments

were incorporated into the couplers, including a design for improved temperature performance. Use of a dichroic reflector on a 50 μm thick substrate between coupler halves reduced assembly time and complexity. This method allows any glass on glass fiber to be utilized in a duplex coupler. Fabrication of a fiber dichroic wafer coupler (FDWC) has become a routine operation. The optical characteristics of the FDWC/FDC are documented in Section 3.0, Table 3-4.

Two SWP couplers were fabricated using the improved assembly technique. The third SWP coupler used the dichroic deposition procedure. Although it appears there is no significant optical difference, the devices using the dichroic wafer were mechanically much easier to assemble. Fabrication of the LWP couplers utilized dichroic deposition directly on the fiber end face.

Throughput coupling efficiency (wavelength independent) for all devices indicated improvements could be made in the assembly technique. The transmission efficiency was better than -1.8 dB. This includes any losses from the dichroic surface. Tapoff coupling efficiency for the 100 μm core fiber was between -1 dB and -4 dB. When assembling the two coupler

halves, excess epoxy can wick over the throughput fiber dichroic interface. This causes a build up of epoxy and limits the separation between the tapoff fiber and the fiber dichroic interface. This accounts for the deviation in tapoff efficiency. Additional development effort to reduce or eliminate this problem is warranted.

Two critical characteristics of a bidirectional coupler are internal generation of optical cross talk and discrimination against link backscatter. Backscatter discrimination levels were measured on all SWP devices using .85 μm LED sources (400Å spectral bandwidth) rather than the preferred laser diode because of availability. The levels measured were between -12 dB and -15 dB. These reflect the out-of-band emission of the LED sources. Significantly better discrimination would be realized with a laser diode (20 Å spectral bandwidth).

The internal optical cross talk of two couplers using the dichroic wafer (SWP-5 and SWP-6) were -40 dB and -53 dB. The SWP coupler with the deposited coating may have had it partially chipped (see Section 3.0 explaining the higher internal cross talk). The wide discrepancy between the cross talk levels in the two couplers is at present unexplained.

Additional effort to identify the cause of the discrepancy is warrented. The backscatter discrimination for the LWP coupler was -11 dB. The optical cross talk was less than -34 dB, limited by source available power (1.06 μm LED).

By inserting an optical absorption filter and index matching the link pigtail, the cross talk can be reduced by an order of magnitude or more, depending on a number of factors discussed in detail in Sections 3.0 and 6.0. The cross talk in the long wavelength detector due to the short wavelength source was -63 dB (SWP-6). This cross talk level may be lower because the index match may not be exact. The cross talk in the short wavelength detector due to the long wavelength source was less than -57 dB. The present cross talk limitation for the SWP coupler is the out-of-band radiation that is transmitted by the laser diode source. The requirement for cross talk levels below -75 dB (digital) will necessitate the addition of in-line source filtering to reduce the out-of-band radiation. This filtering would add -30 dB optical isolation for the short-wave terminal.

An alternative to the fiber dichroic coupler is a lensed bidirectional coupler. Section 7.0 contains a detailed

description. This device exhibits a backscatter discrimination of -40 dB versus -12 dB to -15 dB for a FDWC/FDC. The lensed bi-directional coupler averages approximately -75 dB optical isolation for the short-wave pass coupler, including an optical absorption filter and index matching of the pigtail.

This difference is attributed to the angular orientation of the FDC and its associated finite cone angle. The lensed coupler, on the other hand, employs collimation of the incident light and transmission/reflection on a dichroic at near 0^{o} incidence angle. However, the lensed dichroic coupler is fabricated using custom precision optics, which even in large quantity production, may be expected to be considerably more expensive than the FDC. The reproducibility is similar for both types of duplex coupler. The FDC is probably more rugged due to its fabrication technique and smaller quantity of components compared to the lensed device. Whether a FDC or lensed duplex coupler is utilized is dependent on the particular application. Without any modifications the FDC cross talk is 10 dB worse than the lensed coupler. The transmission/reflection coupling efficiencies are similar.

A system evaluation was performed to determine the maximum bidirectional link length using FDWC/FDC couplers and maintaining a 10^{-8} BER. During the course of the program, the limiting factor in long link length operation was the long wavelength source (-24 dBm coupled optical power). Thus, the intrinsic lower fiber attenuation at the long wavelength could not be fully utilized. The delivered system was evaluated through a 3 km GI link and maintained better than 10^{-10} BER at a data rate of 20 Mb/s (NRZ). The total fiber link attenuation to maintain a 10^{-8} BER was determined to be approximately 12 dB for the long wavelength transmission.

Recently, developmental InGaAsP long wavelength laser diodes have become commercially available. In this case, the GaAlAs laser diode would become the limiting factor in attaining long link lengths. With these long wavelength sources, fiber wavelength duplexing will be able to utilize the low attenuation properties of the fiber. Dichroic coatings can be developed for these longer wavelengths. By properly filtering sources to reduce out-of-band radiation, link lengths significantly greater than 8 km will become assessable along with optical isolation better than -75 dB.

8.2 Conclusions

The following conclusions for full duplex bidirectional link operation are the consequence of the studies and experimental results of this developmental effort. In general, it can be said that:

a. Full duplex bidirectional operation of single fiber channel links can be achieved over very long lengths by using separate wavelength sources and passive wavelength dependent coupling and filtering to achieve minimum cross talk levels.

b. Full duplex bidirectional link operation will be severely limited by fiber distributed and discrete backscattering levels if same wavelength sources are used for each direction.

For all configurations which employ separate wavelengths in each direction it follows that:

a. Couplers which incorporate direct λ duplexing are more efficient than non-duplexing couplers (e.g., fused biconical taper).

b. Source-out-of-band radiation is a limiting factor if additional filtering is not used at sources and detectors.

c. The ultimate system capability using passive techniques only can be achieved using a combination of wavelength duplexing couplers with additional source and detector filtering.

Within the context of the wavelength duplexed bidirectional

link, the choice of coupler will depend on optical performance, environmental suitability, and cost. Relative to these factors, the following conclusions are important:

a. Efficient wavelength duplexing couplers can be implemented using dichroic reflectors in either bulk (lensed) or fiber-integrated configurations.

b. The internal backscatter characteristics and external backscatter rejection capability of the FDWC/FDC coupler is not as good as the Bulk Dichroic Coupler.

c. The mechanical and environmental susceptibly of both types of dichroic coupler need to be determined before a realistic choice can be made between them for various system applications. In particular, the lensed dichroic using graded refractive index lens merits further consideration.

d. Further detailed study of the spectral characteristics of all potential components for bidirectional link operation is needed in order to determine maximum operational capabilities.

e. Further development of the Fiber Dichroic Wafer Coupler and techniques for its fabrication is needed to determine potential cost implications for system implementation.

With the importance of minimizing fiber and cable weight for certain military applications requiring full duplex link operation, the continued development of devices for wavelength duplexing of bidirectional links is highly recommended.

DISTRIBUTION LIST

	Copies
Defense Documentation Center ATTN: DDC-TCA Cameron Station (Building 5) Alexandria, VA 22314	12
Director National Security Agency ATTN: TDL Fort George G. Meade, MD 20755	1
DCA Defense Comm Engrg Ctr ATTN: Code R123, Tech Library 1860 Wiehle Ave Reston, VA 22090	
Defense Communications Agency Technical Library Center Code 205 (P. A. Tolovi) Washington, DC 20305	1
Office of Naval Research Code 427 Arlington, VA 22217	1
GIDEP Engineering & Support Dept TE Section PO Box 398 Norco, CA 91760	1
Director Naval Research Laboratory ATTN: Code 2627 Washington, DC 20375	1
Commander Naval Electronics Laboratory Center ATTN: Library San Diego, CA 92152	1

	Copies
Command, Control & Communications Div Development Center Marine Corps Development & Educ Command Quantico, VA 22134	1
Naval Telecommunications Command Technical Library, Code 91L 4401 Massachusetts Avenue, NW Washington, DC 20390	1
Rome Air Development Center ATTN: Documents Library (TILD) Griffiss AFB, NY 13441	1
AFGL/SULL S-19 HAFB, MA 01731	1
CDR, MIRCOM Redstone Scientific Info Center ATTN: Chief, Document Section Redstone Arsenal, AL 35809	1
Commander HQ Fort Huachuca ATTN: Technical Reference Div Fort Huachuca, AZ 85613	1
Commander US Army Electronic Proving Ground ATTN: STEEP-MT Fort Huachuca, AZ 85613	1
Commander USASA Test & Evaluation Center ATTN: IAO-CDR-T Fort Huachuca, AZ 85613	1
Dir, US Army Air Mobility R&D Lab ATTN: T. Gossett, Bldg 207-5 NASA Ames Research Center Moffett Field, CA 94035	1
HQDA (DAMO-TCE) Washington, DC 20310	1

	Copies
Deputy for Science & Technology Office, Asst Sec Army (R&D) Washington, DC 20310	1
HQDA (DAMA-ARP/DR. F. D. Verderame) Washington, DC 20310	1
Director US Army Human Engineering Labs Aberdeen Proving Ground, MD 21005	1
CDR, AVRADCOM ATTN: DRSAV-E PO Box 209 St. Louis, MO 63166	1
Director Joint Comm Office (TRI-TAC) ATTN: TT-AD (Tech Document Center) Fort Monmouth, NJ 07703	1
Commander US Army Satellite Communications Agency ATTN: DRCPM-SC-3 Fort Monmouth, NJ 07703	1
TRI-TAC Office ATTN: TT-SE (Dr. Pritchard) Fort Monmouth, NJ 07703	1
CDR, US Army Research Office ATTN: DRXRO-IP (Dr. Mink) PO Box 12211 Research Triangle Park, NC 27709	1
Director US Army Material Systems Analysis Actr Attn: DRXSY-MP Aberdeen Proving Ground, MD 21005	1
CDR, US Army Signals Warfare Lab ATTN: DELSW-OS Vent Hill Farms Station Warrenton, VA 22186	1

	Copies
CDR, US Army Signals Warfare Lab ATTN: DELSW-AW Vent Hill Farms Station Warrenton, VA 22186	1
Commander US Army Logistics Center ATTN: ATCL-MC Fort Lee, VA 22801	1
Commander US Army Training & Doctrine Command ATTN: ATCED-TEC Fort Monroe, VA 23651	1
Commander US Army Training & Doctrine Command ATTN: ATCD-TM Fort Monroe, VA 23651	1
NASA Scientific & Tech Info Facility Baltimore/Washington Intl Airport PO Box 8757 Baltimore, MD 21240	1
Advisory Group on Electron Devices 201 Varick Street, 9th Floor New York, NY 10014	1
Advisory Group on Electron Devices ATTN: Secy, Working Group D (Lasers) 201 Varick Street New York, NY 10014	1
TACTEC Battelle Memorial Institite 505 King Avenue Columbus, OH 43201	1
Ketron, Inc. ATTN: Mr. Frederick Leuppert 1400 Wilson Blvd, Architect Bldg Arlington, VA 22209	1

	Copies
R. C. Hansen, Inc. PO Box 215 Tarzana, CA 91356	1
CDR, US Army Avionics Lab AVRADCOM ATTN: DAVAA-D Fort Monmouth, NJ 07703	1
Ballistic Missile Systems Defense Command ATTN: BMDSC-HD (Mr. C. D. Lucus) PO Box 1500 Huntsville, AL 35807	1
Project Manager, ATACS ATTN: DRCPM-ATC (Mr. J. Montgomery) Fort Monmouth, NJ 07703	1
Commander ERADCOM ATTN: DELET-D Fort Monmouth, NJ 07703	1
Commander ERADCOM ATTN: DELSD-L-S Fort Monmouth, NJ 07703	1
Commander ERADCOM ATTN: DELSD-L Fort Monmouth, NJ 07703	1
Commander CORADCOM ATTN: DRDCO-COM-D Fort Monmouth, NJ 07703	1
Commander CORADCOM ATTN: DRDCO-SEI Fort Monmouth, NJ 07703	1

	Copies
Commander CORADCOM ATTN: DRDCO-COM-RM Fort Monmouth, NJ 07703	1
Corning Glass Works Telecommunication Prod Dept Corning, New York 14830	1
Galileo Electro-Optics Corporation Galileo Park Sturbridge, MA 01518	1
Times Fiber Comm, Inc. 358 Hall Avenue Wallingford, CT 06492	1
Bell Northern Research PO Box 3511, Station C Ottawa, Canada K1Y 4H7	1
Valtec Corporation Electro Fiber Optic Division West Boylston, MA 01583	1
Hughes Research Laboratory 3011 Malibu Canyon Road Malibu, CA 90265 ATTN: Dr. R. Abrams	1
Belden Corporation Technical Research Center 2000 South Batavia Avenue Geneva, IL 60134 ATTN: Mr. J. McCarthy	1
Optelecom, Inc. 15940 Shady Grove Road Gaithersburg, MD 20760	1
Bell Telephone Laboratories Whippany Road Whippany, NJ 07981 ATTN: Mr. G. A. Baker	1

	Copies
Deutsch Co. Elec Components Div Municipal Airport Banning, CA 92220	1
General Cable Corporation 15 Prospect Lane Colonia, NJ 07067 ATTN: Mr. I. Kolodny	1
Martin Marietta Corporation Orlando, FL	1
Electronics Group of TRW, Inc. 401 N. Broad Street Philadelphia, PA 19108	1
Hughes Aircraft Corporation Tucson Systems Engr'g Dept. PO Box 802, Room 600 Tucson, AZ 85734 ATTN: Mr. D. Fox	1
GTE Sylvania Inc. Communications System Division 189 B Street Needham Heights, MA 02194 ATTN: Mr. J. Concordia	1
Harris Electronics Systems Division PO Box 37 Melbourne, FL 32901 ATTN: Mr. R. Stachouse Fiber Optics Plant Rodes Boulevard	1
General Cable Corporation Raritan Center 160 Fieldcrest Avenue Edison, NJ 08817 ATTN: Mr. M. Tenzer	1

	Copies
US Army Missile R&D Command Redstone Arsenal, AZ 35809 ATTN: DRDMI-TDD (Mr. R. Powell)	1
Sperry Research Center 100 North Road Sudbury, MA 01776 ATTN: Mr. D. McMahon	1
Westinghouse Advanced Technology Lab PO Box 1521 Baltimore, MD 21203 ATTN: Dr. D. Mergerian Main Stop 3714	1
US Department of Commerce Office of Telecommunications 325 South Broadway Boulder, CO 80302 ATTN: Dr. R. L. Gallawa	1
Carnegie-Mellon University Department of Electrical Engineering Schenley Park Pittsburgh, PA 15213 ATTN: Prof. C. S. Tsai	1
The Mitre Corporation PO Box 208 Bedford, MA 01730 ATTN: J. A. Quarato	1
Naval Ocean System Center, Code 8115 271 Catalina Blvd. San Diego, CA 92152 ATTN: Howard Rast, Jr.	1